Université de Montréal

Histone H3 lysine 56 acetylation and deacetylation pathways as targets for novel antifungal therapies in *Candida albicans*

par

Rahul Ghugari

Département de Biologie Moléculaire

Faculté de Médecine

Thèse présentée a la Faculté de Médecine

en vue de l'obtention du grade de *Philosophiae Doctor* (Ph.D.)

en Biologie Moléculaire

Option Biologie des Systémes

June 2018

Résumé

Candida albicans est un important agent pathogène fongique opportuniste qui est inoffensif pour les individus en bonne santé, mais provoque des infections systémiques potentiellement mortelles chez les personnes dont le système immunitaire est compromis. L'infection invasive causée par *C. albicans* chez les patients immunodéprimés conduit à un taux de mortalité significatif. Les options thérapeutiques actuelles sont limitées par l'émergence de souches pharmaco-résistantes ou d'effets secondaires indésirables. Par conséquent, il existe un besoin urgent de trouver de nouvelles cibles de médicaments spécifiques à ces levures pour surmonter les limites des médicaments existants. Cette thèse consiste en deux articles de recherche.

Le premier article fait l'étude de l'acétylation de l'histone H3 lysine 56 (H3K56), une modification post-traductionnelle abondante qui joue un rôle important dans la survie des dommages à l'ADN et favorise la virulence chez *C. albicans*. H3K56 est acétylée par l'histone acétyltransférase Rtt109 (HAT), et désacétylée par Hst3 (HDAC). Ces deux enzymes ont des propriétés spécifiques aux levures et sont des cibles antifongiques prometteuses. Des études antérieures chez *Saccharomyces cerevisiae* ont montré que les chaperons d'histones ScAsf1 et ScVps75 contrôlent l'activité de ScRtt109 et la spécificité du substrat. ScRttl09 et ScAsfl agissent de manière concertée pour acétyler H3K56, tandis que le complexe ScRttl09-Vps75 acétyle plusieurs résidus de lysine dans la queue N-terminale de l'histone H3. Chez *C. albicans*, les rôles de Rtt109 et H3K56ac dans la survie aux dommages de l'ADN sont conservés. Cependant, les spécificités fonctionnelles et de substrat de CaRtt109 quand elle coopère avec les chaperones d'histone CaAsf1 ou CaVps75 n'ont pas été étudiées. Dans cette étude, nous avons utilisé des méthodes de génétique, de biochimie et de spectrométrie de masse pour identifier et caractériser les rôles de Asf1 ou Vps75 et leur fonctionnement avec Rtt109 chez *C. albicans*. De manière inattendue, les cellules de *C. albicans* dépourvues de Vps75 présentent des niveaux plus faibles de H3K56ac que les cellules de type sauvage et, conséquemment, sont plus résistantes que les cellules de type sauvage au nicotinamide, un inhibiteur de la sirtuine Hst3 qui tue les cellules de *C. albicans* en provoquant une hyperacétylation de H3K56 et des dommages irréparables à l'ADN. Nous mettons en évidence que l'holoenzyme CaRtt109-Vps75 peut directement acétyler H3K56 *in vitro*. Nous montrons également que les faibles niveaux inattendus de H3K56ac trouvés dans des cellules dépourvues de Vps75 peuvent être attribués, au moins en partie, à l'instabilité de Rtt109 en l'absence de son partenaire Vps75. De plus, nos études montrent que, en plus d'aider Rtt109 à promouvoir

H3K56ac, Asf1 est essentiel pour la viabilité de *C. albicans* où il joue un rôle dans le maintien de l'intégrité des chromosomes.

Hst3 appartient à la classe des désacétylases NAD^+, appelées sirtuines, qui peuvent être inhibées par le produit de la réaction nicotinamide (NAM). L'inhibition de Hst3 par NAM conduit à une hyper-acétylation de H3K56, à des dommages catastrophiques à l'ADN et à la létalité. Dans un effort pour améliorer le potentiel clinique de NAM, nous avons étudié son devenir métabolique chez *C. albicans*. NAM est un précurseur d'une voie de sauvetage canonique qui génère NAD^+. Nous avons émis l'hypothèse que les cellules dépourvues de Pnc1 nicotinamidase, qui convertit le NAM en acide nicotinique (NA), seraient plus sensibles au NAM que les cellules de type sauvage. Malgré le fait que Pnc1 était la seule nicotinamidase chez *C. albicans*, les concentrations de NAM et la cytotoxicité étaient, au mieux, légèrement plus élevées chez les mutants pnc1 que chez les cellules de type sauvage. Ces résultats suggèrent l'existence d'un mécanisme indépendant de Pnc1 qui limite l'accumulation de NAM et, par conséquent, restreint sa capacité à inhiber Hst3. Pour identifier le mécanisme sous-jacent, nous avons généré plusieurs mutants dépourvus d'enzymes impliquées dans la biosynthèse de NAD^+ et effectué des expériences avec la NAM marquée aux isotopes lourds et la spectrométrie de masse. Nos résultats démontrent l'existence d'une conversion non-canonique, indépendante de Pnc1, de NAM en NAD^+ qui n'a jamais été rapportée chez les champignons. Nous montrons que cette conversion se produit, au moins en partie, par l'inversion de l'activité de la sirtuine et fournit l'évidence de l'inversion des sirtuines in vivo. Cependant, nous avons pu démontrer que cette voie ne peut pas être la seule source de NAD^+ et maintenir la viabilité aux concentrations physiologiques de NAM.

Mots-clés: *Candida albicans,* l'acétylation de l'histone H3 lysine 56 (H3K56ac), Rtt109, Nicotinamide

Abstract

Candida albicans is a major opportunistic fungal pathogen that is harmless to healthy individuals but causes life-threatening systemic infections in individuals whose immune system is compromised. Invasive infection caused by *C. albicans* in immunocompromised patients leads to a significant mortality. Current therapeutic options are limited by the emergence of drug resistant strains or adverse side effects. Hence, there is an urgent need to find novel fungal-specific drug targets to overcome the limitations of existing drugs. This thesis consists of two research articles.

The first article studies histone H3 lysine 56 (H3K56) acetylation, an abundant post-translational modification that plays an important role in the survival of DNA damage and promotes virulence in *C. albicans.* H3K56 is acetylated by the histone acetyltransferase Rtt109 (HAT), and deacetylated by Hst3 (HDAC). Both of these enzymes have fungal-specific properties and are promising antifungal targets. Previous studies in *Saccharomyces cerevisiae* have shown that the histone chaperones ScAsf1 and ScVps75 control ScRtt109 activity and substrate specificity. ScRtt109 and ScAsf1 act in a concerted fashion to acetylate H3K56, whereas the ScRtt109-Vps75 complex acetylates several lysine residues in the N-terminal tail of histone H3. In *C. albicans*, the roles of Rtt109 and H3K56ac in DNA damage survival are conserved. However, the functional and substrate specificities of CaRtt109 when it co-operates with the histone chaperones CaAsf1 or CaVps75 have not been studied. In this study, we used genetic, biochemical and mass spectrometry methods to identify and characterize the roles of Asf1 or Vps75 when they function with Rtt109 in *C. albicans*. Unexpectedly, *C. albicans* cells lacking Vps75 exhibit lower levels of H3K56ac than wild-type cells and, consistent with this, are more resistant than wild-type cells to nicotinamide, an inhibitor of the sirtuin Hst3 that kills *C. albicans* cells by causing hyperacetylation of H3K56 and irreparable DNA damage. We provide evidence that the CaRtt109-Vps75 holoenzyme can directly acetylate H3K56 *in vitro*. We also show that the unexpectedly low levels of H3K56ac found in cells lacking Vps75 can be attributed, at least in part, to instability of Rtt109 in the absence of its partner Vps75. Our studies also show that, apart from assisting Rtt109 to promote H3K56 acetylation, Asf1 is essential for viability in *C. albicans* where it plays a role in the maintenance of chromosome integrity.

Hst3 belongs to the class of NAD^+-dependant deacetylases called sirtuins, which can be inhibited by the reaction product nicotinamide (NAM). Hst3 inhibition by NAM leads to hyper-acetylation of H3K56, catastrophic DNA

damage and lethality. In an effort to enhance the clinical potential of NAM, we studied its metabolic fate in *C. albicans*. NAM is a precursor of a canonical salvage pathway that generates NAD^+. We hypothesized that cells lacking the Pnc1 nicotinamidase, which converts NAM into nicotinic acid (NA), would be more sensitive to NAM than wild-type cells. Despite the fact that Pnc1 was the sole nicotinamidase in *C. albicans*, NAM concentrations and cytotoxicity were, at best, modestly higher in *pnc1* mutants than in wild-type cells. These results suggest the existence of a Pnc1-independent mechanism that limits the accumulation of NAM and, therefore, restricts its ability to inhibit Hst3. To identify the underlying mechanism, we generated several mutants lacking enzymes involved in the biosynthesis of NAD^+ and performed experiments with heavy isotope-labeled NAM and mass spectrometry. Our results demonstrate the existence of a non- canonical, Pnc1-independent conversion of NAM into NAD^+ that has never been reported in fungi. We show that this conversion occurs, at least in part, through reversal of sirtuin activity and provide the evidence of sirtuins reversal *in vivo*. However, we were able to demonstrate that this pathway cannot serve as the only source of NAD^+ and sustain viability at physiological NAM concentrations.

Keywords: *Candida albicans,* histone H3 lysine 56 acetylation (H3K56ac), Rtt109, nicotimamide

Table of content

List of tables

List of figures

List of abbreviations

5FC	Flucytosine
a.a.	amino acid(s)
AmB	amphotericin B
ATP	adenosine triphosphate
bp	base pair(s)
Ca	*Candida albicans*
CFW	calcofluor white
CGD	*Candida* genome database
CRISPR	Clustered Regularly Interspaced Short Palindromic Repeats
DAPI	4',6-diamidino-2-phenylindole
DNA	deoxyribonucleic acid
DOXY	doxycycline
EtBr	ethidium bromide
gDNA	genomic DNA
GRACE	Gene Replacement And Conditional Expression
H3K56	histone 3 lysine 56
H3K56ac	acetylated histone 3 lysine 56
HAT	histone acetyltransferase
HDAC	histone deacetylases
HEPES	N-2-hydroxyethylpiperazine-N'-2-ethanesulphonic acid
HIV	human immunodeficiency virus
hNAM	tetra deuterated Nicotinamide
HU	hydroxyurea
ICU	intensive care unit
IPTG	isopropyl β-D-1-thiogalactopyranoside
kb	kilobase (1000 nucleotides)
kDa	kilodalton
Mb	megabases (1 million nucleotdies)

MCF	micafungin
MIC	minimal inhibitory concentration
MMS	methyl methane sulfonate
MS	mass spectrometry
NA	nicotinic acid
NaAD	nicotinic acid adenine dinucleotide
NAC	*N*-acetyl-$_{L}$-cysteine
NAD^+	nicotinamide adenine dinucleotide
NAM	nicotinamide
NAMN	nicotinic acid mononucleotide
NBD	nucleotide-binding domain
NMN	nicotinamide mononucleotide
NR	nicotinamide riboside
ORF	open reading frame
PCR	polymerase chain reaction
PI	propidium iodide
RNA	ribonucleic acid
Sc	*Saccharomyces cerevisiae*
SDS-PAGE	sodium dodecyl sulfate-polyacrylamide gel electrophoresis
SEM	standard error of the mean
WT	wild-type

Contribution of authors

Chapter 2. Relative contributions of Rtt109 and histone chaperone-dependent acetylation in the fungal pathogen *Candida albicans*

Sarah Tsao*, **Rahul Ghugari***, Paul Drogaris, Angeli Li, Nebiyu Abshriu, Pierre Thibault and Alain Verreault

RG and ST constructed all mutant strains (cloning and sequencing plasmid constructs). RG and ST designed and performed most experiments; specifically, RG performed experiments for Figure 2.2, Figure 2.3, Figure 2.4 and Figure 2.5A-B. NA and PD performed all the mass spectrometry experiments. RG and ST contributed equally to this work. RG and ST prepared all figures and wrote the manuscript with AV

Chapter 3. Canonical and non-canonical metabolic fates of nicotinamide in the fungal pathogen Candida albicans

Rahul Ghugari*, Sarah Tsao*, Mark Schmidt, Éric Bonneil, Martine Raymond, Charles Brenner and Alain Verreault

RG and ST constructed all mutant strains (cloning and sequencing plasmid constructs). RG carried out western blotting experiments and performed drug susceptibility assays (MIC and GCA assays). RG and ST designed and performed most experiments; specifically, RG performed experiments for Figure 3.2, Figure 3.3, Figure 3.4, Figure 3.5, Figure 3.6 and Figure 3.7. MS and EB performed all the mass spectrometry experiments. Mass spec data was analysed by RG. RG and ST contributed equally to this work. RG and ST prepared all figures and wrote the manuscript with AV. AV, MR and CB oversaw the work.

गुरुर्ब्रह्मा गुरुर्विष्णुर्गुरुर्देवो महेश्वरः ।
गुरु शाक्षात परं ब्रह्म तस्मै श्रीगुरवे नमः ॥१॥

Guru is verily the representative of ***Brahma***, ***Vishnu*** and **Shiva**.
He creates, sustains knowledge and destroys the weeds of ignorance.
Salutations to that Guru.

I dedicate this thesis to all my teachers,
Best of whom was my Dad

Acknowledgement

This thesis represents not only my work at the bench; it is a milestone towards which I have been working for the past decade of my life. My experience at IRIC, UdeM has been nothing short of amazing. Since my first day, I have felt at home. I have been given unique opportunities, and I have taken advantage of them. Throughout these years, I have learned that there are those who build tools and those who use them; my passion is in creating the tools used in innovative research. This thesis is also the result of many experiences I have encountered at IRIC from dozens of remarkable individuals whom I wish to acknowledge.

First and foremost I wish to thank my advisor, Professor Alain Verreault.! For his enthusiasm, guidance and unrelenting support throughout this journey. He has taught me both, consciously and unconsciously how good science is done. I also thank my co-director Professor Martine Raymond for her invaluable insights and suggestions, her moral support during the difficult times I encountered during my Ph.D. and when I was writing this thesis. I am thankful to her for teaching me the importance of critical thinking and scientific integrity.

I thank my committee members Dr. Brian Wilhelm, Prof. Luis Rokeach and Prof. Charles Brenner for their comments and encouragement but also for their hard questions that incented me to widen my research from various perspectives. Special thank you to Dr. Hugo Wurtele for providing his valuable opinion about my research chapters.

I am incredibly grateful to my colleague, mentor and friend, Dr. Sarah Tsao for her guidance, support and all the useful discussions and brainstorming sessions. I am also thankful of all the present and past members of the Verreault lab for their support and for creating an enjoyable work environment. My Colleagues and friends, Eun-hye, Sandra, Yogitha, Aline, Valarie and Dhanaraman..have all extended their support in a special way, and I have gained a lot from them, through their personal and scholarly interactions and their suggestions at various points during my doctoral journey. I am especially grateful to Swati Shetty, a true friend who was always there for a word of encouragement or listening ear.

Last but not the least; I have an amazing family, unique in many ways, and the stereotype of a perfect family in many others. Their support has been unconditional all these years; they have cherished with me every great moment and supported me whenever I needed it. Mom.. Salute you all for the selfless love, care, pain and sacrifice you did to shape my life. A big gratitude to my brother who stood by me like a rock for all these years.

Dad you are forever & always in my thoughts – you are missed

Introduction

1. Introduction

1.1. Medical relevance of fungal infections

The fungal kingdom consists of ~611,000 different species and plays an important role in maintaining the global ecosystem (Mora *et al.* 2011). Among these only small fractions of less than ~500 species are identified as human pathogens that can cause opportunistic fungal infections (Liu 2011). Plant infections resulting from fungal pathogens have presented a worldwide threat to food security in the past. Microbial adaptation to new ecosystem caused by trade and transport, and changes in climate, makes them a global challenge (Fisher *et al.* 2012; Badiee and Hashemizadeh 2014). The challenge of fungal infections on human health has not received due attention, and resulting deaths are often overlooked and misdiagnosed. This is evidenced by the fact that most public health agencies including World Health Organisation have no program on fungal infection. The only exception is U.S. Centers for Disease Control and Prevention (CDC) that has a program on mycological surveillance (Brown *et al.* 2012).

Superficial fungal infections are not life threatening and sometimes relatively easy to cure, but invasive fungal infections can be life threatening and are associated with mortality rates of 40-50% in immunocompromised patients (Pfaller and Diekema 2007; Mohr *et al.* 2008; Brown *et al.* 2012). Cases of invasive fungal infections have increased steadily in recent years due to the ever-expanding population of immunocompromised patients with prolonged hospital stays, placement of central venous catheters and treatment with broad-spectrum antibiotics (Mohr *et al.* 2008; Badiee and Hashemizadeh 2014). Advances made in organ transplantation and cancer chemotherapy have resulted in increased number of immunocompromised patients who are at risk for these infections. In the past, these patients were susceptible to bacterial infections, but new antimicrobial agent discoveries have reduced the mortalities caused by bacterial infections, making these patients at high risk of contracting invasive fungal infections (Fleming *et al.* 2002; Pfaller and Diekema 2004; Pfaller and Diekema 2007). One and half million

people are killed world-wide by invasive fungal infections every year, 90% of which are due to cryptococcosis (*Cryptococcus neoformans* and *Cryptococcus gattii*), candidiasis (*Candida* species), aspergillosis (*Aspergillus* species) and pneumocystosis (*Pneumocystis carinii*) (Pfaller and Diekema 2004; Brown *et al.* 2012).

Fifteen percent of all healthcare-associated infections are attributed to opportunistic fungal pathogens. *Candida* and *Aspergillus* species are the most commonly isolated pathogens from intensive care unit (ICU) patients who are immunocompromised. *Candida* species accounts for 70-90% and *Aspergillus* for 10–20% of all nosocomial invasive fungal infections (Vincent *et al.* 2009; Badiee and Hashemizadeh 2014; Delaloye and Calandra 2014). In conclusion, the ever-increasing pool of immunocompromised patients and external pressure from antibiotic usage is contributing to rise in invasive fungal infections proportionately to medical advances made in last three decades

1.1.1. Candidiasis

Fungal infections caused by different *Candida* species are collectively termed candidiasis (Mohr *et al.* 2008). *Candida* species are commensals in humans and generally harmless. They are part of the human microbiota and commonly found on the mucosal surfaces of gastrointestinal and genitourinary tracts, on the skin, and under fingernails (Lott *et al.* 2005; Kim and Sudbery 2011). Invasive fungal infections caused by *Candida* species vary from catheter-associated infections to widespread disseminated candidiasis (Mohr *et al.* 2008; Delaloye and Calandra 2014). Among other *Candida* species, *Candida albicans* (*C. albicans*) is predominant, accounting for almost two-thirds of all *Candida* infections (Pfaller and Diekema 2007; Delaloye and Calandra 2014). We will discuss in detail about *C. albicans* in section 1.2. Recent epidemiology of candidiasis shows a mycological

shift to non-*albicans Candida* species such as *Candida glabrata*, *Candida krusei*, *Candida tropicalis*, and *Candida parapsilosis* (Delaloye and Calandra 2014; Deorukhkar *et al.* 2014). These non-*albicans Candida* species are emerging with up to 50% of all cases of *Candida* infections attributed to them in different medical centers. The shift towards non-*albicans* species is attributed to increasing use of azole agents in the treatment of fungal infections. These non-*albicans Candida* species show intrinsic resistance (*C. krusei*) and less susceptibility (*C. glabrata*) to commonly used azole agents. Similarly, *C. parapsilosis* shows reduced susceptibility to echinocandins (Oberoi *et al.* 2012; Delaloye and Calandra 2014). However, *C. albicans* remains the single most predominant pathogen isolated from patients.

1.1.2. Aspergillosis

Aspergillus species are the cause of invasive infections in individuals with impaired immune function. Most of the opportunistic infections by *Aspergillus* species are caused primarily by *Aspergillus fumigatus (A. fumigatus)*. *A. fumigatus* spores are abundant in the environment, and commonly found in food, tap water and building surfaces (Mohr *et al.* 2008; Karkowska-Kuleta *et al.* 2009). Immunocompromised patients suffering from neutropenia, solid organ transplant recipients and patients on high-dose corticosteroids are predisposed to life-threatening invasive infections of *A. fumigatus* (Karkowska-Kuleta *et al.* 2009; Brown *et al.* 2012). *Aspergillus* species can cause allergic reactions, lung infections, superficial infection related to local injury, and invasive infections. Lung infections are most prevalent with *Aspergillus* species. Different forms of pulmonary aspergillosis consists of chronic pulmonary aspergillosis (CPA), invasive bronchial aspergillosis (IBA), invasive pulmonary aspergillosis (IPA), and allergic bronchopulmonary aspergillosis (ABPA). These different forms sometimes exhibit overlapping symptoms (Denning *et al.* 2003; Schweer *et al.* 2014). Severity and cause of pulmonary aspergillosis depends on the state of host immune system. Neutropenia is the major risk factor

in developing acute invasive forms of aspergillosis (IA). Invasive pulmonary aspergillosis (IPA) affects severely immunocompromised patients (Berenguer *et al.* 1995; Denning 1998). Despite timely diagnosis and treatment, invasive aspergillosis has a mortality rate of 50%. In case of missed or delayed diagnoses, this rate can go up to 100% (Lin *et al.* 2001; Meersseman *et al.* 2004; Mohr *et al.* 2008).

1.1.3. Cryptococcosis

Cryptococcosis is a pulmonary or disseminated infection caused by encapsulated yeast *Cryptococcus neoformans* or *Cryptococcus gatti*. Pigeon droppings and contaminated soil are the natural habitats of this fungus. Major factors that contribute to the virulence of this pathogen are the polysaccharide capsule, production of melanin, and ability of growth at high temperatures (Hamilton and Goodley 1996; Tenforde *et al.* 2017). The polysaccharide capsule provides protection against host phagocytosis mechanism and it has immunomodulatory effects. Melanin provides protection against host and other environmental stresses. *Cryptococcus* can cause infections in both immunocompromised as well as immunocompetent patients. Individuals with Human immunodeficiency virus (HIV) infection are at major risk of this infection. Lungs are the most common site of infection, but the most common clinical representation of cryptococcosis is cryptococcal meningitis (CM). Every year roughly 1 million cases with 625,000 deaths are reported of CM, majority of them occurring in sub-Saharan countries (Park *et al.* 2009).

1.2. *Candida albicans*

C. albicans is a major opportunistic fungal pathogen and model organism to study fungal pathogenesis. It has been of great interest to the scientific community due to the pathogenic nature of this fungi as well as its impact on the healthcare of immunocompromised patients worldwide. It apparently does not have environmental reservoirs and only grows in association with a mammalian host (Noble and Johnson 2007). It is commensal and resides on the skin, gastrointestinal tract and lower female reproductive tract of 70% of healthy individuals (Sobel *et al.* 1998; Kim and Sudbery 2011). Association of *C. albicans* with humans begins

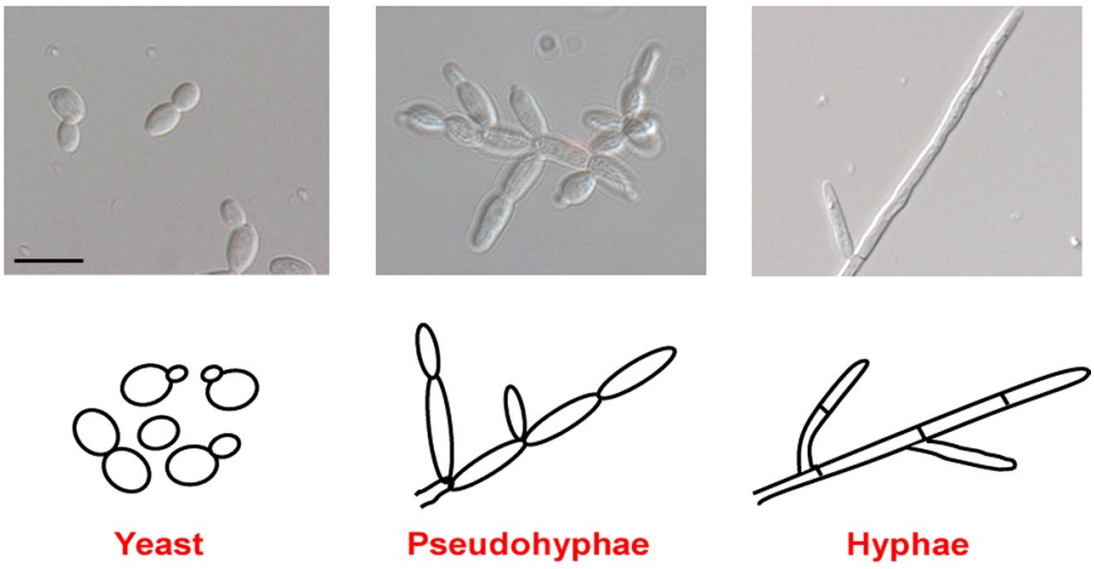

Figure 1.1 Morphologies of *C. albicans*

Morphologies of *C. albicans* cells as visualized by differential interference contrast (DIC) microscopy (bar = 10 μm). (Bottom) Schematic representation of each morphology. **(**Adapted from Thompson *et al.* 2011)

at birth while passing through the birthing canal (Ward *et al.* 2017). Depending upon growth conditions, *C. albicans* can grow in at least three different morphologies: budding yeast cell, pseudohyphal and hyphal (Fig. 1.1). Additionally, they also show opaque form (described in section 1.4.3). In laboratory conditions, *C. albicans* grows as unicellular budding yeast cells (blastoconidia) at 30°C. The yeast form consists of round or oval-shaped cells (Fig. 1.1). They multiply by producing blastoconidia, which are referred as buds. Pseudohyphae are formed when buds are linearly produced from their other cell without separating (Fig. 1.1). When yeast cells grow by extending the apex forming septa to separate the compartments, a structure called hyphae is formed (Fig. 1.1). Sometimes pseudohyphae show a variety of forms between the yeast and the hyphal form making it difficult to distinguish them from true hyphae. Pseudohyphal cells can be differentiated by constrictions at the site of the junction and their shape is ellipsoidal in contrast to hyphal cells, which have parallel sides with uniform width and septa lacking constriction (Thompson *et al.* 2011). *C. albicans* cells that are not able to switch between yeast to hyphal form or vice versa, are avirulent (Gow *et al.* 2002).

C. albicans sometimes causes superficial infections on skin and mucosa in immunocompetent healthy individuals, which are painful and unpleasant but not life-threatening. About 75% of females have at least one episode of vaginal candidiasis during their child-bearing years, and of them 10% suffer from recurrent vulvovaginal candidiasis (Sobel *et al.* 1998; Barousse *et al.* 2005). However, *C. albicans* can cause serious and life-threatening infections in individuals whose immune system is compromised. HIV-positive individuals, patients receiving transplant organ and cancer patients undergoing chemotherapy are predisposed to these infections (Berman and Sudbery 2002; Pfaller and Diekema 2004). Infections caused by *C. albicans* collectively referred to as candidiasis, which are broadly divided into two major categories, mucosal and systemic. Mucosal candidiasis can occur due to localized mucosal injuries, such as burn injury to the skin, surgical procedure or lack of oral hygiene (Peleg *et al.* 2010). These infections can be treated successfully with currently available antifungal agents. On the other hand, systemic candidiasis, which is also referred as candidemia is a life-threatening infection with

mortality rates between 30-40% (Pfaller and Diekema 2007; Mohr *et al.* 2008). In these cases *C. albicans* succeeds in entering the bloodstream by breaching the mucosal membrane and then it disseminates throughout the body, infecting several organs and causing severe and life-threatening invasive illnesses in immunosuppressed patients (Gudlaugsson *et al.* 2003). With the increase in the number of immunocompromised patients due to improvement in medical care facilities, incidences of candidemia have increased dramatically (Abu Al-Melh *et al.* 2005). A long-term epidemiological study of incidences of sepsis in the United States reported an increase of fungal related sepsis by 207% between 1979 and 2000 (Martin *et al.* 2003). Invasive candidiasis is leading cause of mortality among fungal infections, and it is the fourth leading cause of hospital-acquired bloodstream infections (Pfaller and Diekema 2007). This has put an enormous burden on healthcare expenditure; in the United States alone cost due to candidemia is estimated between $1 and $2 billion annually (Wilson *et al.* 2002).

1.2.1. *C. albicans* genetics

C. albicans is the most important fungal pathogen, and its success is attributed to its ability to adapt to a variety of different environmental conditions. It can grow in a pH range of 2.5 to 10, and it can withstand temperatures between 5°C to 46°C (Hubbard *et al.* 1986; Vylkova *et al.* 2011). The adaptive nature of *C. albicans* is in part due to the remarkable genomic plasticity and adaptability of its genome. *C. albicans* achieves genetic diversity by undergoing different events at the genome level, such as translocations, chromosome truncations and rearrangements, supernumerary chromosomes, loss of heterozygosity (LOH) and whole-chromosome aneuploidy (Noble and Johnson 2007; Selmecki *et al.* 2010). These genomic alterations give *C. albicans* selective advantage under stress. Example of this is the formation of isochromosome with two left arms of chromosome 5 as a mechanism of azole resistance. This particular segment of chromosome contains genes involved in ergosterol pathway, which is a target of azole drugs, efflux pumps

and their regulators (see section 1.3.4). This isochromosome formation is reversible in nature (Noble and Johnson 2007; Hnisz *et al.* 2009).

C. albicans is an obligate diploid with 16-Mb (haploid) genome organized into eight diploid chromosomes. It was the first pathogenic fungus whose genome was sequenced. Complete and annotated sequence of clinical isolate SC5314 was published in 2004 (Jones *et al.* 2004). As of August 2017, *C. albicans* has 6046 open reading frames (ORFs) (without dubious ORFS) of which only 1652 have been verified i.e. their functions are identified (www.candidagenome.org). Genome sequencing opened new avenues in molecular manipulation and large-scale transcriptomic and proteomic profiling studies. After the genome sequencing, functional analysis and genes characterization efforts were expedited by large-scale study designs using high-resolution tiling arrays and RNA-sequencing (Bruno *et al.* 2010; Sellam *et al.* 2010). Prior to the genome sequencing, functional studies in *C. albicans* were largely performed by reverse genetics approaches using *Saccharomyces cerevisiae* (*S. cerevisiae*) as a surrogate model. This was due to the availability of advanced functional genomics tools in budding yeast. Many of the *C. albicans* genes were characterized by complementation studies in *S. cerevisiae* (Berman and Sudbery 2002). Genetic analysis in *C. albicans* is complicated compared to other fungi for multiple reasons. *C. albicans* has an unusual codon usage; it translates the CUG codon as a serine instead of leucine (Santos *et al.* 1993). Due to this unusual codon usage, codon optimisation is necessary while performing recombinant protein expression studies in other model systems. Due to genomic plasticity, *C. albicans* shows extensive chromosome polymorphisms which result in translocations, chromosome amplifications, and deletions (Noble and Johnson 2007; Selmecki *et al.* 2010). Being a diploid organism, two rounds of allele deletions are needed to generate a null mutant, and in some cases, further verification has to be done for the absence of more alleles (Selmecki *et al.* 2010). Gene deletion phenotypes are often validated by reintroducing at least one copy of the gene at the original locus. Gene reintroduction should a least partly restore the wild-type (WT) phenotype for the attribution of gene function.

1.2.2. Genetic tools available in *C. albicans*

Compared to *S. cerevisiae,* genetic tools for gene disruption/modification to study gene function are rather limited for *C. albicans*. However, over the years, several groups have developed different techniques for gene deletion (Noble and Johnson 2007). Most studies use auxotrophic strains to perform gene deletion studies. These strains are auxotrophic for certain amino acids or bases due to deletion of genes involved in different metabolic synthesis pathways. BWP17, auxotroph for histidine, arginine, and uracil, and SN148, auxotroph for leucine, histidine, arginine, and uracil, are the most commonly used laboratory strains (Wilson *et al.* 1999; Noble and Johnson 2005). Gene deletions are performed by constructing a cassette containing an auxotrophic marker flanked by at least 100 bp of sequence homology to 5' and 3' of the gene of interest. Restored auxotrophy on drop-out selection medium confirms marker gene insertion. Further verification of gene deletion and insertion of the marker at the right locus needs to be performed by different techniques like polymerase chain reaction (PCR) and sequencing (Gola *et al.* 2003). First such strategy was the "*URA3*-blaster" which utilizes homologous recombination to replace one allele of a target gene using a *URA3* cassette. Successful transformants were selected on a drop-out medium that lacks uridine (Fonzi and Irwin 1993). The recyclable "*URA3* flipper" cassette facilitates generation of multiple gene deletions without loosing markers (Reuss *et al.* 2004). Additionally, there are two dominant selectable markers, which can be used in gene disruptions, mycophenolic acid and nourseothricin (Wirsching *et al.* 2000; Reuss *et al.* 2004).

Regulatable promoters such as tetracycline-repressible or inducible promoters facilitate conditional expression studies of essential genes (Nakayama *et al.* 2000; Park and Morschhauser 2005). The tetracyclin-repressible system allowed the creation of the GRACE library (Gene Replacement And Conditional Expression) where one copy of the gene is deleted, and another copy is placed under the control of a tightly regulatable tetracycline promoter. This library consists of 1105 *C.*

albicans genes sharing homology to known *S. cerevisiae* genes that are essential for growth. This analysis showed that only 61% those genes are essential for growth in *C. albicans* and significant non-overlap exists between two species regarding an essential set of genes (Roemer *et al.* 2003). We have used strains from GRACE collection to study the functions of essential genes for this thesis.

It was easy to make multiple gene deletions without losing any auxotrophic markers with *SAT1*-flipping cassette strategy (Reuss *et al.* 2004). The *SAT1*-flipping strategy uses recyclable dominant selection marker nourseothricin. This cassette consists of the *SAT1* marker, which confers resistance to antibiotic nourseothricin, and the *FLP* gene that encodes the site-specific recombinase Flp. The addition of flanking sequences of the gene of interest allows genomic integration of the cassette by homologous recombination. Nourseothricin-resistance confirms the integration of cassette in the genome. This cassette is bordered by direct repeats of FRT sequences, which are recognized by the Flp recombinase. Expression of *FLP* recombinase precisely removes the whole *SAT1*-fliper cassette leaving behind one copy of *FRT* site in deleted target allele. Two rounds of insertion and recycling generate a homozygous null mutant that differs from WT stain only by the absence of the gene of interest. Using *SAT1*-flipping strategy for reintroducing genes for complementation studies can also be performed (Reuss *et al.* 2004). We have used this cassette to generate double mutants and gene reintroduction successfully. However, multiple rounds of transformations required for generating double mutants and confirmation of recycling of cassette for each deletion can be time-consuming.

More recently, a CRISPR cassette for *C. albicans* has been developed which can target multiple genes and gene families (Vyas *et al.* 2015). This CRISPR cassette facilitates generation of null mutants by mutating both the copies of the gene or multiple genes at high frequency in a single transformation. (Vyas *et al.* 2015). Introduction of silent mutations in the repair template that forms a new restriction site simplifies successful clones screening among CRISPR transformants. Verification of positive clones is done by digesting the PCR product with the enzyme for which the new restriction site has been introduced. Only PCR products from positive clones are digested. This cassette uses *SAT1* marker and has shown

to be efficient with clinical isolates as well (Vyas *et al.* 2015). We used the *Candida* CRISPR system to introduce premature stop codon mutations in target genes.

1.3. Current treatment options against fungal infections

Candida bloodstream infections in ICU remain a major challenge due to limited treatment options. Development of new antifungal agents has lagged behind compared to the development of new antibacterial agents. This is evident by the fact that in the last 30 years, only one new class of antifungal agent has been developed to treat invasive fungal infections (Fig. 1.2) (Butts and Krysan 2012; Roemer and Krysan 2014). In addition, delayed treatment, drug-related toxicity and resistant strains further complicate the situation. Administration of proper antifungal agent early in the treatment is necessary to decrease the mortality associated with fungal infections (Garey *et al.* 2006; Mohr *et al.* 2008). Treatment of patients suffering from candidiasis is hampered due to their compromised immune system. There are four major classes of antifungal agents used for the treatment of candidiasis. They are polyenes, flucytosine, azoles, and echinocandins. Each one these antifungal agents have their limitations along with their advantages (Chapman *et al.* 2008; Roemer and Krysan 2014). These limitations include lack of spectrum activity, route of administration, toxicity and drug interactions. In the mjority of the times antifungal treatment failures are caused by the emergence of drug- resistant fungal cells. Broadly, resistance is divided into two types, intrinsic and acquired. Intrinsic resistance means fungal cells showing resistance to the drug that they have never exposed to such as *C. krusei* and shows intrinsic resistance to azoles. Fungal cells can also acquire resistance after exposure to the drug, which is called acquired resistance (Marie and White 2009; Maubon *et al.* 2014). As the both mammalian host and its fungal pathogen are eukaryotes, many essential biological processes are conserved, making it difficult to target only

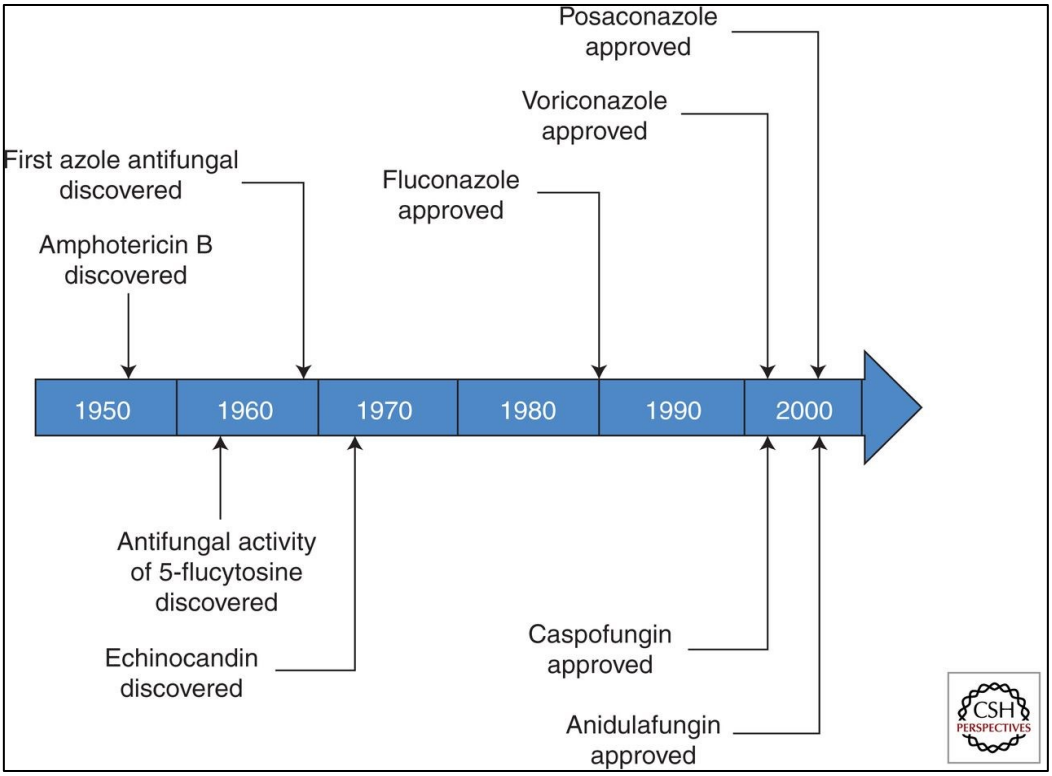

Figure 1.2 Timeline of antifungals development

(Adapted from Roemer and Krysan 2014)

the pathogen (Brown *et al.* 2012; Pierce and Lopez-Ribot 2013). The cell membrane, the cell wall, and DNA and RNA synthesis are the main targets of current drugs used to treat invasive fungal infections (Chapman *et al.* 2008; Roemer and Krysan 2014). This section describes the four major classes of antifungals currently used for this purpose with their advantages and limitations.

1.3.1. Polyenes

These are the first class of antifungals developed back in 1954. Bacterial genus *Streptomyces noursei* produces polyenes. There are several hundred different drugs

in this class, but Amphotericin B (AmB) is the most commonly used drug (Mohr *et al.* 2008; Robbins *et al.* 2016). AmB is a polyene macrolide that acts by targeting ergosterol, a major lipid in the fungal cell membrane. AmB binding to ergosterol leads to the formation of pores in the fungal cell membrane, causing cell leakage and depolarization and ultimately cell death. It is fungicidal, i.e., lethal to fungal cells and shows broad-spectrum activity against a wide variety of fungal species (Chapman *et al.* 2008; Robbins *et al.* 2016). AmB shows little intrinsic oracquired resistance. AmB treatment has been the gold standard for many decades, but large doses of AmB are associated with nephrotoxicity in the host. AmB has a strong affinity for ergosterol binding, but it also binds to cholesterol-containing membranes present in humans. This accounts for toxic effects including nephrotoxicity, anemia, anaphylaxis and infusion-related reactions in the human host (Chapman *et al.* 2008; Mohr *et al.* 2008; Robbins *et al.* 2016). There have been efforts to develop a safer alternative to AmB to minimise the toxicity to host by making lipid formulations of the drug. Lipid formulations of drug improve the drug uptake and distribution to target organs. This helps in reducing kidney concentrations of drug which minimizes nephrotoxicity, but these formulations are expensive and sometimes not available in certain regions (Day *et al.* 2013; Robbins *et al.* 2016). However, studies indicate that after using different lipid formulations of AmB for more than two decades, there is no conclusive data suggesting lipid formulations of AmB are superior to AmB (Robbins *et al.* 2016).

1.3.2. Flucytosine

Flucytosine (5FC) is a pyrimidine analog with antifungal properties that was originally discovered in 1957 as an antitumor drug (Chaudhuri *et al.* 1958). 5FC inhibits both DNA and RNA synthesis. 5FC is transported into the fungal cell by cytosine permease and converted by fungal-specific cytosine deaminase into 5-fluorouracil (5FU). 5FU metabolic product, 5-fl uorodeoxyuridine monophosphate (FdUMP) inhibits thymidylate synthase, a key enzyme in DNA synthesis. In fungal

cells, 5FU can be converted into 5-fluorouridine triphosphate (FUTP), which is incorporated into fungal RNA that affects the aminoacylation of tRNA resulting in protein synthesis inhibition (Diasio *et al.* 1978; Waldorf and Polak 1983). Human cells lack cytosine deaminase hence cannot metabolize 5FC to 5FU. 5FC is active against *Cryptococcus* species and *Candida* species, but it is ineffective against filamentous fungi such as *A. fumigatus.* A major limitation of 5FC is that it is fungistatic (arrests cell growth) leading to the rapid emergence of resistance against the drug. Thus, it is commonly used in a combination therapy with AmB rather than as a monotherapy (Vermes *et al.* 2000; Day *et al.* 2013).

1.3.3. Azoles

Azole class of antifungals target ergosterol, an essential component of cell membranes in fungi (Fig. 2D-E) (Chapman *et al.* 2008; Maubon *et al.* 2014). Ergosterol is not part of mammalian cell membranes, making azoles fungal-specific. Azoles target both cellular and mitochondrial membranes in fungi. They inhibit ergosterol biosynthesis. Azoles inhibit cytochrome P450-dependent 14α-lanosterol demethylation, leading to decrease in cellular ergosterol and accumulation of methylated toxic sterol intermediate in the fungal cells (Fig. 1.3D-F) (Chapman *et al.* 2008; Mohr *et al.* 2008; Maubon *et al.* 2014). The azole antifungals used in the clinic are classified into two groups based on number of nitrogens in their azole ring, i) the imidazoles (miconazole and ketoconazole) and, ii) the triazoles (fluconazole, itraconazole, voriconazole, and posaconazole) (Chapman *et al.* 2008; Mohr *et al.* 2008). Imidazole derivatives have complex mode of action and inhibits several membrane-bound enzymes as well as membrane lipid biosynthesis that includes cholesterol synthesis in humans. Triazoles show greater affinity for fungal cytochrome P-450 enzymes rather than mammalian enzyme, making them a better choice to treat invasive fungal infections (Ghannoum and Rice 1999; Sheehan *et al.* 1999).

Due to its broad-spectrum activity, which includes *Candida*, and *Cryptococcus,* as well as dimorphic and dermatophyte fungi, fluconazole is the most widely used first-line antifungal in the clinic to treat invasive fungal infections (Denning and Hope 2010; Robbins *et al.* 2016). Oral fluconazole is easy to administer, and it is relatively inexpensive as the patent has expired and generic versions of the drug are available. Azoles have mild side effects compared to treatment-limiting nephrotoxicity in case of patients treated with AmB (Chapman *et al.* 2008). However, azoles are fungistatic and some *Candida* species such as *C. glabrata* and *C. krusei* show intrinsic resistance to fluconazole. This frequently leads to the emergence of azole resistant strains (Pfaller and Diekema 2004; Pfaller and Diekema 2007). In addition, this class of antifungals gives rise to many drug-drug interactions. They interfere with hepatic and intestinal cytochrome P-450 enzymes, which leads to increased metabolism and reduction in blood concentration of the drug resulting in treatment failure (Chapman *et al.* 2008).

Efficacy of azoles is decreased in clinical isolates of *C. albicans* due to various mechanisms of drug resistance (Chapman *et al.* 2008; Maubon *et al.* 2014; Robbins *et al.* 2016). Mechanisms of azoles drug resistance have been studied in detail over the years. The common mechanism by which drug resistance is acquired in *C. albicans* is by target alteration. Point mutations in *ERG11* (e.g. R467K amino acid substitution) cause conformational change in the protein structure. These alterations prevent effective binding of azoles to their target without compromising its normal function (Fig. 1.3F) (Chapman *et al.* 2008; Maubon *et al.* 2014; Robbins *et al.* 2016). High intracellular concentration of Erg11 can also reduce the efficacy of the drug. *ERG11* constitutive overexpression is brought about either by gain-of-function mutations in its transcriptional activator *UPC2* or by genomic re-arrangements (Chapman *et al.* 2008; Marie and White 2009). The genome of *C. albicans* is remarkably plastic and tolerant of aneuploidies and chromosome re-arrangements (Noble and Johnson 2007; Selmecki *et al.* 2010). The genomic re-arrangements happening in the form of aneuploidy results in an increase in the copy number of chromosomes.

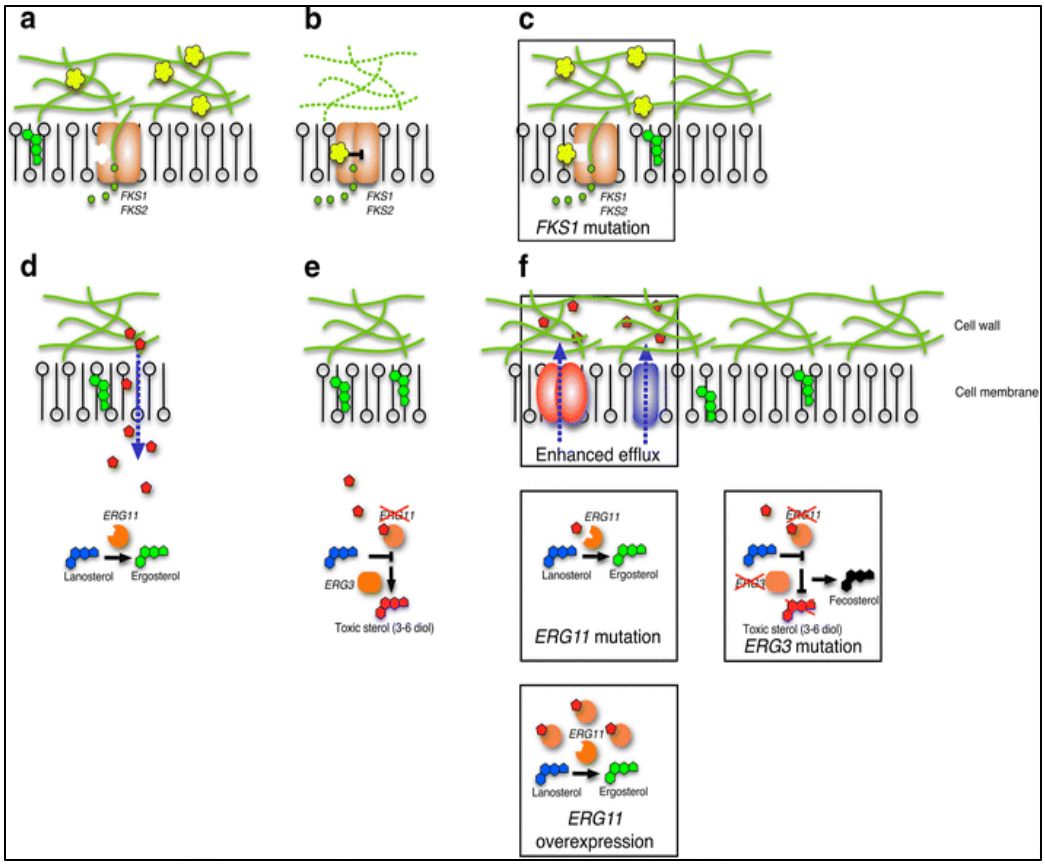

Figure 1.3 Molecular mechanisms of echinocandin and azole resistance in *C. albicans*.

A) β-1, 3-glucan synthesis in fungal membrane. B) Echinocandins inhibiting Fks1 and Fks2 blocks cell wall synthesis C) Echinocandin resistance mechanism. Mutations in *FKS1* and *FKS2* compromises drug binding. The target enzyme is less sensitive to echinocandins, allowing the production of β-1, 3-glucans. D) Ergosterol synthesis at the endosplamic reticulum and uptake of azole antifungal drugs into the cytosol of the fungal cell. E) Azole molecules inhibit the Erg11, leading to membrane ergosterol depletion and the production of toxic sterols via Erg3. F) Azole resistance due to (1) the overproduction of transporters, increasing azole efflux, (2) alteration of the target enzyme by mutations of *ERG11*, (3) Erg11 overproduction, (4) mutations of *ERG3* preventing the azole-mediated production of toxic sterols which are substituted by the non-toxic fecosterol (Adapted from Maubon *et al.* 2014)

The increase in copy number of chromosome 5, on which *ERG11* resides, is associated with the emergence of azole resistance in *C. albicans* (Selmecki *et al.* 2006; Noble and Johnson 2007; Marie and White 2009). Another mechanism frequently linked with azole drug resistance is active drug efflux leading to a

reduction in intracellular drug concentration. Overexpression of efflux pumps is often associated with drug resistance in fungi. In *C. albicans,* the transporters of ATP-Binding Cassette (ABC) and Major Facilitator Superfamily (MFS) play a significant role in azole resistance. Azole efflux is mediated by overexpression of two ABC transporters, Cdr1 and Cdr2*,* and one MFS pump Mdr1. Overexpression of the Cdr1, Cdr2, and Mdr1 efflux pumps is due to gain-of-function mutations in the transcription activators Tac1 and Mrr1, respectively (Noble and Johnson 2007; Chapman *et al.* 2008). Finally, mutations in *ERG3* create a metabolic bypass that leads to the synthesis of fecosterol, which can replace ergosterol, causing resistance to azoles (Fig. 1.3F) (Marie and White 2009; Maubon *et al.* 2014).

C. albicans acquire azole resistance by different mechanisms however; high levels of resistance are acquired by multiple mechanisms accumulating over time in fungal cells. The Center for Disease Control and Prevention (CDC) has reported fluconazole resistant *Candida* infections as a serious threat, with roughly 3,400 cases with 220 deaths (more than 7%) yearly associated with it (Http://Www.Cdc.Gov/Drugresistance/Threat-Report-2013.). To combat the *Candida* infections and menace of drug-resistant clinical isolates, we need novel therapeutic approaches (see section 1.4).

1.3.4. Echinocandins

Echinocandins are the newest class of antifungals approved by U.S. Food and Drug Administration (FDA) for intravenous (IV) therapy of invasive candidiasis. There are three echinocandins available for use in the clinic: caspofungin, micafungin, and anidulafungin (Robbins *et al.* 2016). Echinocandins disrupts fungal cell wall biosynthesis by noncompetitively inhibiting the enzyme that synthesizes β-(1,3)-glucan, the most abundant fungal cell wall component (Fig. 1.3A-C) (Denning and Hope 2010; Maubon *et al.* 2014). β-(1,3)-glucan synthase subunits are encoded by the *FKS1* and *FKS2* genes. Echinocandins are fungicidal for *Candid*a and

fungistatic for *Aspergillus* species but are not effective against *Cryptococcus* (Denning 2003; Chapman *et al.* 2008). They have little toxicity to the host and limited drug-drug interaction, making them the preferred drug for the treatment of invasive fungal infections. However, their major limitation is daily IV dosing regimens. Due to their poor oral bioavailability, they have to be administered by slow IV infusion (Denning 2003; Chapman *et al.* 2008; Robbins *et al.* 2016). Efforts are underway to synthesize orally active formulation of the echinocandin class drugs (Robbins *et al.* 2016).

Resistance to echinocandins is not due to drug efflux as they are poor substrates for drug efflux transporters. Echinocandin resistance occurs mainly by target alteration. In echinocandin-resistant *C. albicans* clinical isolates, *FKS1* and *FKS2* are found to be mutated, causing the enzyme to be less sensitive to the drug (Fig. 1.3A-C) (Chapman *et al.* 2008; Maubon *et al.* 2014). *C. neoformans* is intrinsically resistant to echinocandins despite that its glucan synthase is inhibited by echinocandins (Chapman *et al.* 2008; Marie and White 2009).

1.4. Antifungal target discovery

Development of new antifungals is more challenging than antibacterials because of differences in the cellular structure of fungi and bacteria. Bacteria being prokaryotes offer numerous targets that are unique to the pathogen. On the other hand, fungi, being eukaryotes, are closely related to human host with many biological functions conserved among them, thus making it difficult to target pathogen only (Brown *et al.* 2012; Roemer and Krysan 2014). As a result, only a few classes of antifungals are available to treat many different fungal infections. None of the available class of antifungals meet the key criteria to be an ideal antifungal agent (Chapman *et al.* 2008; Brown *et al.* 2012). The steady increase in the number of invasive infections over the years, with the emergence of other non-*albicans Candida* species highlights the shortcomings of current antifungals.

Resistance mechanisms (intrinsic and acquired) and host related side effects limit the current therapeutic options available to treat invasive fungal infections. New therapeutic approaches are needed to reduce the unacceptably high mortality rates of invasive fungal infections. Hence, there is an urgent need to develop more effective and relatively safe antifungals. This section will discuss recent advances made in identifying new targets.

1.4.1. Recent advances in identifying new targets

Finding fungal-specific targets has been an attractive idea as it limits the off-target effects in the human host. The current classes of antifungals target either the cell wall (echinocandins) or the cell membrane (azoles and polyenes). These likely represent a minor fraction of potential fungal-specific processes that can be targeted. There are several proteins currently been explored as potential drug targets to develop new therapeutic options (Lopes Da Rosa and Kaufman 2013; Robbins *et al.* 2016). There is a new paradigm that is unexploited in drug discovery regarding choosing drug targets. For instance, is it possible to target virulence factor or does it have to be protein essential for survival, making it a fungicide target? Even though essential genes remain attractive targets, genes involved in fungal virulence has their own advantages. Currently used antifungal drugs target cell viability either by killing (-cidal) or by inhibiting the growth (-static). This puts selective pressure on the pathogens that stimulate the emergence of drug- resistant strains (Clatworthy *et al.* 2007). The advantages of targeting virulence are: a) it will expand the number of potential targets for new drug discovery, b) it will preserve the host microbiome which is commensal in nature, and c) it will exert weaker selective pressure on pathogens for the emergence of drug resistance (Clatworthy *et al.* 2007). In this section, I will discuss potential drug targets that contribute to processes that affect fungal virulence as well as viability.

Eukaryotic membranes contain a variety of sphingolipids including fungal-specific glucosylceramides (GlcCer) that play a role in signal transduction, cell regulation and virulence of pathogenic fungi (Thevissen *et al.* 2007). *C. albicans* mutant for sphingolipid biosynthesis is avirulent, making sphingolipid synthesis a potential target for antifungal drug development (Noble *et al.* 2010; Robbins *et al.* 2016). The genetic study indicates that small molecule inhibitors of sphingolipid biosynthesis pathway can block fungal virulence. A screen consisting of small molecules to identify inhibitors of fungal sphingolipid GlcCer yielded two molecules that showed activity against a wide variety of fungal pathogens. However, these compounds showed poor activity against *C. albicans* (Mor *et al.* 2015).

In the quest for novel antifungal targets, the heat shock protein 90 (Hsp90) is being explored due to its role in acquired antifungal resistance (Cowen and Lindquist 2005). Hsp90 is a molecular chaperone that orchestrates a protein-folding response to drug-induced cellular stresses. Genetic inactivation or pharmacological inhibition of Hsp90 impairs emergence of azole resistance, annuls the acquired resistance and transforms azoles into a fungicidal drug (Cowen and Lindquist 2005; Cowen *et al.* 2006). Hsp90 inhibition in combination therapy with current antifungal drugs exert potent activity in broad-spectrum of fungal pathogens. (Singh-Babak *et al.* 2012; Lamoth *et al.* 2013). Hsp90 inhibition studies performed in a variety of *in vivo* infection models with fungal pathogens *C. albicans* and *A. fumigatus* have shown to abrogate virulence of the pathogen (Cowen *et al.* 2009; Shapiro *et al.* 2009; Lamoth *et al.* 2014). Hence, using inhibitors of Hsp90 as antifungals in combination with currently available drugs is a promising therapeutic treatment option to treat fungal infections.

Another fungal-specific target is the glycosylphosphatidylinositol (GPI) anchor biosynthesis pathway. GPI anchored proteins are required for the adhesion of pathogenic fungi to the human epithelium. They play a role in fungal wall biosynthesis and maintenance of homeostasis, making them a fungal-specific target (Liu *et al.* 2016). A *C. albicans gpi7* mutant, whose gene product plays a major role in GPI-anchor synthesis, shows less virulence and abnormal morphology (Richard

et al. 2002). In *A. fumigatus,* downregulation of genes involved in GPI anchor synthesis attenuates virulence and show increased cell death (Li *et al.* 2007; Yan *et al.* 2013).

Alternatively, a number of metabolites from various natural sources have been shown to inhibit pathogenic fungi. There are many different classes of these compounds ranging from furanones, quinines, cinnamodial sterols and resorcinols (Treyvaud Amiguet *et al.* 2006; Vengurlekar *et al.* 2012). Two active molecules isolated from *Pleodendron costaricense,* cinnamodial and cinnamosmolide, have shown potent *in vitro* antifungal activity against *C. albicans* (Vengurlekar *et al.* 2012). Similarly, an antimicrobial peptide (Vv-AMP1), isolated from *Vitis vinifera* (common grape vine variety), has shown broad-spectrum antifungal activity. Recombinant Vv-AMP1 alters the membrane permeability of fungal membranes (Vengurlekar *et al.* 2012).

Additionally, recent studies provided convincing evidence that chromatin regulates fungal virulence as well as fitness and targeting chromatin remodelers represents a novel therapeutic strategy (Wurtele *et al.* 2010; Lopes Da Rosa and Kaufman 2013; Kuchler *et al.* 2016), as explained in the following section.

1.4.2. Chromatin-modifying enzymes as drug targets

In eukaryotes, genetic information is stored in a nucleoprotein complex called chromatin. In eukaryotic cells, DNA is packaged into chromatin consisting of repeating units of the nucleosome. Each nucleosome is made up of 147 bp of DNA wrapped around a histone octamer composed of two histone H2A-H2B dimers and one histone (H3-H4) tetramer (Luger *et al.* 1997). The primary function of histone proteins is to package long DNA into compact nucleosome structure. Histone proteins harbor many covalent modifications to modulate their function during nucleosome assembly, transcription, genome stability and DNA repair (Allard *et al.* 2004; Millar and Grunstein 2006; Kouzarides 2007). Acetylation, methylation,

phosphorylation, ubiquitylation, and sumoylation are the major post-translational modifications (PTMs) histone proteins undergo to regulate different biological processes. These modifications indicate the expression state of chromatin, in the so-called histone code (Kouzarides 2007; Ruthenburg *et al.* 2007). This histone code is brought about by a series of "writers" and "erasers" histone-modifying enzymes. Writers are enzymes that catalyze a chemical modification of a particular residue, for example, histone acetyltransferases (HATs) that acetylate lysine residues. Erasers are enzymes that remove a chemical modification, for example, histone deacetylases (HDACs) that remove acetylation from lysine residues to restore its positive charge (Chi *et al.* 2010). There is growing evidence that these chromatin-modifying enzymes play a crucial role in fungal virulence and represent promising antifungal targets (Wurtele *et al.* 2010; Hnisz *et al.* 2011; Robbins *et al.* 2016). These enzymes contribute to the virulence of pathogen in multiple ways. Here are a few examples of chromatin remodeling enzymes and their role in pathogenicity.

The first evidence of a chromatin-modifying enzyme playing a role in the pathogenicity of *C. albicans* was the Set1 histone methyltransferase (HMT). An immunological screen performed with *C. albicans* proteins recognized by sera from HIV-positive patients suffering from oral candidiasis identified immunogene Set1 (Raman *et al.* 2006). Set1 mono-, di-, or tri-methylates histone 3 lysine 4 (H3K4), a modification associated with active gene transcription and DNA damage resistance (Faucher and Wellinger 2010; Guillemette *et al.* 2011). *C. albicans* cells lacking Set1 lose H3K4 methylation and cannot adhere to mammalian cells *in vitro*. *set1* null mutants failed to colonize different organs and cause mortality in murine systemic candidiasis (Raman *et al.* 2006).

The multi-subunit complex, SWI/SNF is a chromatin-remodeling complex that promotes transcription of inducible genes. SWI/SNF complex provides transcription machinery access to DNA by sliding the nucleosomes (Cote *et al.* 1994; Kwon *et al.* 1994). This complex plays a role in virulence of *C. albicans*. The SWI/SNF complex facilitates transcription of hyphae-specific genes. Mutants of *SWI1* or *SNF2* that encode DNA binding/transcription co-activator and ATPase subunits, respectively, abrogate pathogenicity of *C. albicans* in a murine model of

systemic candidiasis. These mutants fail to express hyphae-inducing genes resulting in loss of pathogenicity (Mao *et al.* 2006).

Among other, chromatin remodeling enzymes HATs and HDACs have been extensively studied for their role in fungal virulence (Wurtele *et al.* 2010; Lopes Da Rosa and Kaufman 2013; Kuchler *et al.* 2016; Robbins *et al.* 2016).

1.4.3. HATs and HDACs as target for new therapeutic strategies

Recent studies indicate that several HATs and HDACs regulate fungal virulence traits and drug resistance by modulating the histone acetylation profile in *C. albicans* (Lopes Da Rosa *et al.* 2010; Wurtele *et al.* 2010; Hnisz *et al.* 2011; Nobile *et al.* 2014; Roemer and Krysan 2014; Kuchler *et al.* 2016). The *C. albicans* genome encodes eight putative HATs and twelve HDACs that are evolutionarily conserved among fungal species (Kuchler *et al.* 2016). These HATs and HDACs play a crucial role in the chromatin-mediated transcriptional regulation of a variety of biological processes that are essential for fungal cells (Hnisz *et al.* 2009; Hnisz *et al.* 2011). Here are few examples of HATs and HDACs playing a role in fungal virulence and fitness.

C. albicans can switch between two morphologies, which can be distinguished by colony size, shape, and color. This system is referred as white-opaque switching. In "white" phenotype *C. albicans* forms white and hemispherical colonies, whereas in "opaque" phenotype they form large, flat and opaque colonies (Slutsky *et al.* 1987). White round colonies are made up of round cells, and opaque flat colonies are made up of elongated cells. This difference in colony shape is due to the cell shape and volume (Slutsky *et al.* 1987). White and opaque cells show strikingly different properties for various traits including mating competency, virulence, and niche specificity, but they have the same genome. Interestingly, only opaque cells are mating-competent whereas white cells are mating-incompetent (Miller and Johnson 2002; Lohse and Johnson 2009; Mallick *et al.* 2016). White and opaque cells show increased virulence depending upon the site of infection. This white- opaque

switching is regulated by multiple transcriptional feedback loops that are conserved over generations. The Set3/Hos2 HDAC complex regulates phenotypic switching in an H3K4 methylation-dependent manner (Hnisz *et al.* 2009; Morschhauser 2010). Moreover, the role of the Rtt109 HAT and the Hst3 HDAC is also well established in the regulation of white-opaque switching (Stevenson and Liu 2011). Gcn5 is a conserved HAT that is responsible for the acetylation of several lysine residues on histones. *C. albicans* cells lacking Gcn5 show decreased virulence. A recent review by Kuchler *et al*. 2016, summarises the role of different HATs and HDACs in *C. albicans* fitness and virulence, making a strong case to utilize them as targets for novel antifungal drug development. One particular histone modification that has been characterized in our lab is acetylation and deacetylation of lysine 56 of histone H3 (H3K56), which can be exploited as a potential target for drug discovery (Wurtele *et al.* 2010).

Acetylation and deacetylation of histone proteins is a very crucial PTM in the regulation of gene expression. Acetylation and deacetylation is tightly regulated by specific HATs and HDACs respectively. In *S. cerevisiae* during the S-phase of the cell cycle, all the newly synthesized histones that are deposited throughout the genome are acetylated at H3K56 (H3K56ac). Lysine 56 is deacetylated from the majority of histone H3 molecules during G2 or M phase in the absence of any DNA damage, thus making acetylation and deacetylation of H3K56 a feature of yeast cell cycle (Masumoto *et al.* 2005; Schneider *et al.* 2006; Tang *et al.* 2008). H3K56ac is an abundant PTM also found in *C. albicans*. In *C. albicans*, enzymes that have fungal- specific properties regulate H3K56 acetylation and deacetylation. It is acetylated by the HAT Rtt109 and deacetylated by HDAC Hst3 (Fig. 1.4). Both hypo- or hyper- acetylation of H3K56 resulting from the inhibition of these enzymes led to the accumulation of spontaneous DNA damage, growth defects and reduced virulence in *C. albicans* (Lopes Da Rosa *et al.* 2010; Wurtele *et al.* 2010).

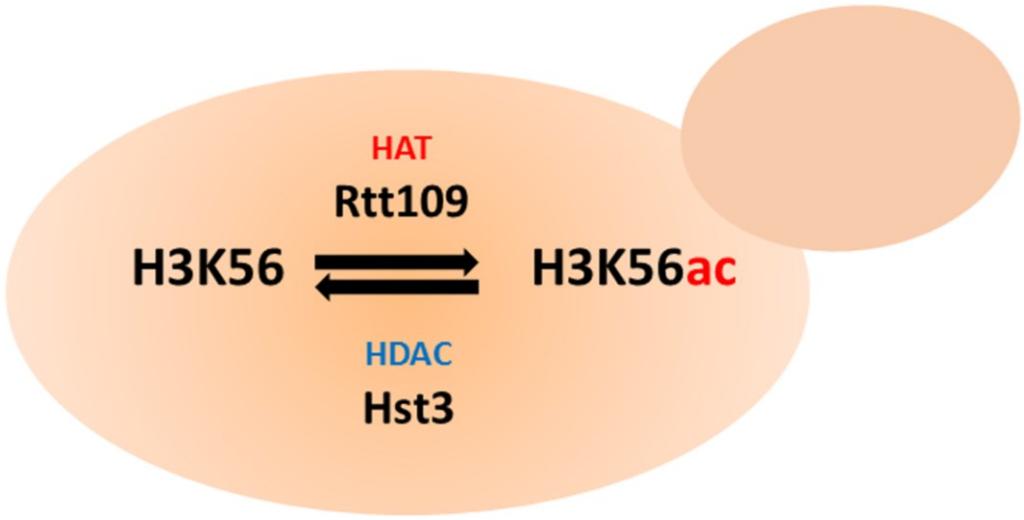

Figure 1.4 Acetylation and deacetylation of Histone H3 lysine 56 (H3K56)

In *C. albicans* acetylation of H3K56 is a reversible post-translational modification (PTM). It is carried out by histone acetyltransferase (HAT) Rtt109 and it is deacetylated by histone deacetylase (HDAC) Hst3.

Asynchronously growing *C. albicans* cells have 20-27% of all histones H3 acetylated at lysine 56. In humans, only about 0.03% of histones H3 are acetylated at H3K56. This clearly indicated that H3K56ac is not a feature of the human cell cycle and makes it an appealing target for developing novel antifungal therapy (Wurtele *et al.* 2010; Drogaris *et al.* 2012).

1.4.3.1. H3K56 acetylation pathway as a target

Histone post-translation modifications are often associated with gene expression, but they also play an important role in DNA damage checkpoint signaling and DNA repair (Allard *et al.* 2004; Moore and Krebs 2004). One such example is H3K56ac brought by HAT Rtt109 (Repressor of Ty-1 Transposition 109). Rtt109 is a unique HAT that does not have sequence homology with other HATs outside the fungal kingdom (Schneider *et al.* 2006). Detailed bioinformatics analysis revealed that

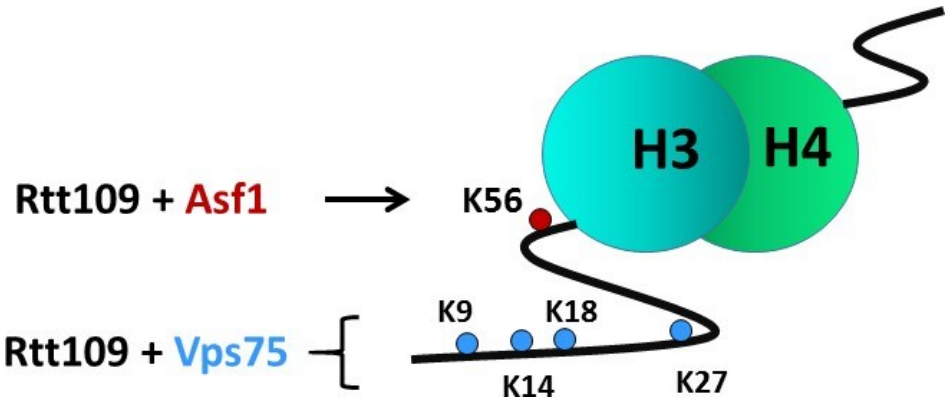

Figure 1.5 Rtt109 site specificity in *S. cerevisiae*

HAT Rtt109 needs co-factors for its catalytic activity. Rtt109-Asf1 exclusively acetylates H3K56 residue. Rtt109-Vps75 acetylates different N-terminal sites on histone H3 (K9, K14, K18 and K27).

Rtt109 is highly diverged relative to mammalian HAT p300 that does not share its catalytic activity and site specificity. Studies from *S. cerevisiae* showed that Rtt109 requires two cofactors, Asf1 or Vps75, for its catalytic activity and site specificity (Tang *et al.* 2008; D'arcy and Luger 2011; Abshiru *et al.* 2013). Rtt109, together with co-factor Asf1, is the sole HAT responsible for H3K56ac (Fig. 1.5). On the other hand, Rtt109-Vps75 acetylates different sites on the N-terminal tail of H3, namely K9, K14, K23 and K27 (Fig. 1.5) (Wurtele *et al.* 2010; D'arcy and Luger 2011; Abshiru *et al.* 2013). Deletion of *RTT109* or a point mutation of H3 lysine 56 residue into an amino acid that cannot be acetylated renders hypersensitivity to genotoxic stress and DNA damaging agents (Tang *et al.* 2008). This implies an essential role of Rtt109 in genome stability and DNA damage response to genotoxic agents. *rtt109* null mutant completely lacks H3K56ac in *C. albicans.* Deleting *RTT109* in *C. albicans* strikingly reduces mortality in a mouse model of systemic candidiasis and show reduced fungal loads in heart and kidney compared to wild-type (WT) strains (Lopes Da Rosa *et al.* 2010; Wurtele *et al.* 2010). Notably, *rtt109* mutant cells cannot colonize the kidneys during acute or prolonged infections. Loss of Rtt109 renders *C. albicans* cells susceptible to macrophages compared to WTcells (Lopes Da Rosa *et al.* 2010). In *C. albicans*, Rtt109 and H3K56ac provide

protection from genotoxic stress which is essential to survive phagocytosis by macrophages (Lopes Da Rosa and Kaufman 2013). Thus, inhibition of Rtt109 represents a novel strategy for the development of new antifungal therapies. Previous studies to find inhibitors of Rtt109 in cell-free high-throughput assays yielded only one compound that showed inhibitory activity against Rtt109 *in vitro* (Dahlin *et al.* 2013; Lopes Da Rosa *et al.* 2013). However, these assays were performed using the *S. cerevisiae* Rtt109 complex. The activity of this compound against *C. albicans* Rtt109 HAT complex has never been tested. Rtt109 HAT activity and its site specificities together with its co-factors are not studied in *C. albicans.* In Chapter 2, we studied the catalytic activity of Rtt109 and its dynamic interaction with Asf1 and Vps75 in *C. albicans.*

1.4.3.2. NAD^+-dependent HDAC Hst3

As previously mentioned, H3K56ac is removed genome-wide by the Hst3 HDAC in *C. albicans* (Fig. 1.4). (Wurtele *et al.* 2010). Hst3 belongs to a class of HADCs called sirtuins that depends on NAD^+ for its action. Sirtuins are evolutionarily conserved from bacteria to humans, with more than 60 homologues found in bacteria, plants, invertebrates and vertebrates. However, the Hst3 orthologues that deacetylate histone H3K56 exhibit fungal-specific properties. Fungal Hst3 members have conserved sequence motifs that human sirtuins lack, making them potential targets for antifungal drug development (Frye 2000; Schemies *et al.* 2010; Wurtele *et al.* 2010). Sirtuins mediated deacetylation reaction is coupled to NAD^+ hydrolysis. In deacetylation reaction, one NAD^+ molecule is cleaved into ADP-ribose and nicotinamide (NAM) per acetyl group removed from lysine. This removed acetyl group is transferred to the ADP-ribose moiety, forming the product 2-O-acetyl-ADP-ribose (Fig. 1.6) (Sauve *et al.* 2001; Tanny and Moazed 2001). NAM, which is a reaction product of sirtuins catalyzed deacetylation reaction, can

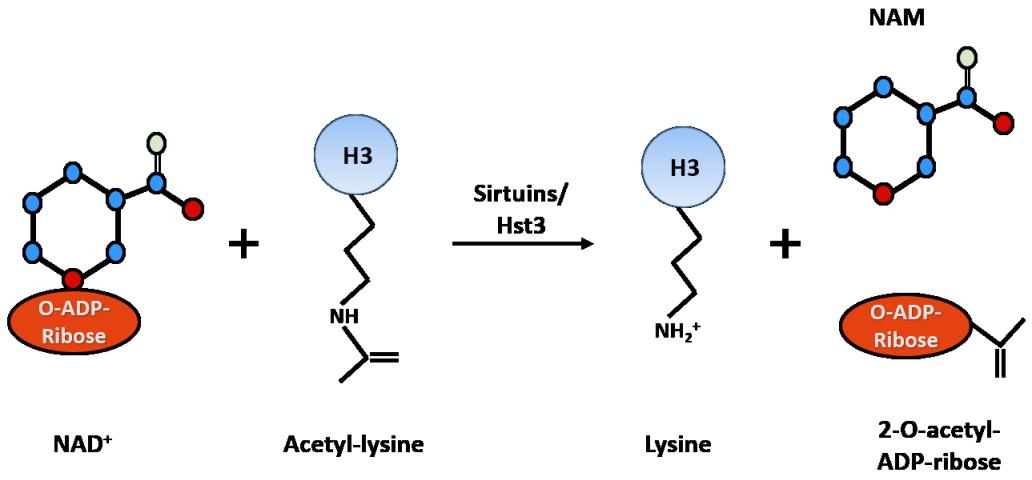

Figure 1.6 NAD^+-dependent sirtuins/Hst3 deacetylation reaction

Hst3 belongs to a class of NAD^+-dependent lysine deacetylases called sirtuins. During the reaction, acetyl group is transferred to ADP-ribose moiety and NAM is released.

also inhibit the reaction making it endogenous inhibitor (Sauve *et al.* 2001; Tanny and Moazed 2001). *HST3*, which encodes the sole HDAC responsible for deacetylation of H3K56, is an essential gene in *C. albicans*. Inhibition of *HST3* by conditional gene repression in *C. albicans* leads to hyperacetylation of H3K56 followed by cell death associated with histone degradation, abnormal filamentous growth, and DNA damage. In a mouse model of *C. albicans* infection, *HST3* downregulation showed reduced virulence. Pharmacological inhibition of Hst3 with NAM phenocopies the effect of *HST3* conditional repression. *C. albicans* cells treated with NAM showed H3K56 hyperacetylation followed by cell death associated with histone degradation, DNA damage and abnormal filamentous growth (Wurtele *et al.* 2010). With this background, we decided to study the metabolic fate of NAM to enhance its potential as an antifungal agent.

1.4.4. Nicotinamide (NAM) – a potential antifungal agent

An ideal antifungal agent to treat invasive fungal infections should meet the following criteria. 1) It should target a fungal-specific enzyme or pathway, resulting in minimal side effects in the human host. 2) It should be fungicidal, therefore the chances of emergence of drug-resistant clones could be lower. 3) It should have limited drug-drug interactions. Drug-drug interactions can decrease absorption or increase the drug metabolism, resulting in low blood and tissue concentrations. This can lead to treatment failure. 4) An easy mode of administration and stability are added advantages (Chapman *et al.* 2008; Mohr *et al.* 2008). These considerations are important, as invasive fungal infections occur in patients undergoing cancer chemotherapy, HIV AIDS patients, and patients suffering from neutropenia. These patients are typically very ill, with an already weakened immune system. As discussed in section 1.3, none of these currently available drugs meet all those criteria. Hence, it is essential to find an antifungal agent that satisfies the key criteria.

Previous studies have shown that NAM is fungicidal and exerts its effect through inhibition of Hst3 resulting in hyperacetylation of H3K56. Deleterious effects of NAM through hyperacetylation of H3K56 is evidenced by the fact that *rtt109* null mutants are resistant to NAM treatment (Wurtele *et al.* 2010). NAM is a form of vitamin B3, an FDA approved food supplement that is not toxic to humans. Dosage up to 6 g/day for extended periods have shown a low incidence of side effects in clinical trials for various human conditions (Knip *et al.* 2000; Wurtele *et al.* 2010; Mackay *et al.* 2012; Libri *et al.* 2014). NAM also inhibited the growth of azole- or echinocandin-resistant *C. albicans* clinical isolates as well as non-*albicans* species *C. krusei*. It was effective against medically relevant and non-*Candida* species *A. fumigatus,* showing a broad-spectrum activity against different pathogenic fungi. In a mouse model of fungal infection, mice injected with NAM showed lower fungal kidney loads (Wurtele *et al.* 2010). Thus, NAM meets the key criteria to be an ideal antifungal agent. However, NAM inhibits the growth of *C. albicans* in the millimolar range, and its pharmacokinetics issues limit its use in therapy (Knip *et*

al. 2000). NAM is a vitamin, and it is ingested quickly and circulated into the blood and is rapidly cleared from all tissues. It reaches its peak plasma concentration in humans within 1 hour of ingestion. NAM has a high hepatic extraction rate that reduces its concentration in circulation (Knip *et al.* 2000; Libri *et al.* 2014).

1.4.4.1. NAD^+ metabolism in fungi

We propose that better understanding NAM metabolism in *C. albicans* could increase its potential as a therapeutic agent. NAM is a precursor of nicotinamide adenine dinucleotide (NAD^+) in cells. NAD^+ is essential for cell viability in yeast and human cells. Numerous enzymes use NAD^+ and its reduced form NADH as coenzymes in redox reactions. NAD^+ serves as a substrate for three large groups of enzymes: ADP-ribosyltransferases, cyclic ADP-ribose synthetases, and sirtuins (Bogan and Brenner 2008; Canto *et al.* 2015). In *S. cerevisiae,* there are two major ways to generate NAD^+. The *de novo* pathway to generate NAD^+ starts from tryptophan, and with the help of six enzymes (catalyzed by Bna1-2, and Bna4-7), reaches nicotinic acid mononucleotide (NaMN) (Fig. 1.7) (Bogan and Brenner 2008). The salvage pathway starts from any one of the forms of vitamin B3. There are three forms of vitamin B3: NAM, nicotinic acid (NA), and nicotinamide riboside (NR) (Bieganowski and Brenner 2004; Bogan and Brenner 2008). Salvage of NAM, NA and NR can also generate NaMN. NAM is converted into NA by a fungal-specific nicotinamidase, Pnc1 (Fig. 1.7) (French *et al.* 2010). NA imported from the environment or generated by the action of Pnc1 is converted into NaMN by nicotinic acid phosphoribosyltransferase, Npt1 (Fig. 1.7) (Bieganowski and Brenner 2004; Bogan and Brenner 2008). NR joins NAM salvage pathway by nucleoside splitting activities of Pnp1, Urh1 and Meu1 (Tempel *et al.* 2007;Bogan and Brenner 2008). NR can be phosphorylated by the action of nicotinic acid riboside (Nrk1) into nicotinamide mononucleotide (NMN) (Fig. 1.7) (Bieganowski and Brenner 2004; Bogan and Brenner 2008). Conversion of NR into NMN can be reversed by 5'-nucleotidase activities of Sdt1 and Isn1 (Tempel *et al.* 2007). Nicotinic acid mononucleotide adenylyltransferase 1-2 (Nma1 and Nma2) can

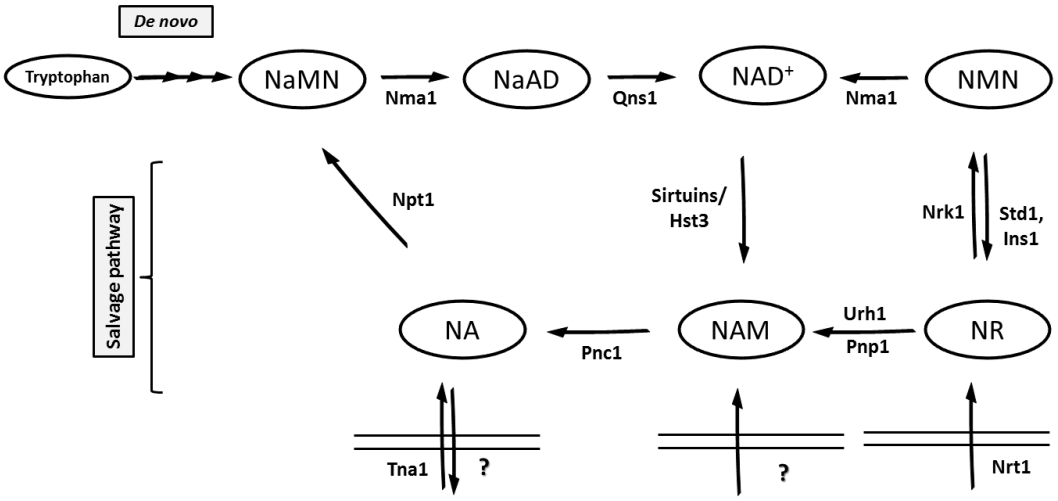

Figure 1.7 Fungal NAD^+ biosynthesis pathway

S. cerevisiae enzymes involved in this pathway are listed. In fungi, NAD^+ can be synthesized via two pathways, *de novo* and *salvage*. The *de novo* pathway starts from tryptophan and in six enzymatic steps (gene products of Bna1-2 and Bna4-7) it is converted into NaMN. The products of Nma1/2 adenylates NaMN to NaAD. Further, NaAD is converted into NAD^+ by glutamine-dependent NAD^+ synthetase Qns1. NAD^+ can also be generated by the *salvage* of either NAM, NA, or NR. NAM is converted to NA by nicotinamidase Pnc1. Npt1, phosphoribosyl transferase converts NA into NaMN. NR can be converted to NMN by Nrk1, which is then converted into NAD^+ by gene products of Nma1/2. NAM is produced as a reaction product of sirtuin-mediated NAD^+ dependant deacetylation reaction. NAM can also be generated in two steps from NMN. First NMN is converted into NR by 5'-nucleotidase Sdt1/Isn1 then resulting NR is converted into NAM by the second salvage pathway route by the gene products of Pnp1/Urh1/Meu1.

adenylate NaMN and NMN into nicotinic acid adenine dinucleotide (NaAD) and NAD^+ respectively. Qns1, a glutamine-dependent NAD^+ synthetase, converts NaAD to NAD^+ (Fig. 1.7) (Bieganowski and Brenner 2004; Bogan and Brenner 2008). NAD^+ is broken down into NAM and 2-O-acetyl-ADP-ribose by the activity of sirtuins (Fig. 1.7) (Sauve *et al.* 2001).

NAD^+ metabolism pathway and genes involved in it are not characterized in *C. albicans.* A better understanding of NAM metabolism and genes involved in NAD^+ biosynthesis might provide additional targets for antifungal therapy. In Chapter 3, we have studied the metabolic fate of NAM in *C. albicans,* using genetic and mass spectrometry approaches.

1.5. Thesis rationale, hypotheses and objectives

Invasive fungal infections constitute a pressing global health challenge. High mortality rates associated with invasive fungal infections are partly due to the limitations of currently available drugs. Despite the availability of different classes of drugs to treat these infections, mortality rates remain high and the problem of resistance is persistent. Treatment of these infections puts an enormous burden on healthcare expenses. Therefore, there is an urgent need for better therapeutic options to treat invasive fungal infections. Regarding the development of new therapeutic avenues, a major challenge is to find fungal-specific targets, which can limit the toxic side effects to the human host. Promising advances are made in the field to improve the current drugs, to overcome their limitations and to find novel targets for antifungal drug discovery.

Enzymes modulating fungal-specific post-translational modifications that play a crucial role in the virulence of pathogen can be potential targets for developing new antifungal strategies. Acetylation and deacetylation of lysine 56 residue on histone H3 are an important post-translational modification that has been shown to be essential for the virulence of *C. albicans*. This modification is a feature of the fungal cell cycle but not of mammalian cell cycle hence an ideal target for antifungal drug discovery. Both hypo- and hyper- acetylation of H3K56 leads to accumulation of DNA damage, growth defects and reduced virulence in *C. albicans*. HAT Rtt109 that shows fungal-specific properties is responsible for this modification. Most of the knowledge of Rtt109 HAT complex comes from studies performed in *S. cerevisiae*, however relying on a surrogate model for studying *C. albicans* pathway poses obvious limitations. We wanted to study *C. albicans* Rtt109 HAT complex using genetic, biochemical and mass spectrometry approaches. We proposed that a better understanding of Rtt109 HAT complex, both *in vivo* and *in vitro,* and its interaction with its co-factors in the modulation of H3K56ac in *C. albicans* could assist in developing more targeted screen designs for finding novel inhibitors of this fungal-specific pathway. Our objectives are to study the catalytic mechanism of Rtt109, study its co-factors Asf1 and Vps75, and their relative contribution in

promoting H3K56ac in *C. albicans*

Previous studies have shown that NAM at sufficiently high concentration inhibits the essential enzyme Hst3, which is a NAD^+-dependent HDAC that exhibits fungal-specific properties. Hst3 inhibition with NAM results in hyper-acetylation of H3K56 followed by cell death. NAM meets the key criteria of an effective antifungal agent. NAM is FDA approved food supplement that has been tested in clinical trials for various human conditions at high doses without any side effects. Physiological conditions when intracellular NAM levels are high will interfere with the activity of Hst3 resulting in H3K56 hyperacetylation associated phenotypes. Therefore, we anticipated that a better understanding of NAM metabolism in *C. albicans* would enhance its therapeutic potential. Studying the fate of NAM in *C. albicans* cells might provide additional fungal-specific targets that will increase its therapeutic efficacy. We want to study the NAM metabolism in WT and mutant strains that lack enzymes involved in NAD^+ biosynthesis in *C. albicans* using a combination of quantitative mass spectrometry and genetic tools. Our objectives are to study genes involved in NAD^+ biosynthesis and understand the metabolic fate of NAM in *C. albicans*.

Chapter 2

Rtt109-dependent and chaperone-assisted histone acetylation in the fungal pathogen *Candida albicans*

Rtt109-dependent and chaperone-assisted histone acetylation in the fungal pathogen *Candida albicans*

Running title: Histone chaperones and Rtt109-mediated acetylation in *C. albicans*

Sarah Tsao[1,*], **Rahul Ghugari[1,2,*],** Paul Drogaris[1], Nebiyu Abshiru[1,3], Angeli Li[1], Hugo Wurtele[4,5], Pierre Thibault[1,3], and Alain Verreault[1,6#]

[1] Institut de Recherche en Immunologie et Cancérologie, Université de Montréal, C.P. 6128, Succursale Centre-Ville, Montréal, QC, H3C 3J7, Canada
[2] Programme de Biologie Moléculaire, Université de Montréal, C.P. 6128, Succursale Centre-Ville, Montréal, QC, H3C 3J7, Canada
[3] Département de Chimie, Université de Montréal, C.P. 6128, Succursale Centre-Ville, Montréal, QC, Canada, H3C 3J7
[4] Maisonneuve-Rosemont Hospital Research Center, 5415 L'Assomption Boulevard, Montreal, H1T 2M4, Canada.
[5] Department of Medicine, Université de Montréal, P.O. Box 6128, Succursale Centre-ville, Montreal, H3C 3J7, Canada.
[6] Département de Pathologie et Biologie Cellulaire, Université de Montréal, C.P. 6128, Succursale Centre-Ville, Montréal, QC, Canada, H3C 3J7

* These authors contributed equally to this work.

Corresponding author:
Alain Verreault, Institut de Recherche en Immunologie et Cancérologie, Université de Montréal, C.P. 6128, Succursale Centre-Ville, Montréal, QC, H3C 3J7, Canada.
Phone: (514) 343-6816. Fax: (514) 343-5839. E-mail: alain.verreault@umontreal.ca

2.1 Abstract

Candida albicans is an opportunistic fungal pathogen that is harmless to healthy individuals but causes life-threatening systemic infections in individuals with a crippled immune system. Previous studies showed that histone H3 lysine 56 (H3K56) acetylation is an abundant mark of newly synthesized histones that plays an important role in response to DNA damage and promotes virulence in *C. albicans.* In *Saccharomyces cerevisiae,* Rtt109 is an acetyltransferase whose activity and substrate specificity is dictated by the histone chaperones Asf1 and Vps75; Rtt109 and Asf1 act in a concerted fashion to acetylate H3K56, whereas the Rtt109-Vps75 complex acetylate N-terminal lysine residues of H3. *C. albicans* possesses homologues of ScAsf1 and ScVps75 that have not yet been studied. In contrast to budding yeast, we find that *C. albicans* cells lacking CaVps75 exhibit lower levels of H3K56ac than wild-type cells; we also provide evidence that the CaRtt109-Vps75 holoenzyme directly acetylates H3K56 *in vitro* and that CaRtt109 is destabilized in the absence of CaVps75 *in vivo*. In striking contrast to the mild phenotypes of CaVps75-deficient cells, conditional repression of the *CaASF1* gene resulted in chromatin structural defects and loss of viability. Thus, independently of assisting CaRtt109 promote acetylation of H3K56, CaAsf1 plays an essential role in the maintenance of chromosome integrity that was unsuspected from studies of other fungal species such as *S. cerevisiae* and *S. pombe*.

2.2 Introduction

Fungal infection and global health concern

Serious fungal diseases kill more than 1.5 million people globally every year, more than malaria and similar to the tuberculosis death toll (Bongomin *et al.* 2017), http://www.life-worldwide.org/). Steadily increased number of immunocompromised patients, such as those undergoing chemotherapy or infected with HIV are the major drivers of fungal infections in both developed or developing countries. *Candida, Aspergillus* and *Pneumocystis* species remain the fungal pathogens responsible for majority of cases of serious fungal infections. Current antifungal therapy is often limited by the emergence of drug-resistant strains or high toxicity side effects, underscores the unmet medical need for a safe and cross-species therapeutic strategy. In line with this, recent antifungal drug development research has been focusing on targeting essential molecular mechanisms that are common across the fungal kingdom and responsible for fungal virulence and viability (Kuchler *et al.* 2016; Robbins *et al.* 2016).

Studying of fungal chromatin for new antifungal target discovery

In all eukaryotes, DNA is compacted into chromatin containing histone proteins. Chromatin has been seen as an instructive DNA scaffold that respond to cellular cues to dynamically modulate the access of DNA, such as DNA replication, repair and transcription. Appropriate regulation of chromatin is therefore crucial for many cellular events, stress responses and cell growth. Histone lysine acetyltransferases (HATs) and lysine deacetylases (HDACs) catalyze the addition or removal of acetyl groups from the ε-amino group of lysines. These post-translational modifications on histones subsequently result in changes in chromatin structure, followed by diverse downstream cellular consequences (Lopes Da Rosa and Kaufman 2012; Dahlin *et al.* 2014). Recent studies have shown that modulating the activity of fungal HATs and/or HDACs resulted in reduced virulence and growth of *C. albicans*, as well as decreased their tolerance and resistance to existing antifungal drugs (Wurtele *et al.* 2010; Lopes Da Rosa and Kaufman 2012; Garnaud *et al.* 2016; Kuchler *et al.* 2016; Robbins *et al.* 2016).

Broad spectrum HDAC inhibitor trichostatin-A (TSA) has been shown to sensitize *C. albicans* to azoles (Smith and Edlind 2002; Garnaud *et al.* 2016). This agent inhibits the upregulation of *ERG* genes (encoding azole targets) and *CDR/MDR* genes (encoding multidrug transporters) in *C. albicans* cells treated with azoles (Smith and Edlind 2002). It has also been demonstrated that addition of TSA inhibits *C. albicans* classes I and II HDACs (Rpd3, Hos2 and Hda1) (Hnisz *et al.* 2010; Kuchler *et al.* 2016) and remarkably, phenocopies pharmacological inhibition of Hsp90 in numerous *Candida* species (Robbins *et al.* 2012; Li *et al.* 2017). Hsp90 is a central molecular chaperone that governs drug resistance, morphogenesis and virulence in *C. albicans* (O'meara et al. 2017). Targeting Hsp90 function is a promising strategy in combinational therapy as it orchestrates crucial cellular responses to drug-induced stresses in fungi (Robbins *et al.* 2016). Recently, a more selective, fungal-specific Hos2 HDAC inhibitor has been developed, MGCD290 (Mirati Therapeutics, San Diego, CA), that is currently in clinical trial as a potent synergen with the two major classes of antifungal agents, azoles and echinocandins against a broad range of fungi (Pfaller *et al.* 2009; Pfaller *et al.* 2015).

Targeting histone H3K56ac levels

Previously we and others demonstrated that a coordinated maintenance of histone H3 lysine 56 acetylation (H3K56ac) levels is important for *C. albicans* cell growth, virulence and morphogenesis (Lopes Da Rosa *et al.* 2010; Wurtele *et al.* 2010; Stevenson and Liu 2011). The function of H3K56ac was first identified and intensively studied in the model yeast *Saccharomyces cerevisiae,* all newly synthesized histone H3 molecules are acetylated at H3K56 by *S. cerevisiae* Rtt109 (ScRtt109) (Driscoll *et al.* 2007; Han *et al.* 2007a). Following their acetylation, new H3 molecules are deposited onto DNA throughout the genome during DNA replication (Masumoto *et al.* 2005). As the cell cycle progresses into the G2/M phase, H3K56ac is removed by the NAD^+-dependent histone deacetylases Hst3 and Hst4 (Masumoto *et al.* 2005; Celic *et al.* 2006). In *C. albicans*, conditional repression of Hst3 results in the accumulation of H3K56ac to a toxic level accompanied by excessive spontaneous DNA damage; these cells were observed

with aberrant morphology comparable to that of genotoxic stress-induced filamentous cells with perturbed cell cycle progression (Shi *et al.* 2007; Wurtele *et al.* 2010). Hst3 is a member of the class III HDAC, a nicotinamide adenine dinucleotide (NAD^+)-dependent sirtuin that couples lysine deacetylation to NAD^+ hydrolysis. The deacetylation reaction produces nicotinamide (NAM), which itself could inhibit sirtuin activity. Indeed, we previously reported that NAM could inhibit cell growth through inhibition of Hst3-mediated H3K56 deacetylation and diminishes *C. albicans* virulence in mice (Wurtele *et al.* 2010). Similar inhibitory effects have also been observed in a wide range of fungal species, including drug-resistant *C. albicans* clinical strains and *Aspergillus* species (Wurtele *et al.* 2010). NAM is a form of vitamin B3 that is quickly metabolized to NAD^+ *in vivo* (Sauve 2008), therefore, it remains to be evaluated if NAM could provide therapeutic benefit against fungal infections by effectively targeting fungal Hst3 in clinical trials.

Targeting fungal HAT Rtt109 as a new antifungal strategy

Targeting Rtt109 HAT responsible for H3K56ac for antifungal drug discovery has also been established with strong biological rationale. First, H3K56ac is an important histone PTM involved in nucleosome assembly. H3K56ac quantitatively marks all newly synthesized histones in the model yeast *Saccharomyces cerevisiae*, stimulating their association with nucleosome assembly proteins that deposit them onto DNA throughout the genome during DNA replication (Kaplan *et al.* 2008). In the presence of DNA damage, H3K56ac contributes to a chromatin environment that favors for DNA repair (Masumoto *et al.* 2005; Dahlin *et al.* 2014). Mutant cells lacking H3K56ac have reduced cell growth, exhibited extreme susceptibility to genotoxic stress, underscoring important functional roles of H3K56ac (Masumoto *et al.* 2005; Dahlin *et al.* 2014). It has also been shown that Rtt109 mutation is epistatic to all phenotypes caused by the absence of H3K56ac and Rtt109 is the sole enzyme responsible for H3K56ac in *S. cerevisiae* (Recht *et al.* 2006; Schneider *et al.* 2006; Han *et al.* 2007b). *C. albicans* cells lacking Rtt109-mediated H3K56ac are extremely susceptible to the antifungal agent echinocandins, exhibited a reduced

pathogenicity in mice and were more susceptible to killings by macrophages than wild-type cells *in vitro* (Lopes Da Rosa et al. 2010; Wurtele et al. 2010). Interestingly, functional Rtt109 orthologs have also been characterized in *Pneumocystis* spices, suggesting a possible conserved functional role among pathogenic fungi (Dahlin *et al.* 2014). Second aspect of the rationale is the fungal specificity. Although H3K56ac has been detected in mammalian cells, it is far less abundant than in fungi, suggesting an evolutionary diverged, less central role of H3K56ac in mammalian cells (Drogaris *et al.* 2012). Notably, Rtt109 has no detectable sequence homology to other HAT family members in mammalian cells but unexpectedly shares a similar tertiary fold as compared to mammalian p300/CBP (a distant homolog of fungal Rtt109) (Tang *et al.* 2008). Taken together, targeting Rtt109-mediated H3K56ac would bring towards the goals of developing broad-spectrum antifungal strategy with minimized toxicity to human (Dahlin *et al.* 2013; Lopes Da Rosa *et al.* 2013).

Although campaigns for small-molecules targeting Rtt109 HAT in academic drug discovery has been intense but unfortunately there is very little evidence for useful compounds emerged having been further developed and clinically progressed (Dahlin *et al.* 2013; Lopes Da Rosa *et al.* 2013) . This is partly due to the fact that there exists a high proportion of small molecules in high-throughput screening (HTS) libraries are thiol-reactive that interferes with the indirect thiol-scavenging HAT assays in screening assays (Dahlin *et al.* 2013; Baell and Miao 2016; Dahlin *et al.* 2017). Recently, a breakthrough discovery from a pharmaceutical research laboratory reported a selective, drug-like catalytic inhibitor of p300/CBP by utilizing *in silico* HTS screen followed by direct radioactive HAT assays (Lasko *et al.* 2017). This finding underlines the fact that Rtt109 remains a feasible target for antifungal drug discovery, however, further knowledge of the function and regulation of Rtt109 in the pathogenic fungi would contribute to rational approaches to refine and establish tailored HTS screening strategies.

Current understanding of chaperone-dependent Rtt109 activation

Molecular, biochemical and structural characterization of Rtt109 has been extensively studied in *S. cerevisiae* (Han *et al.* 2007b; Tang *et al.* 2008; D'arcy and Luger 2011; Dahlin *et al.* 2014). Collectively, these studies showed that Rtt109 HATs are subject to complex regulation, including some unique features. Unlike other HATs, acetylation by Rtt109 *in vitro* is extremely inefficient in the absence of either of two histone chaperones, Asf1 and Vps75 (Recht *et al.* 2006; Han *et al.* 2007b; Tsubota *et al.* 2007; D'arcy and Luger 2011). Surprisingly, while Asf1 is required for H3K56ac acetylation, the major binding partner for Rtt109 is Vps75, whose deletion has little effect on bulk H3K56ac levels (Han *et al.* 2007b; Tsubota *et al.* 2007; D'arcy and Luger 2011). Recent studies utilizing mass spectrometry techniques showed that, depending on chaperone association (Asf1 or Vps75) and substrate (H3, H3/H4 heterodimer or heterotetramer), different levels of Rtt109 activation and substrate specificity (H3K56 or H3-N-terminal tail acetylations) could be observed *in vitro* (Abshiru et al. 2013; Kuo and Andrews 2013). Importantly, these studies indicated that H3K9 and H3K23 are the primary sites acetylated by Rtt109-Vps75, whereas Rtt109- Asf1 showed a far greater site-specificity towards H3K56 (Abshiru *et al.* 2013; Kuo and Andrews 2013). Current knowledge of detailed Rtt109-dependented H3K56ac pathway in *C. albicans* is limited and other components of this pathway have not yet been identified. In this study, we provided evidences that while the catalytic mechanism of CaRtt109 is conserved as to that of ScRtt109; chaperone proteins CaVps75 and CaAsf1 do not function in a manner parallel to that of ScVps75 and ScAsf1.

2.3 Results

C. albicans Rtt109 preserved the catalytic mechanism of H3K56ac

Loss of *C. albicans RTT109* abolishes H3K56ac and causes sensitivity to DNA damaging drugs, including reactive oxygen species (ROS) (Lopes Da Rosa *et al.* 2010; Wurtele *et al.* 2010). We sought to directly link the catalytic activity of

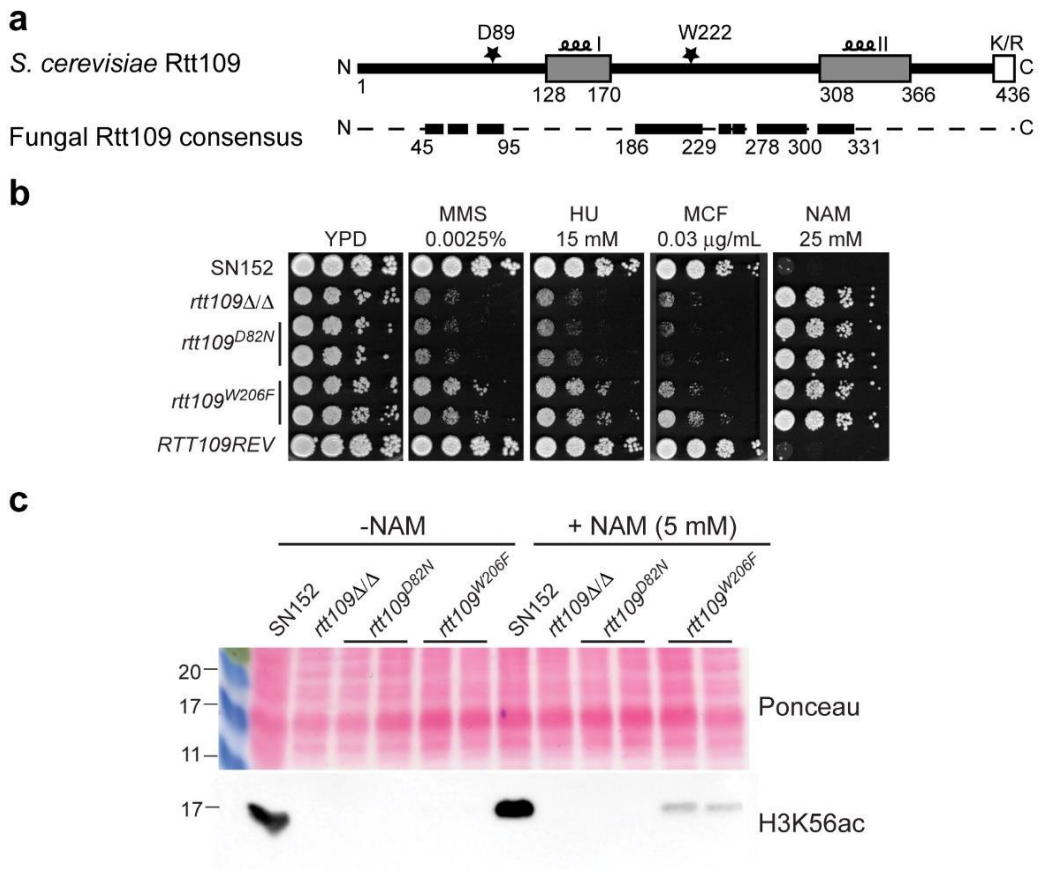

Figure 2.1. *C. albicans* Rtt109 has evolutionally conserved catalytic residues for H3K56 acetylation.

(a) Schematic representation of *S. cerevisiae* Rtt109 as well as the sequence consensus of fungal Rtt109 homolog. Residues that are critical for catalyzing H3K56ac are indicated with star symbols of *S. cerevisiae* Rtt109. Rtt109 forms a strong complex with Vps75, two interfaces with Vps75 are boxed in grey and indicated with spiral symbols. A K/R-rich C-terminus domain that has been implicated for Vps75-depedent H3K56ac is boxed in white. A consensus sequence that is maximally representative of fungal Rtt109 sequences obtained from the Candida genome database (www.canadidagenome.org) was constructed and mapped according to the *S. cereveisiae* Rtt109 sequence (http://mergealign.appspot.com); highly conserved region (score 8 out of 10) is presented as a thick black line. (b) *C. albicans rtt109* catalytic mutants phenocopy the *rtt109* null mutant. Ten-fold serial dilutions of cells from WT, *rtt109* null mutant, catalytic mutant alleles (rtt109D82N, rtt109W206F) *or rtt109* null mutant carrying one *RTT109* WT allele (RTT109REV) were spotted on YPD plates with indicated concentrations of testing chemicals; plates were incubated at 30°C for 48 h. Two independently generated catalytic mutants are shown. MMS (methylmethane sulfonate), HU (hydroxyurea), MCF (micafungin), NAM (nicotinamide) (c) *C. albicans rtt109* catalytic mutants lack H3K56 acetylation. Log phase WT and *rtt109* null mutant cells (OD_{600} ~0.8) were grown in the presence or absence of NAM (5 mM) for 4 h followed by total cell lysis and immunoblotting using the specific anti-H3K56ac antibody.

CaRtt109 to these phenotypes. Previous structural studies of ScRtt109 protein revealed two residues that are particularly important for H3K56 acetylation, Asp 89 (D89) and Trp 222 (W222) (Tang *et al.* 2008). These two sites appear to influence acetyl-coenzyme A (acetyl-CoA) binding (Tang *et al.* 2008) and are highly conserved among fungal Rtt109 homologs (Fig 2.1A). Consistent with this, *rtt109* null mutant cells carrying a single $rtt109^{D82N}$ mutant allele are as sensitive to the genotoxins methyl methanesulfonate (MMS) and hydroxyurea (HU) as *rtt109* null mutants (Fig 2.1B) with abolished H3K56ac (Fig 2.1C). These cells are also hyper-susceptible to the antifungal agent micafungin (MCF), which elicits oxidative stress and causes DNA damage (Kelly *et al.* 2009; Wurtele *et al.* 2010). As is the case for *rtt109* null mutants, $rtt109^{D82N}$-expressing cells are insensitive to nicotinamide (NAM), a potent inhibitor of the essential H3K56ac histone deacetylase CaHst3 (Wurtele *et al.* 2010). On the other hand, while $rtt109^{W206F}$ cells are also resistant to NAM up to 25 mM, this mutation only resulted in a moderately increased sensitivity to genotoxic agents (Fig 2.1B). This is in agreement with the fact that we detected residual H3K56ac in the NAM- treated $rtt109^{W206F}$ cells (Fig 2.1C). Taken together, our results suggested that D82 is a critical residue for the CaRtt109 catalytic activity while W206 plays a less important role. Furthermore, we demonstrated that the catalytic mechanism of *C. albicans* Rtt109 is evolutionally conserved and its ability to acetylate H3K56 is important for *C. albicans* cells to survive DNA damage conditions.

C. albicans Vps75 is required for the optimal H3K56 acetylation

Two lines of evidence from *S. cerevisiae* studies indicate that surfaces of ScRtt109 contributing to Vps75 binding are important for its function: i) binding of ScVps75 stimulates the catalytic activity of ScRtt109, ii) ScVps75 binding via the interacting loop I (ScRtt109 residues 128-170) protects ScRtt109 from proteolysis *in vivo* (Berndsen *et al.* 2008; Keck and Pemberton 2011; Su *et al.* 2011; Tang *et al.* 2011). Intriguingly, these functional domains are not well conserved among fungal species, implying the regulatory mechanism(s) of Rtt109 by Vps75 could be evolutionarily diverged (Fig 2.1 and 2.S1). We identified the gene encoding

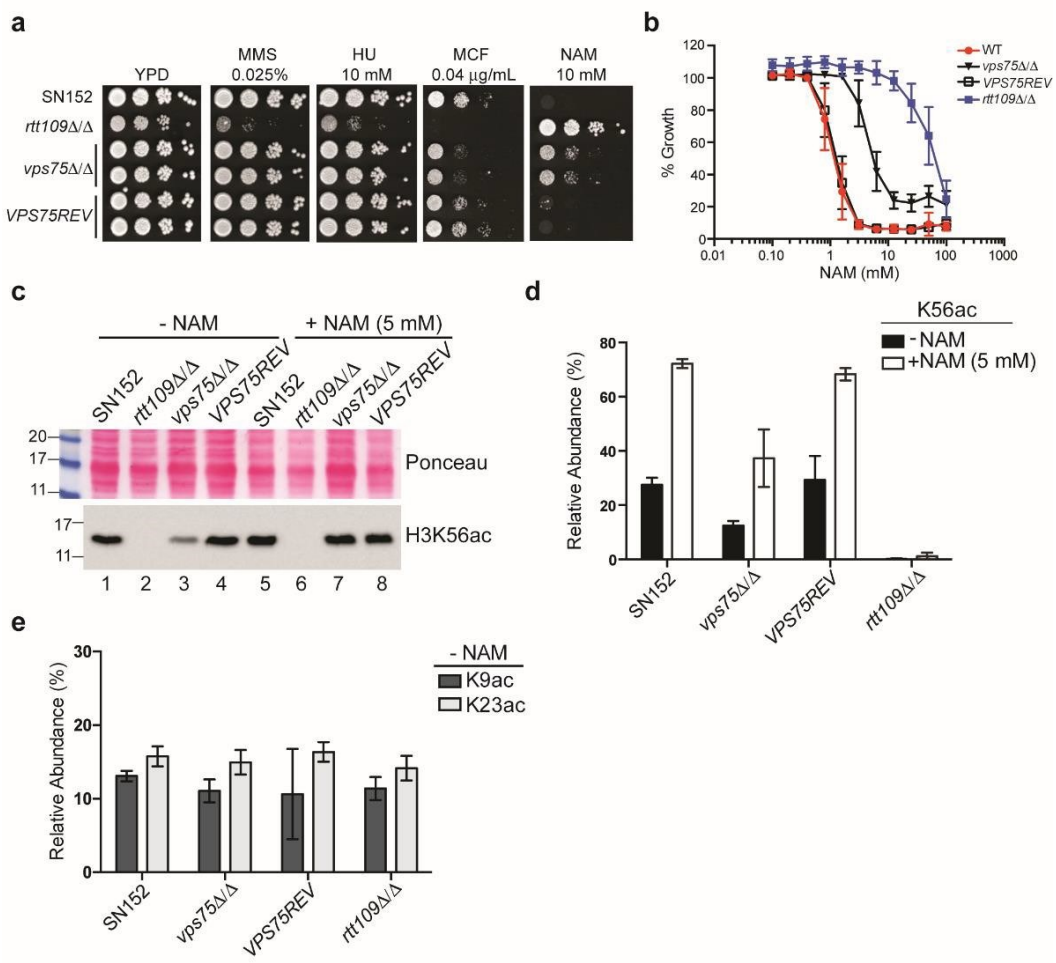

Figure 2.2. *C. albicans* lacking *VPS75* exhibited similar phenotypes associated with partial loss of H3K56ac

(a) Strains lacking *VPS75* are mildly susceptible to MCF, moderately resistant to NAM but are not susceptible to genotoxic agents MMS and HU. Serial 10-fold dilutions of the cells from indicated strains, starting at an OD_{600} of 0.1, were spotted onto YPD plates containing testing chemicals at concentrations as indicated. Plates were incubated at 30 ^{o}C for 48 h. (b) Fold-increase in NAM resistance in strains lacking *RTT109* or *VPS75* were quantified using the liquid MIC assay (c) *C. albicans vps75* null mutant showed a decreased in H3K56 acetylation. Log phase *C. albicans* cells (OD_{600} ~0.8) were grown in the presence or absence of NAM (5 mM) for 4 h followed by total cell lysis and immunoblotting using the specific anti-H3K56ac antibody. (d) Levels of H3K56ac in cells grown in absence or presence of NAM were determined by mass spectrometry and expressed as percent relative abundance. Relative abundance was calculated as H3K56ac/(H3K56ac+H3K56pr) x 100%; H3K56pr (propionylated H3K56 peptide). (e) Levels of H3K9ac and H3K23ac in asynchronously growing cells were determined by mass spectrometry and expressed as percent relative abundance.

putative *C. albicans* Vps75 (CR_05890C), we generated the *vps75* null mutant strains and tested their susceptibility to genotoxic as well as antifungal agents. We

found that while *vps75* null mutants are not sensitive to genotoxic agents MMS and HU compared to WT cells, they exhibited a modest growth impairment in the presence of MCF (Fig 2.2A). Interestingly, *vps75* null mutant cells are also more resistant to NAM than WT or *VPS75* revertant (*vps75*Δ/Δ+*VPS75*) (Fig 2.2A-B), the phenotype that is closely associated with a decreased of H3K56ac levels in *C. albicans*, suggesting that Vps75 could be involved in promoting H3K56ac. Indeed, immunoblotting analyses showed a reduced H3K56ac in exponentially growing *vps75* null mutant, while re-introduction of one copy of *VPS75* (*VPS75* revertant) restored WT levels of H3K56ac (Fig 2.2C). Using quantitative mass spectrometry, we consistently detected a ~50% reduction in the levels of H3K56 stoichiometry in *vps75* null mutant cells as compared to WT or *VPS75* revertant strains irrespective of NAM treatment (Fig 2.2D). In *S. cerevisiae*, H3 N-terminal lysines H3K9 and H3K27 have been identified as primary acetylation sites for ScRtt109-Vps75 (Abshiru *et al.* 2013; Kuo and Andrews 2013); however, changes on H3 N-terminal tail acetylation, if any, were not significant in *C. albicans* cells lacking Vps75 (Fig 2.2E). The fact that a similar level of N-terminus acetylation also observed in the *rtt109* null mutant, consistent with the notion that the H3 N-terminus acetylation is also targeted by other HAT, such as GCN5 (Tang *et al.* 2011; Su *et al.* 2016).

It has been demonstrated that ScVps75 stabilizes ScRtt109 via binding to the loop I (Fig 2.1A) (Keck and Pemberton 2011), therefore it is possible that the reduced H3K56ac levels in *C. albicans vps75* null mutant observed reflected the amount of CaRtt109 protein *in vivo*. However, residues of CaRtt109 117-158 are poorly conserved to the corresponding ScRtt109 loop I; intriguingly, this region is often completely absent in other fungi (Fig 2.S1), thus prompting us to investigate if the stability Rtt109 is affected by Vps75 in *C. albicans*. Analyzing total protein lysate followed by immunoblotting, we detected a slightly lower signal corresponding to Rtt109-HA in two independent exponentially growing cells in *vps75* null mutants as compared to that in the *VPS75* revertant strains (Fig 2.3A). We also determined the stability of Rtt109-HA as a function of time after the addition of cycloheximide to arrest protein synthesis and found that Rtt109-HA is less stable in *vps75* null mutant as compared to *VPS75* revertant (Fig 2.3B).

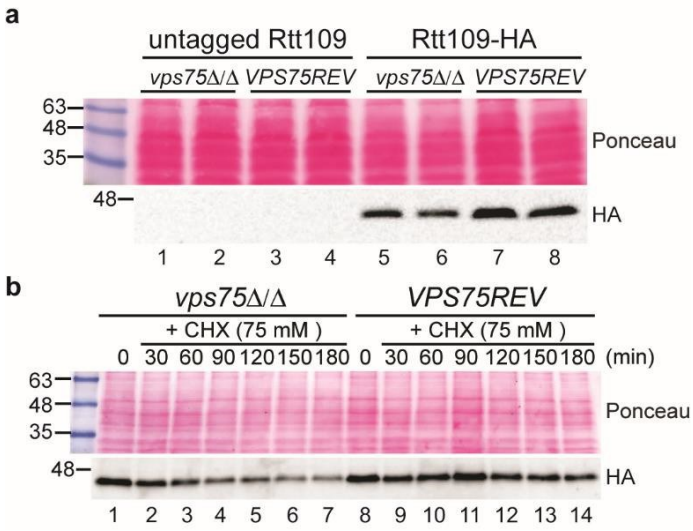

Figure 2.3. The stability of CaRtt109 is affected in the absence of CaVps75

(a) Rtt109-HA was detected in whole cell lysate of the indicated strains by Western blot analysis. Slightly weaker signals corresponding to RTT109-HA were consistently observed in the *vps75* null strain as compared it to that of the *VPS75* revertant strains (lanes 5-6 vs 7-8). This is a representative blot from n=3 experiments. (b) Cycloheximide-chase assays were performed to assess the stability of Rtt109-HA in the *vps75* null versus *VPS75* revertant strains. Time after cycloheximide (75 mM) addition are indicated. Western blots were probed with the anti-HA antibody. This is a representative experiment from n=2 assays.

These results suggest that reduced H3K56ac in the *vps75* null mutant may be attributable, at least in part, to the effect of CaVps75 on CaRtt109 stability. We next performed *in vitro* HAT assays to evaluate whether *C. albicans* Rtt109-Vps75 could directly acetylate H3K56. Full-length recombinant 6xHis-Rtt109 and 6xHis-Rtt109-Vps75 holoenzymes, as well as histone H3-H4 and the non-H3K56 acetylatable H3K56R-H4 were purified (Fig 2.4A). We performed *in vitro* HAT assays with recombinant 6xHis-Rtt109 at an enzyme to substrate ratio of 1:10 and 6xHis-Rtt109-Vps75 at an enzyme to substrate ratio of 1:10, 1:25, 1:100, 1:250 using purified ScH3-H4 as substrates. Western blot as well as quantitative mass spectrometry analyses of the HAT reaction product showed a very low H3K56 acetylation in the absence of recombinant CaVps75 (Fig 2.4B-C, sample 2). Signals corresponding to H3K56ac were easily detected in samples containing recombinant *C. albicans* 6xHis-Rtt109-Vps75 holoenzyme in an enzyme to substrate ratio-dependent manner (Fig 2.4B and 4C, samples 3-6), strongly suggests that Vps75 is an active component of Rtt109 complex for H3K56

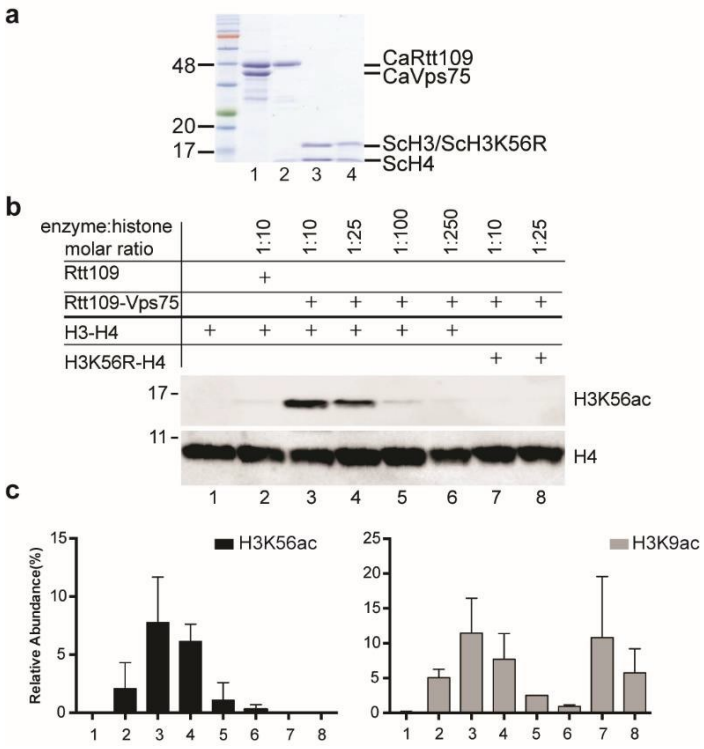

Figure 2.4 CaVps75 promotes H3K56ac and H3K9ac *in vitro*

(a) Purified *C. albicans* 6xHis-RTT109-Vps75, 6xHis-RTT109, and *S. cerevisiae* H3/H4 and H3K56R/H4 were separated on 12% SDS gel followed by coomassie-blue staining. (b) *In vitro* HAT assay performed using purified *C. albicans* 6xHis-RTT109, 6xHis-RTT109-Vps75 and *S. cerevisiae* H3/H4 or H3K56R/H4. Final amount of 0.4-11 pmol of Rtt109 alone or in complex with Vps75 were mixed with 110 pmole of H3/H4 or H3K56R/H4 in a final of 10 µM of acetyl-CoA assay. This is a representative blot of at least 2 independent experiments. (c) Relative abundance of H3 acetylation in HAT reaction samples as listed in panel b were quantified by mass spectrometry.

acetylation. No western blot signals were detected in samples containing mutant histone substrates H3K56R-H4, confirming the specificity of our antibody (Fig 2.4B, samples 7 and 8). Finally, we also showed that *C. albicans* Rtt109-Vps75 holoenzyme promotes histone H3K9 acetylation and that the level of H3K9ac was independent to the acetylation status of H3K56ac (Fig 2.4C). Taken together, our results provide the first *in vivo* and *in vitro* evidence for the dual functions of *C. albicans* Vps75 in achieving optimal H3K56ac, i.e., direct promotion of H3K56 acetyltransferase reaction and stabilization of Rtt109.

ASF1 influences chromatin structure and is an essential gene in *C. albicans*

In *S. cerevisiae*, Asf1 binds to histone H3-H4 dimers, promotes Rtt109-dependent H3K56ac, and releases K56 acetylated H3 to downstream histone chaperones for nucleosome assembly (Fillingham *et al.* 2008; Dahlin *et al.* 2014). Unlike in *S. cerevisiae*, where *asf1*Δ is viable, *C. albicans* Asf1 (CR_07860c) has been reported to be an essential gene due to lack of success in generating null mutant (Tscherner *et al.* 2015). In order to evaluate the essentiality of *C. albicans ASF1* for cell viability, we used a conditional repression *asf1*Δ*/pTET-ASF1* strain, in which the expression of the functional *ASF1* allele of the heterozygous deletion strain is placed under a doxycycline (DOX)-repressible promoter (Roemer *et al.* 2003). Immunoblotting analyses showed that addition of DOX to the medium caused time-dependent decrease in Asf1 protein levels accompanied by concomitant decrease in H3K56ac signals, confirming the contribution of *C. albicans* Asf1 to H3K56ac (Fig 2.5A). We next evaluated the viability of *asf1*-downregulated cells grown in media +/- DOX for 24 h. We found that only less than 1% of *asf1*Δ*/pTET-ASF1* cells could survived after 24 h DOX treatment and proliferated in the DOX-free media (Fig 2.5B). This observation suggested that under expression of Asf1 has negative impact on cell viability and corroborated with previous reports of inability to construct homozygous deletion mutant for *ASF1* (Tscherner *et al.* 2015). To test if the lethality of *C. albicans asf1* strain was due to severe defects in chromatin structure, we measured changes in chromatin structure affected by *ASF1* downregulation in micrococcal nuclease (MNase) assay. *C. albicans asf1*Δ*/pTET-ASF1* strain was treated or not with DOX for 8 h prior to cell wall digestion with lyticase; spheroplasted cells were treated with MNase (1.43 U) in a function of time (Fig 2.5C). Depending on concentration and time of treatment, low concentrations of MNase digestion generally produce one dobule-stranded cut every 10 to 50 nucleosomes, therefore we could compare the MNase digestion pattern (nucleosome repeat leangth of bulk chromatin) in the condition where Asf1 is downregulated in the presence of DOX to that of the untreated cells (Fig 2.5C). In our testing condition, we observed a massive degradation of gDNA in Asf1-depleted cells (+DOX, 8h) and a significant increased of mononucleosome-length DNA after only 2 min of MNase treatment.

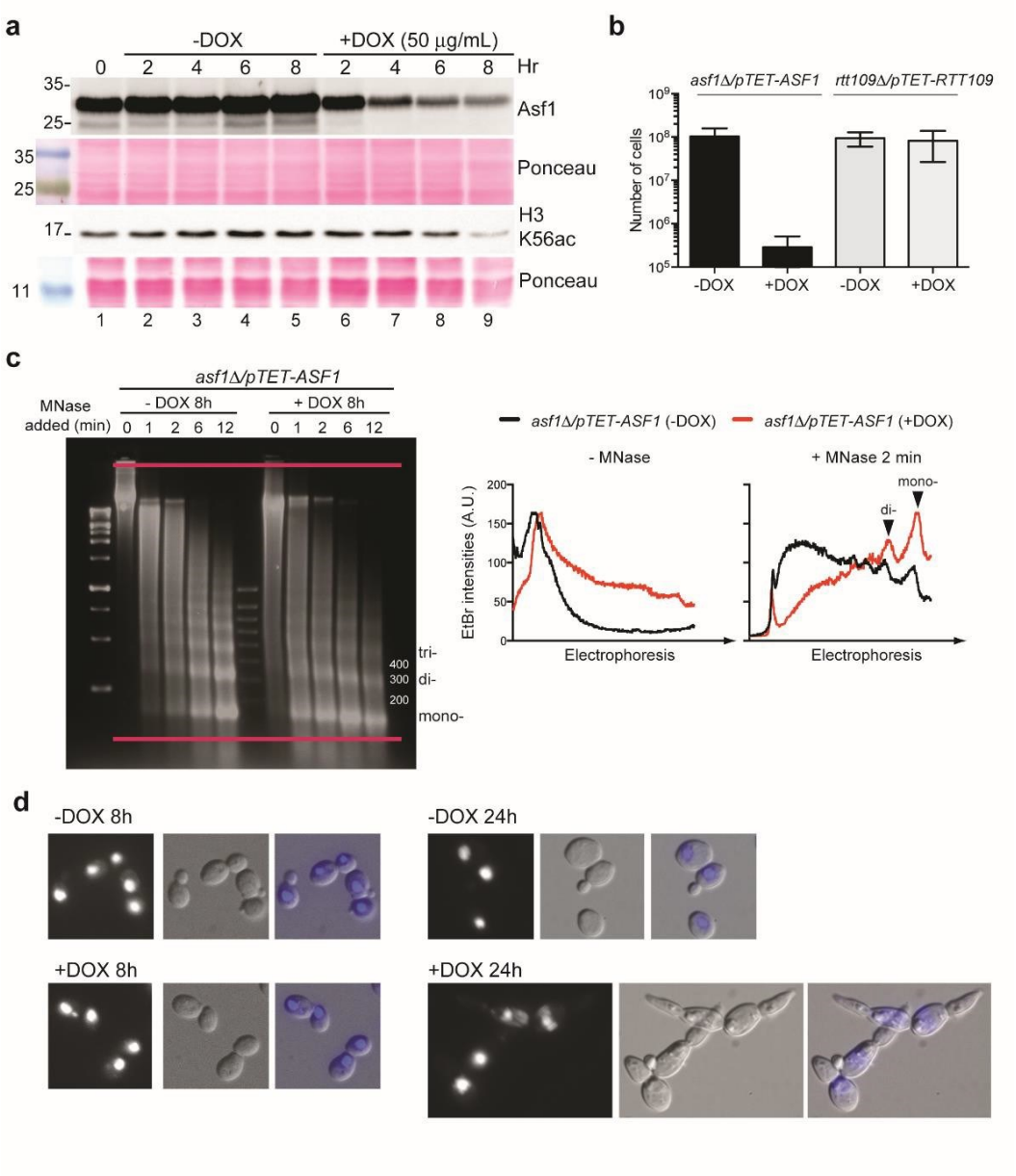

Figure 2.5. *C. albicans ASF1* is an essential gene

(a) In the presence of doxycycline, the expression of Asf1 gradually diminishes, concomitantly with the H3K56ac levels, as detected using the specific anti-Asf1 and anti-H3K56 antibodies, respectively. (b) Conditional gene repression strains of *ASF1* or *RTT109* were grown in YPD with or without doxycycline for 24 hours. Cells were then harvested, washed and serially diluted in microtiter plates containing no doxycycline and incubated for 2-3 days at 30 ºC. Number of colonies formed was scored representing the number of viable cells. (c) MNase nuclease assay revealed that down-regulation of Asf1 resulted in a defect in nucleosome structure. Nuclei prepared from control and DOX-treated cells were exposed to MNase (1.43 U) in a function of time. MNase-digested DNA was purified, resolved by agarose gel electrophoresis and detected by ethidium bromide (EtBr) staining. (d) Asf1 depletion triggers an aberrant cell morphology, DNA stained with DAPI and cell morphology transition were monitored after 8 h or 24 h following DOX addition.

Our results indicate that chromatin is strongly sensitized to MNase digestion in Asf1-depleted cells, suggesting that lack of Asf1 causes anomalies in chromatin structure. Finally, previous studies show that *C. albicans* cells with unregulated levels of H3K56ac are accompanied by an abnormal cellular morphology with elongated cells; furthermore, similar morphology has also been observed in *C. albicans* cells treated with genotoxic agents HU or MMS (Shi *et al.* 2007; Wurtele *et al.* 2010; Loll-Krippleber *et al.* 2014), suggesting extensive DNA damage in *C. albicans* could be responsible for abnormal polarized growth. We monitored the morphology of *asf1Δ/pTET-ASF1* cells that were grown in the presence of DOX for 8 and 24 hours and observed elongated cells at the later time point (Fig 2.5D). Taken together, our results demonstrate that Asf1 depletion causes decreased H3K56ac levels, chromatin structure defects and loss of cell viability.

2.4 Discussion

Crucial roles of H3K56 acetylation in nucleosome assembly and genomic stability in fungi have been well documented; moreover pharmacological modulation of H3K56ac levels has been proposed as a potential antifungal therapeutic strategy (Wurtele *et al.* 2010; Kottom *et al.* 2011; Lopes Da Rosa and Kaufman 2012; Dahlin *et al.* 2014). Further understanding of the regulatory as well as chemical mechanisms of Rtt109-catalyzed H3K56 acetylation in *C. albicans* is important toward designing pharmacological agents targeting this pathway. Structural studies of ScRtt109-Vps75-(acetyl-CoA) complexes recently highlighted unusual mechanistic aspects of Rtt109-dependent acetylation reactions (Tang *et al.* 2008; D'arcy and Luger 2011; Su *et al.* 2011; Tang *et al.* 2011). Briefly, Rtt109 does not have a defined general base (glutamate) acting as a catalyst to deprotonate lysine on the histone substrate prior to the acetylation reaction; instead, Rtt109 relies on Vps75 to orientate substrates toward the hydrophobic core of the Rtt109-Vps75 holoenzyme, where the substrate lysine is expriencing different chemical environment resulting a lower p*Ka* of the substrate lysine, allowing the acetylation reaction to occur at catalytic rates. Such general mechanism by simply decreasing the lysine p*Ka* could explain the promiscuity of Rtt109 to acetylate multiple lysine

residues (Dahlin *et al.* 2014; Mccullough and Marmorstein 2016). Sequence alignment of Rtt109 homologs from several fungal species revealed a high degree of conservation among regions associated with acetyl-CoA binding. However, the interfaces with Vps75 are less conserved or even absent in several fungal species, implying a possible evolutionary diverged catalytic or regulatory mechanisms of Rtt109 homologs (Fig 2.1A). In this study, we characterized important residues for the catalytic activity of *C. albicans* Rtt109 for H3K56 acetylation as well as the function and contribution of histone chaperones that are predicted to cooperate and regulate CaRtt109 for promoting H3K56ac.

We showed that the two highly conserved residues of the of acetyl-CoA binding pocket of CaRtt109, D89 and W222, are necessary for its catalytic activity and mutation of these two residues largely abolished H3K56ac and caused increased sensitivity to genotoxic as well as antifungal agents, confirming a conserved catalytic mechanism of Rtt109 between *S. cerevisiae* and *C. albicans* (Fig 2.1). Despite the conserved region that is likely to associate with acetyl-CoA and substrate binding, ScRtt109 segments that were reported to be in direct contact with ScVps75 are less conserved among fungal Rtt109 homologs. For example, *C. albicans* Rtt109 has more acidic residues in the region corresponding to ScRtt109-Vps75 interacting loop I, which has mostly basic residues (Fig 2.S1 and (Dahlin *et al.* 2014)); furthermore, CaRtt109 is transcribed from a much shorter sequence of only 1080 nucleotide base pairs while the average length of fungal Rtt109 homologs is 1275 nucleotide base pairs. Secondary structure alignment of *C. albicans* Rtt109 to the crystal structure of ScRtt109 (3Q66) revealed that CaRtt109 completely lacks the last helical loop along with the Lys/Arg-rich C-terminus (Fig 2.S1), a small basic patch that has been reported to be required for Asf1-dependent activation of Rtt109-mediated H3K56 acetylation, and compete with Vps75 binding (ScVps75 could promote H3K56ac with C-terminally truncated ScRtt109) (Radovani *et al.* 2013; Lercher *et al.* 2017). These observations are implying a possible alternative cooperation relationship between *C. albicans* Rtt109 and Vps75 in promoting H3K56 acetylation. Indeed, our data show that contrasting to the findings in *S. cerevisiae*, where deletion of Vps75

showed no obvious phenotype relating to H3K56ac and genotoxic sensitivity, CaVps75 directly contributes to H3K56ac both *in vivo* and *in vitro*. We observed a moderately increased susceptibility of *vps75* null mutant to the antifungal agent MCF and increased resistance to NAM, phenotypes associated with a partial loss of H3K56 acetylation levels (Fig 2.2-4). Furthermore, we also noted that Rtt109 is less stable in the absence of Vps75 in *C. albicans*, an observation that has been previously reported in *S. cerevisiae* (Fig 2.3). Our results support dual functions of Vps75 in promoting Rtt109-associated H3K56ac, whereby Vps75 directly participates in H3K56 acetylation and contributes to Rtt109 stability *in vivo*.

We also demonstrated that in this study, *C. albicans* Asf1 is an abundant and stable protein, consistent with its evolutionarily conserved roles in histone binding and trafficking (English *et al.* 2006). Unexpectedly, while Asf1 is not an essential gene in *S. cerevisiae* or in *Schizosaccharomyces pombe* (Recht *et al.* 2006; Tanae *et al.* 2012), we showed that Asf1 is essential in *C. albicans*. Previous studies showed that *C. albicans rtt109* null mutant with a complete lack of H3K56ac remain viable, suggesting that a significant loss in H3K56ac level in the *asf1* null mutant did not result in its lethality (Lopes Da Rosa *et al.* 2010; Wurtele *et al.* 2010). Instead, Asf1-downregulated cells showed defects in nucleosomal structure accompanied by genotoxic-stress induced polarization morphology (Fig 2.5), suggesting that *C. albicans* is sensitive to the changes of nucleosome structure as resulted from the deregulation of *Asf1*.

Functional regulators of chromatin are in general conserved among pathogenic fungi, and have been proposed as potential broad-spectrum antifungal pharmacological targets (Pfaller *et al.* 2009; Wurtele *et al.* 2010; Hnisz *et al.* 2011; Pfaller *et al.* 2015; Kuchler *et al.* 2016). Our study provides experimental evidences suggesting that dynamic interactions between Rtt109 and histone chaperones may be targeted for antifungal purposes. Furthermore, the essential role of *C. albicans* Asf1 suggest that it could serve as a better antifungal target than Rtt109. Asf1 is composed of a highly conserved N-terminal histone-binding

domain from yeast and a more diverged C-terminal tails (English *et al.* 2006). Recently, small molecules that inhibit the binding of human Asf1-H3/H4 have been identified using virtual screen of 140,000 compounds (Miknis *et al.* 2015). However, since mammalian Asf1 are essential for viability (Sanematsu *et al.* 2006), these molecules are expected to serve as chemical probes in validating biological pathways rather than toward therapeutic purposes. Development of small molecules specifically targeting fungal Asf1 but not mammalian Asf1 will require the identification of fungal-specific residues or surfaces that lie in close proximity to the Asf1-histone binding pocket. Taken together, our studies of Rtt109 HAT complex in *C. albicans* showed unexpected phenotype, stressing the importance of characterizing potential antifungal targets directly in the pathogenic fungi. Future structural studies of *C. albicans* Asf1 would provide invaluable information and contribute to structural-aided drug design as a part of the new antifungal drug screen campaign.

2.5 Materials and Methods

Chemicals and reagents were purchased from Sigma, unless otherwise stated. Additional details can be found in the *Supporting Information*-Materials and Methods section.

Strains, plasmids and culture conditions

The *C. albicans* strains and plasmids used in this study are listed in Table S1. All *C. albicans* strains were derived from the common laboratory strain SN152 (Noble and Johnson 2005) or CaSS1 (Roemer *et al.* 2003). *C. albicans* cells were grown routinely at 30^{o}C in YPD liquid (1% yeast extract, 2% peptone and 2% glucose). For solid media, 2% agar was added. *Escherichia coli* DH10B cells were used for DNA cloning procedures. *E. coli* cells were grown in LB medium to which appropriate antibiotics were added. Concentrations of antibiotics used in this study were chloramphenicol (34 μg/ml), ampicillin (100 μg/ml) and nourseothricin (200 μg/ml; Werner BioAgents). Hyper-acetylation of H3K56 were elicited in *C.*

albicans by growing cells in the presence of nicotinamide (NAM, 5 mM) at 30ºC for 4 h, unless otherwise specified.

Conditional inactivation of *ASF1* or *RTT109* and viability assay

ASF1 or *RTT109* conditional mutants were derived from the *C. albicans* CaSS1 strain that expresses a tetracycline-dependent transactivation fusion protein (TetR-ScGal4AD) (Roemer *et al.* 2003). For *Tet* promoter repression, saturated cell cultures were diluted to OD_{600} of 0.005 with or without doxycycline (DOX, 40 µg/mL) in the fresh media and grown at 30ºC with shaking for 24 h. After incubation, cells were harvested and washed in media without DOX. Colony formation assay was performed in liquid medium as previously described (Tsao *et al.* 2009; Wurtele *et al.* 2010). Briefly, a 200 µl culture was transferred to the first column of a 96-well plate. Cells in the first column was then serially diluted 1:10 (20 µl culture in 180 µl YPD) eleven times across a 96-well microtiter plate, with new tips for each dilution. The plate was then incubated in a humid chamber without agitation at 30ºC for 3-4 days. Number of colonies formed were scored and used to multiply the dilution factor of that well, the product represents the number of viable cells in the initial culture. The relative percent survival was calculated as the percent of cells in (DOX-treated)/(untreated). The graph was plotted from at least two independent experiments each with more than 6 technical replicates.

Growth inhibition assays

Spot dilution assays were performed as described previously (Wurtele *et al.* 2010). Briefly, cells were grown overnight in YPD at 30ºC and diluted to OD_{600} of 0.1. Ten-fold serial dilutions of each strain were spotted onto YPD plates containing methyl methanesulfonate (MMS), hydroxyurea (HU), micafungin (MCF, Astellas Pharma) or NAM and incubated at 30ºC for 48 h. Minimum inhibitory concentrations (MIC) assays were performed in growth media in a 96-well plate as described previously (Wurtele *et al.* 2010). Saturated cells were diluted to OD_{600} of 10^{-4} and grown in the presence of increasing concentrations of NAM at 30ºC for 24 h. Endpoint cell viability was measured spectrophotometrically using

a microplate reader at OD_{620} (Tecan).

Total protein extraction and immunoblotting

Whole-cell lysates were prepared from at least 2 mL of OD_{600} of 1.0 cells (2 OD unit of cells) using an alkaline extraction method (Kushnirov 2000). Proteins were separated by SDS–PAGE (12% or 15% acrylamide gels). The gels were either stained with Coomassie blue or transferred to a nitrocellulose membrane with a Trans Blot SD Semi-Dry transfer apparatus (Bio-Rad). Membranes were stained with Ponceau S reagent (0.1% Ponceau S in 5% acetic acid) prior to immunodetection. Primary antibodies used in this study: α-H3K56ac antibody (AV105-GE; 1:500 dilution) (Masumoto *et al.* 2005), α-H3 (AV71/72; 1:1000 dilution). Proteins on membranes were visualized on a Typhoon-9410 variable mode imager and analyzed using ImageQuant software (GE Healthcare). For cycloheximide (CHX)-chase assay, actively growing Rtt109-HA cells (OD_{600} of 1.0) were grown in YPD or YPD containing 75 mM CHX at 30ºC (Manoharlal *et al.* 2008). Equivalent of 10 OD unit of cells per time point (0, 30, 60, 90, 120, 150 and 180 min) were collected and immediately mixed with 30 mM of sodium azide (NaN_3) on ice to stop further protein degradation for the duration of the chase. Total protein lysate extractions and immunoblotting were prepared as described above, Rtt109-HA was detected using α-HA antibody (12CA5, Roche, 1:1000 dilution).

Histone sample preparation and mass spectrometry

Histones were acid extracted from actively growing 100 OD unit of *C. albicans* cells (OD_{600} of 0.8-1.6) as described earlier (Edmondson and Russell 1996; Guillemette *et al.* 2011). Briefly, immediately after cells were harvested, the cell pellet was washed once in sterile water, resuspended in 8 mL of 0.1 mM Tris (pH 9.4)/10 mM DTT and incubated at 30ºC for 15 min with gentle shaking. The cells were centrifuged and washed twice in 8 mL Sorbitol/HEPES buffer (1.2 M Sorbitol/20 mM HEPES, pH 7.4). Cell wall digestion: cells were resuspended in the same buffer with a cocktail of protease inhibitors (4 mM of AEBSF, 5 µg/mL of each pepstatin, aprotinin, leupeptin and E-64) and 5 mg of zymolyase (100T)/g

(wet weight of the cell pellet). Cells were incubated at 30ºC for 30 min with gentle shaking. Cells were immediately cooled down by mixing with 12.5 mL of ice-cold 1.2 M Sorbitol/20 mM PIPES/1 mM $MgCl_2$ (pH 6.8) followed by a low speed centrifugation (3,500*g*) at 4ºC for 5 min. Cell pellets were resuspended in 8 mL ice-cold nuclei isolation buffer (NIB, 0.25 M sucrose, 60 mM KCl, 14 mM NaCl, 5 mM $MgCl_2$, 1 mM $CaCl_2$, 15 mM MES at pH 6.6, 0.8% Triton X100, protease inhibitors) and held on ice/water for 20 min. Cells were pelleted as described above at the low speed centrifugation and the pellets were resuspended in the wash buffer "A" (10 mM Tris at pH 8.0, 0.5% NP-40, 75 mM NaCl, 30 mM sodium butyrate, protease inhibitors) and held on ice/water for 15 min, spun cells again and repeated wash A and ice/water incubation one more time. The cell pellet was then washed twice in the "B" wash (10 mM Tris at pH 8.0, 0.4 M NaCl, 30 mM sodium butyrate, protease inhibitors), held on ice/water for 5 min. Acid extraction: the cell pellet was resuspended in 2 ml/g (of the initial pellet weight) of ice-cold H_2O, add 5 N HCl to a final concentration of 0.25 N to extract histones. Samples were held on ice/water for 30 min and vortex occasionally. Following the incubation, cell debris were removed from the solution by centrifuge. The supernatant, which contains the extracted histones, was precipitated by adding 100% TCA to a final concentration of 20% and incubated at 4ºC overnight. Histone pellets were collected by centrifugation at the maximum speed of 13,000*g* at 4ºC for 30 min and washed once with acidified acetone (2 ml cold acetone, 0.5% HCl) and spun at 13,000*g* at 4ºC for 10 min. Histone pellets were washed twice with 1 mL cold acetone then air dried. Histone pellets were resuspended in 20 □L H_2O and stored at -20ºC.

Acid-extracted histones were further purified by reverse phase HPLC followed by propionylation, tryptic digestion and peptide sequencing by LC-MS/MS (Abshiru *et al.* 2013). Briefly, samples were derivatized with propionic anhydride as previously described (Drogaris *et al.* 2008). After two sequential rounds of derivatization, the samples were evaporated to dryness, then digested using trypsin (1:10 enzyme:substrate ratio, Promega) at 37ºC for 18 hours. Protein digests were acidified with 5% % trifluoroacetic acid (TFA) in water (v/v) prior to nanoscale LC-MS/MS analysis. Tryptic digests were then loaded onto an EXP stem trap column (3 µm EXP C18, Optimize

Technologies) and separated using a 15 cm length, 150 μm i.d. analytical column packed in-house with 3 μm C18 particles (Jupiter 300 Å, Phenomenex, Torrance, CA). The mobile phases consisted of 0.2% formic acid in water (v/v, solvent A) and 0.2% formic acid in acetonitrile (v/v, solvent B). Samples were loaded onto the trap column at 1 μL/min, followed by separation at 0.6 μL/min. Peptide elution was achieved using a linear gradient of 5 to 50% solvent B over 60 minutes. Nano LC-MS/MS analyses were performed using an Easy nLC II or nLC-1200 (Thermo Fisher scientific) coupled to Q-Exactive HF biopharma hybrid quadrupole-Orbitrap mass spectrometer (Thermo Fisher scientific). A Nanospray Flex ion source (Thermo Fisher scientific) fitted with a fused silica emitter was used as the nanoelectrospray interface. The mass spectrometer was operated in positive ion mode, and MS1 scans were acquired in the Orbitrap mass analyzer from m/z 300 to 1200 in data dependent acquisition (DDA) mode. Fragments ions were generated in the HCD collision cell with a NCE of 25. Protein identification was performed using PEAKS studio 8.5 database searching with the following variable modifications: acetylation (K, N-terminal, +42.01 Da), propionylation (K, +56.03 Da), deamidation (NQ, +0.98 Da), and oxidation (M, +15.99 Da). Relative peptide quantitation was performed by generating extracted ion chromatograms (XICs) of each peptide within a 10 ppm mass accuracy tolerance. The three most intense isotopes were extracted, summed together, and peak areas integrated using Xcalibur software. The identity of integrated peptide peak areas was confirmed by MS/MS sequencing. To compensate for differences in the amount of peptide loaded on-column between each sample, the histone H3 tryptic peptide YKPGTVALR was used to normalize the peptide intensities detected. The relative stoichiometryof histone H3 acetylation at different sites (K9, K14, K18, K23 and K56) was determined based on the normalized peak area ratios of the acetylated and propionylated forms of the tryptic peptides generated. An average of at least 2 biological replicates are presented

Recombinant protein expression and purification

Recombinant *C. albicans* 6xHis-Rtt109/Vps75 and 6xHis-Rtt109 were expressed and purified according to methods reported by Tang *et al*. with modifications

(Tang *et al.* 2011). Full-length *C. albicans RTT109* and *VPS75* were cloned into the BamHI/SalI and NdeI/XhoI sites, respectively, of the 6xHis-TEV-pCDF-Duet1 vector (Tang *et al.* 2011). As *C. albicans* decodes CUG codon as serine instead of leucine, three CUG codons of Rtt109 (L321/L336/L339) were all mutated to serine (AGC) for expression in bacteria. CaRtt109/Vps75 or CaRtt109 were expressed in *E. coli* BL21 (DE3) RIL cells. Cells were grown to OD_{600} of 0.8 and induced with 1 mM 1-thio-β-D-galactopyranoside (IPTG) at 18 ºC overnight. Cells were harvested by centrifugation and lysed by sonication in the lysis buffer (20 mM sodium phosphate, pH 7.8, 150 mM NaCl, 5 mM β-mercaptoethanol and 0.4 mM AEBSF protease inhibitor cocktail (Bio-Basic). Recombinant 6xHis-Rtt109/Vps75 was purified using nickel-nitrilotriacetic acid (Ni-NTA) affinity purification (Qiagen). The eluate was further purified by the MonoQ anion exchange chromatography with a NaCl gradient from 20 mM to 1,000 mM in 5 mM HEPES buffer, pH 8.0 and 5 mM β-mercaptoethanol (Tang *et al.* 2011). Recombinant 6xHis-Rtt109 was purified similarly except the Ni-NTA eluate was subjected to MonoSP cation exchange liquid chromatography. Purified recombinant proteins were further dialyzed in the sample buffer (5 mM HEPES, pH 8.0, 20 mM NaCl and 1 mM β-mercaptoethanol) that is compatible for subsequent *in vitro* assays and mass spectrometry analyses. Proteins were also concentrated using Amicon ultra centrifugal columns (Millipore), and aliquotes were stored at -80 °C with 10% glycerol until further use. Protein quantifications were performed using absorbance readings at 280 nm.

S. cerevisiae histone proteins were expressed from plasmids pET-Duet-H3/H4 or pET-Duet-H3-K56R/H4 from *E. coli* strain BL21(DE3) RIL (Kingston *et al.* 2011). Cells were grown to OD_{600} of 0.6 and induced with 0.3 mM IPTG at 37 °C for 6 hours. Cells were sonicated in the lysis buffer containing 500 mM NaCl, 20 mM Tris-HCl, pH 8.0, 0.1 mM EDTA, 10 mM β-mercaptoethanol, complete mini, EDTA-free protease inhibitor cocktail and 0.4 mM AEBSF (Bio-Basic). The supernatant was loaded onto a 5-ml HiTrap heparin column (GE Healthcare) and eluted with a NaCl gradient from 50 to 2,000 mM. Fractions containing histone complexes were further purified by size exclusion chromatography in buffer

containing 2M NaCl, Tris-HCl, pH 8.0, 0.1 mM EDTA, 10 mM β-mercaptoethanol. Purified histone complexes were directly dialyzed in the sample buffer (5 mM HEPES, pH 8.0, 20 mM NaCl and 1 mM β-mercaptoethanol) or distilled water.

Histone acetyltransferase (HAT) enzyme assay

In vitro HAT assays were performed as previously described (Abshiru *et al.* 2013) with minor modifications: 110 pmoles of ScH3/H4 or ScH3-K56R/H4 per reaction were mixed with purified 6xHis-Rtt109/Vps75 or 6xHis-Rtt109 at different concentrations on ice, giving ratios of enzymes to substrate at 1:10, 1:25, 1:100 and 1:250 (11-0.4 pmoles of enzymes) in the reaction buffer (5 mM HEPES, pH 8.0, 20 mM NaCl and 1 mM β-mercaptoethanol). Samples were equilibrated at 30°C for 2 minutes, 10 μM acetyl-coA (AcCoA) were added to the samples to initiate the reaction. After 30 minutes incubating at 30°C, reactions were terminated by mixing with the 2xSDS sample buffer followed by boiling for 5 minutes. Western blot analyses of HAT reactions were performed as described in immunoblotting section. Samples for mass spectrometry analyses were quenched with 5% TFA in water (v/v) instead of the addition of 2xSDS buffer and boiling, and analyzed as described above. No reversed-phase HPLC fractionation was performed on HAT enzyme assay samples.

Micrococcal nuclease accessibility assay

Equivalent of 100 OD_{600} of cells per sample was suspended in yeast lytic enzyme buffer [1M sorbitol, 5 μM β-mercaptoethanol and 4 mg/mL lyticase (≥200 U/mg)] with the addition of proteinase inhibitors (1 mM AEBSF and 7 μM Pepstatin) on ice. Cells were lysed by incubating samples at 30°C on a rotating wheel until at least 90% lysis was achieved. Spheroplasts were immediately pelleted at 1,000*g* at 4°C for 5 min in a centrifuge and washed twice with 1M sorbitol containing proteinase inhibitors. Spheroplasts were then resuspend in 1.2 mL of MNase digestion buffer [1M sorbitol, 50 mM NaCl, 10 mM Tris-HCl (pH7.5), 1 mM $CaCl_2$, 1 mM β-mercaptoethanol, 0.5 mM spermidine, 0.075% Nonidet P-40, 1 mM AEBSF, 7 μM Pepstatin and 20 μM E-64] and incubated at 37°C for 5 min.

To initiate the MNase digestion, 1.43 U of MNase (Thermo Scientific, 300U/µL) was added to each sample. After various time points, 200 µL of samples were removed and transferred to a microfuge tube containing 10 µL stop buffer (2.5 M EDTA/10%SDS). The DNA was extracted and purified by standard phenol/chloroform/isoamylalcohol procedures. Digested chromatin was analysed on a 2% agarose gel with ethidium bromide. Band intensities were quantified with ImageJ and analysed with GraphPad Prism software.

Morphological observations

Microscopy was performed by differential interference contrast (DIC) and epifluorescence microscopy with a Zeiss Axio-Imager Z1 microscope. Image analysis was carried out with the Zeiss AxioVision 4.8 software. DAPI staining of DNA was performed as previously described (Wurtele *et al*. 2010).

Multiple sequence alignments

Multiple sequence alignment of fungal proteins was performed by using Clustal Omega (http://www.ebi.ac.uk/Tools/msa/clustalo/). Secondary structure-based protein alignment was performed using ESpript (http://espript.ibcp.fr/ESPript/ESPript/; [58]. Mergealign was used to calculate the conservation of each residues: (http://mergealign.appspot.com).

2.6 Acknowledgements

ST was the recipient of Fonds de recherché santé (FRQS) postdoctoral fellowship. RG was the recipient of Mitacs Accelerate awards. Research in AV's laboratory was supported by funds from the "Fonds de Partenariat pour un Québec Innovant en Santé" (FPQIS). Authors also thank Eun-Hye Lee and Zhe Yin for technical assistance; M. Raymond for *C. albicans* plasmids pCaMPY-3HA-SAT1 and ASF1-/RTT109-GRACE strains; M.R. Singleton for pET-H3/H4 plasmid; P. Kaufman for the anti-Asf1 antibody.

2.7 Author contributions

Conceived and designed the experiments: ST, RG, AV; Performed the experiments: ST, RG, AL, PD, NA; Analyzed the data: ST, RG, PD, NA, AV; Contributed reagents/materials/analysis tools: PT and MR; Wrote the paper: ST, RG, HW, AV.

2.8 Supplementary information

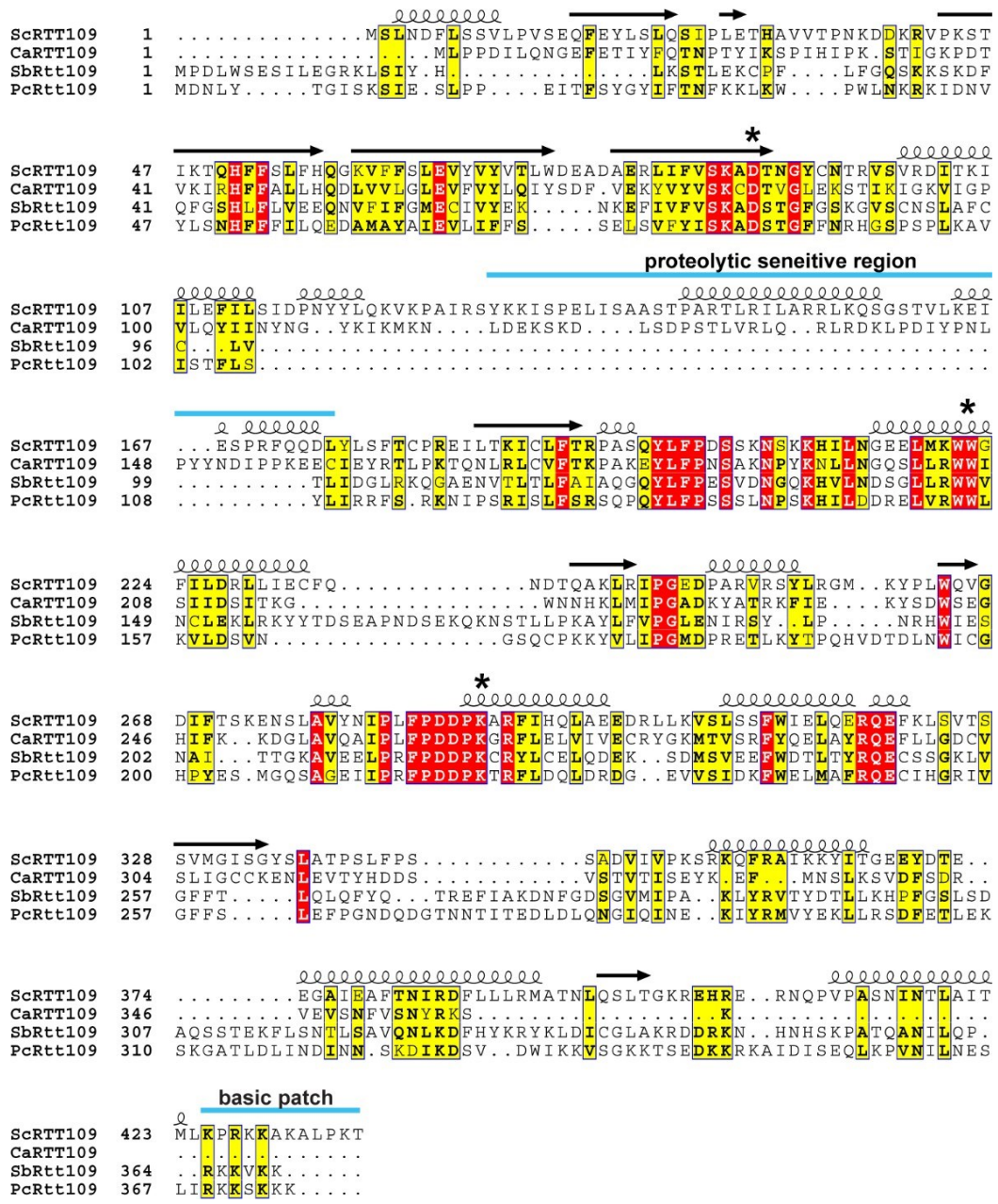

Figure 2.S1 Secondary structural alignment of fungal Rtt109.

Crystal structure of the full-length *S. cerevisiae* Rtt109 (PBD: 3Q66) was used as the template for structure-based sequence alignment with other fungal orthologs found in *C. albicans*, *S. pombe* and *P. carinii*. Secondary structures (α-helices or β-sheets) are indicated as spirals or arrows on the top of sequence alignment.

Table 2.S1 *C. albicans* strains, plasmids and primers used in this study

A. Strains used in this study

Description	Name	Genotype	Reference
WT	SN152	*ura3*::imm^{434}::*URA3/ura3*::imm^{434} *iro1::IRO1/iro1*::imm^{434} *his*1::hisG/*his1*::hisG *leu2/leu2 arg4/arg4*	Noble and Johnson 2005
*rtt109*Δ/Δ	*rtt109*Δ/Δ	As SN152, *rtt109*Δ*::C. dubliniensis ARG4/rtt109*Δ*::C. dubliniensis HIS1*	Wurtele *et al.* 2010
RTT109Rev	*rtt109*$^{Δ/Δ}$*::RTT109*	As *rtt109*$^{Δ/Δ}$, *RTT109-FRT/rtt109*Δ*::C. dubliniensis HIS1*	Wurtele *et al.* 2010
RTT109^{D82N}*#1*	CaST64	As *rtt109*$^{Δ/Δ}$, *RTT109D82N-FRT/ rtt109*Δ*::C. dubliniensis ARG4*	This study
RTT109^{D82N}*#2*	CaST67	As *rtt109*$^{Δ/Δ}$, *RTT109D82N-FRT/ rtt109*Δ*::C. dubliniensis ARG4*	This study
RTT109^{W206F}*#1*	CaST69	As *rtt109*$^{Δ/Δ}$, *RTT109W206F-FRT/ rtt109*Δ*::C. dubliniensis HIS1*	This study
RTT109^{W206F}*#2*	CaST71	As *rtt109*$^{Δ/Δ}$, *RTT109W206F-FRT/ rtt109*Δ*::C. dubliniensis ARG4*	This study
*vps75*Δ/Δ #1	CaST82	As SN152, *vps75*Δ*::C. dubliniensis ARG4/vps75*Δ*::C. dubliniensis HIS1*	This study
*vps75*Δ/Δ #2	CaST88	As SN152, *vps75*Δ*::C. dubliniensis ARG4/vps75*Δ*::C. dubliniensis HIS1*	This study
VPS75Rev#1	CaST99	As *vps75*$^{Δ/Δ}$, *VPS75-FRT/ rtt109*Δ*::C. dubliniensis HIS1*	This study
VPS75Rev#2	CaST101	As *vps75*$^{Δ/Δ}$, *VPS75-FRT/ rtt109*Δ*::C. dubliniensis ARG4*	This study
Asf1GRACE	*tetO-ASF1*/*asf1*Δ	*ura3::imm*^{434}*/ura3::imm*^{434} *his3::hisG/his3::hisG leu2::tetR-GAL4AD-URA/LEU2 asf1::HIS3/SAT1-tetp-ASF1*	Roemer *et al.* 2003

Rtt109GRACE	*tetO-RTT109/rtt109Δ*	*ura3::imm^{434}/ura3::imm^{434} his3::hisG/his3::hisG leu2::tetR-GAL4AD-URA/LEU2 rtt109::HIS3/SAT1-tetp-RTT109*	Wurtele *et al.* 2010
Rtt109-HA *vps75Δ/Δ* #1	CaST229	As CaST82 *rtt109-FRT/ RTT109-3xHA-SAT1*	This study
Rtt109-HA *vps75Δ/Δ* #2	CaST232	As CaST82 *rtt109-FRT/ RTT109-3xHA-SAT1*	This study
Rtt109-HA Vps75Rev#1	CaST237	As CaST99 *rtt109-FRT/ RTT109-3xHA-SAT1*	This study
Rtt109-HA Vps75Rev#2	CaST238	As CaST99 *rtt109-FRT/ RTT109-3xHA-SAT1*	This study

B. Plasmids used in this study

Plasmid	**Parent**	**Insert**	**Reference**
pMPY-3HA			Schneider *et al.* 2006
pCaMPY-3HA-SAT1	pMPY-3HA		This study
pSFS2A			Reuss *et al.* 2004
pRTT109Rev	pSFS2A		Wurtele *et al.* 2010
pRtt109D82N	pRTT109Rev	As pRTT109Rev, *RTT109^{D82N}*	This study
pRtt109W206F	pRTT109Rev	As pRTT109Rev, *RTT109^{W206F}*	This study
pVps75Rev	pSFS2A		This study
6HIS-TEV-pCDF-Duet1			Tang, Y. *et al* 2011
CaDuet-Rtt109	6HIS-TEV-pCDF-Duet1	Ca*RTT109*$^{L321S/L336S/L339S}$	This study
CaDuet-Rtt109-Vps75	6HIS-TEV-pCDF-Duet1	Ca*RTT109*$^{L321S/L336S/L339S}$, Ca*VPS75*	This study
pETDuet-H3-H4			Kingston, I. J *et al* 2011
pETDuet-H3K56R-H4	pCDFDuet-H3-H4	Sc*HHT1*^{K56R}	This study

Table 2.S2 Oligonucleotide primers used in this study

Oligos used for site-directed mutagenesis (5'->3')		
oST67	Rtt109D82NF	GTTTACGTATCCAAATGTAATACTGTTGGATTAGAAAAA
oST68	Rtt109D82NR	TTTTTCTAATCCAACAGTATTACATTTGGATACGTAAAC
oST69	Rtt109W206FF	GACAGTCTCTCTTGAGATGGTTTATATCAATAATTGATAG CAT
oST70	Rtt109W206FR	ATGCTATCAATTATTGATATAAACCATCTCAAGAGAGACT GTC
oST135	RTT109L321SF	GAGGTTACATATCACGATGATAGCGTTTCAACTGTGACAA TTTCA
oST136	RTT109L321SR	TGAAATTGTCACAGTTGAAACGCTATCATCGTGATATGTA ACCTC
oST137	RTT109L336SF	AATATAAAGAGTTTATGAACAGCTTGAAGCTGGTTGATTT TAG
oST138	RTT109L336SR	CTAAAATCAACCAGCTTCAAGCTGTTCATAAACTCTTTAT ATT
oST139	RTT109L339SF	GTTTATGAACAGCTTGAAGAGCGTTGATTTTAGTGATCGT
oST140	RTT109L339SR	ACGATCACTAAAATCAACGCTCTTCAAGCTGTTCATAAAC
oST282	ScH3K56RF	ATCAGCAGTTCGGTGCTTCTCTGAAAACGACGAATTTC
oST283	ScH3K56RR	GAAATTCGTCGTTTTCAGAGAAGCACCGAACTGCTGAT
Oligos used for cloning in pSFS2A (5'->3')		
oST86	VPS75DelUP	TTCAGTTTCAATTCTAAAAAATTATATTTTTCTTTCAAGTT TCACAATAACATATACGTATGTGGAATTGTGAGCGGATA
oST87	VPS75DelUP2	TTGAAAACGGAACGAAGAAAATAGGACCATCAAGAATA AAACACGTTTAGAAAGTCAATTTTCAGTTTCAATTCTAAA AA
oST88	VPS75DelDN	CTTTCATATAGTCAACTTATTAAATACTATCTGCTATATAT ACAGACCTGAGTAATTCTTGTTTTCCCAGTCACGACGTT
oST89	VPS75DelDN2	TTGATTGCAGTTGCAGTCGATGGGACAAGTGTGCAAAAA TGAATTTCTGAAATACATTTACTTTCATATAGTCAACTTAT
oST108	VPS75RevUPSA	CGATCCGCGGGCCCACAATGGGAGAGAAACTCATCCAAA
oST109	VPS75RevUPN	GCATGAAGCGGCCGCTCCCGGACTCTTGCGAGAGCTTTAC
oST110	VPS75RevDNX	GCATGACTCGAGACTCACTTTTAAATCCAAAGACGAT
oST111	VPS75RevDNA	TGAATAGGGCCCCAAATAGCTCCGGTGCACCTTGATC
Oligos used for cloning for protein expression (5'->3')		
oST149	RTT109BHF	CGATATGGATCCATGCTTCCTCCAGATATATTAC
oST150	RTT109SlR	CGATCCCGTCGACCTATTTTGATTTTCTATAATTACTTAC
oST155	VPS75BHF	CGATATGGATCCATGACAGAGAAAGATGAAGGAAAACG
oST156	VPS75SlR	CGATCCCGTCGACTTATTTGGATTTTTTTGTCGCATGTTC
Construction of the HA tagging plasmid (pMPY-SAT1)		

oMR1837	ACT1TF	GCGTCTAGATAGTAAGAGTGAAATTCTGGAAATCTGGAAA
oMR1838	URA3TR	CGCGGGCCCCTGCAGGACCACCTTTGATTGTAAA
Primer for Rtt109 HA tagging		
oST159	RTT109HATagF	GTTGATTTTAGTGATCGTGTTGAAGTTAGTAATTTTGTAA GTAATTATAGAAAATCAAAAAGGGAACAAAAGCTGG
oST160	RTT109HATagF2	TCTGGTTTCAACTGTGACAATTTCAGAATATAAAGAGTTT ATGAACCTGTTGAAGCTGGTTGATTTTAGTGATCGTGT
oST161	RTT109HATagR	CCCAGGTTTTAATCGAACTGGCCCCAATGCAATTACGTAT CGTGTGAGGTTATCGTCGATCTATAGGGCGAATTGG
oST162	RTT109HATagR2	CATCTATACTCTAATCACAATATATGATAAAATAATGACA GAGGTCAAGACCAATCGGTCCCAGGTTTTAATCGAACT

2.9 References

1) Abshiru, Ippersiel, Tang, Yuan, Marmorstein *et al.*, 2013 Chaperone-mediated acetylation of histones by Rtt109 identified by quantitative proteomics. J Proteomics 81**:** 80-90.
2) Baell, and Miao, 2016 Histone acetyltransferase inhibitors: where art thou? Future Med Chem 8**:** 1525-1528.
3) Berndsen, Tsubota, Lindner, Lee, Holton *et al.*, 2008 Molecular functions of the histone acetyltransferase chaperone complex Rtt109-Vps75. Nat Struct Mol Biol 15**:** 948-956.
4) Bongomin, Gago, Oladele and Denning, 2017 Global and Multi-National Prevalence of Fungal Diseases-Estimate Precision. J Fungi (Basel) 3.
5) Celic, Masumoto, Griffith, Meluh, Cotter *et al.*, 2006 The sirtuins hst3 and Hst4p preserve genome integrity by controlling histone h3 lysine 56 deacetylation. Curr Biol 16**:** 1280-1289.
6) D'arcy, and Luger, 2011 Understanding histone acetyltransferase Rtt109 structure and function: how many chaperones does it take? Curr Opin Struct Biol 21**:** 728-734.
7) Dahlin, Kottom, Han, Zhou, Walters *et al.*, 2014 Pneumocystis jirovecii Rtt109, a novel drug target for Pneumocystis pneumonia in immunosuppressed humans. Antimicrob Agents Chemother 58**:** 3650-3659.
8) Dahlin, Nelson, Strasser, Barsyte-Lovejoy, Szewczyk *et al.*, 2017 Assay interference and off-target liabilities of reported histone acetyltransferase inhibitors. Nat Commun 8**:** 1527.
9) Dahlin, Sinville, Solberg, Zhou, Han *et al.*, 2013 A cell-free fluorometric high-throughput screen for inhibitors of Rtt109-catalyzed histone acetylation. PLoS One 8**:** e78877.
10) Driscoll, Hudson and Jackson, 2007 Yeast Rtt109 promotes genome stability by acetylating histone H3 on lysine 56. Science 315**:** 649-652.

11) Drogaris, Villeneuve, Pomies, Lee, Bourdeau *et al.*, 2012 Histone deacetylase inhibitors globally enhance h3/h4 tail acetylation without affecting h3 lysine 56 acetylation. Sci Rep 2**:** 220.
12) Drogaris, Wurtele, Masumoto, Verreault and Thibault, 2008 Comprehensive profiling of histone modifications using a label-free approach and its applications in determining structure-function relationships. Anal Chem 80**:** 6698-6707.
13) Edmondson, and Russell, 1996 Evaluation of matrix-assisted laser desorption ionization-time-of-flight mass measurement accuracy by using delayed extraction. J Am Soc Mass Spectrom 7**:** 995-1001.
14) English, Adkins, Carson, Churchill and Tyler, 2006 Structural basis for the histone chaperone activity of Asf1. Cell 127**:** 495-508.
15) Fillingham, Recht, Silva, Suter, Emili *et al.*, 2008 Chaperone control of the activity and specificity of the histone H3 acetyltransferase Rtt109. Mol Cell Biol 28**:** 4342-4353.
16) Garnaud, Champleboux, Maubon, Cornet and Govin, 2016 Histone Deacetylases and Their Inhibition in Candida Species. Front Microbiol 7**:** 1238.
17) Guillemette, Drogaris, Lin, Armstrong, Hiragami-Hamada *et al.*, 2011 H3 lysine 4 is acetylated at active gene promoters and is regulated by H3 lysine 4 methylation. PLoS Genet 7**:** e1001354.
18) Han, Zhou, Horazdovsky, Zhang, Xu *et al.*, 2007a Rtt109 acetylates histone H3 lysine 56 and functions in DNA replication. Science 315**:** 653-655.
19) Han, Zhou, Li, Xu and Zhang, 2007b Acetylation of lysine 56 of histone H3 catalyzed by RTT109 and regulated by ASF1 is required for replisome integrity. J Biol Chem 282**:** 28587-28596.
20) Hnisz, Majer, Frohner, Komnenovic and Kuchler, 2010 The Set3/Hos2 histone deacetylase complex attenuates cAMP/PKA signaling to regulate morphogenesis and virulence of Candida albicans. PLoS Pathog 6**:** e1000889.
21) Hnisz, Tscherner and Kuchler, 2011 Targeting chromatin in fungal pathogens as a novel therapeutic strategy: histone modification gets infectious. Epigenomics 3**:** 129-132.
22) Kaplan, Liu, Erkmann, Holik, Grunstein *et al.*, 2008 Cell cycle- and chaperone-mediated regulation of H3K56ac incorporation in yeast. PLoS Genet 4**:** e1000270.
23) Keck, and Pemberton, 2011 Interaction with the histone chaperone Vps75 promotes nuclear localization and HAT activity of Rtt109 in vivo. Traffic 12**:** 826-839.
24) Kelly, Rowan, Mccann and Kavanagh, 2009 Exposure to caspofungin activates Cap and Hog pathways in Candida albicans. Med Mycol 47**:** 697-706.
25) Kingston, Yung and Singleton, 2011 Biophysical characterization of the centromere-specific nucleosome from budding yeast. J Biol Chem 286**:** 4021-4026.
26) Kottom, Han, Zhang and Limper, 2011 Pneumocystis carinii expresses an active Rtt109 histone acetyltransferase. Am J Respir Cell Mol Biol 44**:** 768-776.

27) Kuchler, Jenull, Shivarathri and Chauhan, 2016 Fungal KATs/KDACs: A New Highway to Better Antifungal Drugs? PLoS Pathog 12**:** e1005938.
28) Kuo, and Andrews, 2013 Quantitating the specificity and selectivity of Gcn5-mediated acetylation of histone H3. PLoS One 8**:** e54896.
29) Kushnirov, 2000 Rapid and reliable protein extraction from yeast. Yeast 16**:** 857-860.
30) Lasko, Jakob, Edalji, Qiu, Montgomery *et al.*, 2017 Discovery of a selective catalytic p300/CBP inhibitor that targets lineage-specific tumours. Nature 550**:** 128-132.
31) Lercher, Danilenko, Kirkpatrick and Carlomagno, 2017 Structural characterization of the Asf1-Rtt109 interaction and its role in histone acetylation. Nucleic Acids Res.
32) Li, Robbins, O'meara and Cowen, 2017 Extensive functional redundancy in the regulation of Candida albicans drug resistance and morphogenesis by lysine deacetylases Hos2, Hda1, Rpd3 and Rpd31. Mol Microbiol 103**:** 635-656.
33) Loll-Krippleber, D'enfert, Feri, Diogo, Perin *et al.*, 2014 A study of the DNA damage checkpoint in Candida albicans: uncoupling of the functions of Rad53 in DNA repair, cell cycle regulation and genotoxic stress-induced polarized growth. Mol Microbiol 91**:** 452-471.
34) Lopes Da Rosa, Bajaj, Spoonamore and Kaufman, 2013 A small molecule inhibitor of fungal histone acetyltransferase Rtt109. Bioorg Med Chem Lett 23**:** 2853-2859.
35) Lopes Da Rosa, Boyartchuk, Zhu and Kaufman, 2010 Histone acetyltransferase Rtt109 is required for Candida albicans pathogenesis. Proc Natl Acad Sci U S A 107**:** 1594-1599.
36) Lopes Da Rosa, and Kaufman, 2012 Chromatin-mediated Candida albicans virulence. Biochim Biophys Acta 1819**:** 349-355.
37) Manoharlal, Gaur, Panwar, Morschhauser and Prasad, 2008 Transcriptional activation and increased mRNA stability contribute to overexpression of CDR1 in azole-resistant Candida albicans. Antimicrob Agents Chemother 52**:** 1481-1492.
38) Masumoto, Hawke, Kobayashi and Verreault, 2005 A role for cell-cycle-regulated histone H3 lysine 56 acetylation in the DNA damage response. Nature 436**:** 294-298.
39) Mccullough, and Marmorstein, 2016 Molecular Basis for Histone Acetyltransferase Regulation by Binding Partners, Associated Domains, and Autoacetylation. ACS Chem Biol 11**:** 632-642.
40) Miknis, Stevens, Smith, Ostrov and Churchill, 2015 Development of novel Asf1-H3/H4 inhibitors. Bioorg Med Chem Lett 25**:** 963-968.
41) Noble, and Johnson, 2005 Strains and strategies for large-scale gene deletion studies of the diploid human fungal pathogen Candida albicans. Eukaryot Cell 4**:** 298-309.
42) O'meara, Robbins and Cowen, 2017 The Hsp90 Chaperone Network Modulates Candida Virulence Traits. Trends Microbiol 25**:** 809-819.
43) Pfaller, Messer, Georgopapadakou, Martell, Besterman *et al.*, 2009 Activity of MGCD290, a Hos2 histone deacetylase inhibitor, in combination with

azole antifungals against opportunistic fungal pathogens. J Clin Microbiol 47**:** 3797-3804.
44) Pfaller, Rhomberg, Messer and Castanheira, 2015 In vitro activity of a Hos2 deacetylase inhibitor, MGCD290, in combination with echinocandins against echinocandin-resistant Candida species. Diagn Microbiol Infect Dis 81**:** 259-263.
45) Radovani, Cadorin, Shams, El-Rass, Karsou *et al.*, 2013 The carboxyl terminus of Rtt109 functions in chaperone control of histone acetylation. Eukaryot Cell 12**:** 654-664.
46) Recht, Tsubota, Tanny, Diaz, Berger *et al.*, 2006 Histone chaperone Asf1 is required for histone H3 lysine 56 acetylation, a modification associated with S phase in mitosis and meiosis. Proc Natl Acad Sci U S A 103**:** 6988-6993.
47) Robbins, Leach and Cowen, 2012 Lysine deacetylases Hda1 and Rpd3 regulate Hsp90 function thereby governing fungal drug resistance. Cell Rep 2**:** 878-888.
48) Robbins, Wright and Cowen, 2016 Antifungal Drugs: The Current Armamentarium and Development of New Agents. Microbiol Spectr 4.
49) Roemer, Jiang, Davison, Ketela, Veillette *et al.*, 2003 Large-scale essential gene identification in Candida albicans and applications to antifungal drug discovery. Mol Microbiol 50**:** 167-181.
50) Sanematsu, Takami, Barman, Fukagawa, Ono *et al.*, 2006 Asf1 is required for viability and chromatin assembly during DNA replication in vertebrate cells. J Biol Chem 281**:** 13817-13827.
51) Sauve, 2008 NAD+ and vitamin B3: from metabolism to therapies. J Pharmacol Exp Ther 324**:** 883-893.
52) Schneider, Bajwa, Johnson, Bhaumik and Shilatifard, 2006 Rtt109 is required for proper H3K56 acetylation: a chromatin mark associated with the elongating RNA polymerase II. J Biol Chem 281**:** 37270-37274.
53) Shi, Wang, Zheng, Lee and Wang, 2007 Critical role of DNA checkpoints in mediating genotoxic-stress-induced filamentous growth in Candida albicans. Mol Biol Cell 18**:** 815-826.
54) Smith, and Edlind, 2002 Histone deacetylase inhibitors enhance Candida albicans sensitivity to azoles and related antifungals: correlation with reduction in CDR and ERG upregulation. Antimicrob Agents Chemother 46**:** 3532-3539.
55) Stevenson, and Liu, 2011 Regulation of white and opaque cell-type formation in Candida albicans by Rtt109 and Hst3. Mol Microbiol 81**:** 1078-1091.
56) Su, Hu, Zhou, Thompson, Xu *et al.*, 2011 Structure and histone binding properties of the Vps75-Rtt109 chaperone-lysine acetyltransferase complex. J Biol Chem 286**:** 15625-15629.
57) Su, Lu and Liu, 2016 N-acetylglucosamine sensing by a GCN5-related N-acetyltransferase induces transcription via chromatin histone acetylation in fungi. Nat Commun 7**:** 12916.
58) Tanae, Horiuchi, Matsuo, Katayama and Kawamukai, 2012 Histone chaperone Asf1 plays an essential role in maintaining genomic stability in fission yeast. PLoS One 7**:** e30472.

59) Tang, Holbert, Delgoshaie, Wurtele, Guillemette *et al.*, 2011 Structure of the Rtt109-AcCoA/Vps75 complex and implications for chaperone-mediated histone acetylation. Structure 19**:** 221-231.
60) Tang, Holbert, Wurtele, Meeth, Rocha *et al.*, 2008 Fungal Rtt109 histone acetyltransferase is an unexpected structural homolog of metazoan p300/CBP. Nat Struct Mol Biol 15**:** 738-745.
61) Tsao, Rahkhoodaee and Raymond, 2009 Relative contributions of the Candida albicans ABC transporters Cdr1p and Cdr2p to clinical azole resistance. Antimicrob Agents Chemother 53**:** 1344-1352.
62) Tscherner, Zwolanek, Jenull, Sedlazeck, Petryshyn *et al.*, 2015 The Candida albicans Histone Acetyltransferase Hat1 Regulates Stress Resistance and Virulence via Distinct Chromatin Assembly Pathways. PLoS Pathog 11**:** e1005218.
63) Tsubota, Berndsen, Erkmann, Smith, Yang *et al.*, 2007 Histone H3-K56 acetylation is catalyzed by histone chaperone-dependent complexes. Mol Cell 25**:** 703-712.
64) Wurtele, Tsao, Lepine, Mullick, Tremblay *et al.*, 2010 Modulation ofhistone H3 lysine 56 acetylation as an antifungal therapeutic strategy. Nat Med 16**:** 774-780.

Chapter 3

Canonical and non-canonical metabolic fates of nicotinamide in the fungal pathogen *Candida albicans*

Canonical and non-canonical metabolic fates of nicotinamide in the fungal pathogen *Candida albicans*

Short title: Metabolic fates of nicotinamide in *Candida albicans*

Rahul Ghugari*[1], Sarah Tsao*[1], Mark Schmidt[2], Éric Bonneil[1], Martine Raymond[1, 3], Charles Brenner[2] and Alain Verreault[1, 4, #]

[1] Institute for Research in Immunology and Cancer, Université de Montréal, Montreal, QC, Canada

[2] Department of Biochemistry, Carver College of Medicine, University of Iowa, Iowa City, Iowa, USA

[3] Département de Biochimie, Université de Montréal, Montréal, QC, Canada

[4] Département de Pathologie et Biologie Cellulaire, Université de Montréal, Montréal, QC, Canada

* These authors contributed equally to this work

Corresponding author: Alain Verreault, Institute for Research in Immunology and Cancer, Université de Montréal, P.O. Box 6128, Station Centre-Ville, Montreal, QC, Canada H3C 3J7. Phone: +1 (514) 706-9667. Fax: (514) 343-5839. E-mail: alain.verreault@umontreal.ca

3.1 Abstract

Candida albicans is a fungal pathogen that causes systemic infections and mortality in immunosuppressed individuals. We previously demonstrated that deacetylation of histone H3 lysine 56 by Hst3 is essential for *C. albicans* viability. Hst3 is a member of the sirtuin family of NAD^+-dependent deacetylases and, as expected of a sirtuin, our previous studies showed that Hst3 is inhibited by nicotinamide (NAM). However, supra-physiological concentrations (SPCs) of NAM (2-3mM) are required for NAM's cytotoxicity in *C. albicans*. Based on this, we speculated that a thorough understanding of NAM's metabolic fate might help uncover strategies to enhance its therapeutic potential.

Here, we demonstrate that *C. albicans* can synthesize NAD^+ through conversion of NAM into nicotinate (NA) catalyzed by the fungal-specific nicotinamidase Pnc1. NA then serves as precursor of NAD^+ through the canonical Preiss-Handler salvage pathway. Unexpectedly, we found that cells lacking Pnc1 were, at best, mildly sensitive to NAM. This suggested the existence of non-canonical fates for NAM. Using heavy isotope labeling and mass spectrometry, we provide evidence for the existence of two non-canonical fates for NAM. First, non-canonical incorporation of NAM into NAD^+ occurred through sirtuin-dependent NAM exchange, a well-established reaction by which NAM inhibits sirtuins by reacting with a deacetylation intermediate and regenerating NAD^+. The second non-canonical fate of NAM was its incorporation into NMN, an immediate precursor of NAD^+. Collectively, our results suggest that supra-physiological NAM concentrations lead to at least two distinct fates for NAM. We discuss the implications of these findings on the cytotoxicity of NAM and future improvements of NAM's therapeutic potential.

3.2 Introduction

Candida albicans is an opportunistic fungal pathogen that normally resides in the mouth, throat, and the gastrointestinal and urogenital tracts of healthy individuals. *C. albicans* causes vulvovaginal infections that are not life-threatening, but nonetheless very painful and often recurrent (Pfaller and Diekema 2010; Kim and Sudbery 2011; Neville *et al.* 2015; Jabra-Rizk *et al.* 2016). In addition, *C. albicans* can instigate oropharyngeal infections in AIDS patients, and systemic infections in immunocompromised individuals suffering from HIV infections, patients treated with cancer chemotherapeutic agents or patients deliberately immunosuppressed in preparation for hematopoietic stem cell or solid organ transplantation (Pfaller and Diekema 2010; Kim and Sudbery 2011; Neville *et al.* 2015; Jabra-Rizk *et al.* 2016). In patients with crippled immunity, systemic dissemination of *C. albicans* and invasion of vital organs can result in considerable morbidity or mortality (Pfaller and Diekema 2010; Kim and Sudbery 2011). Cases of invasive fungal infections have steadily augmented over time due to the increased number of patients needing cancer chemotherapy or hematopoietic stem cell transplantation (Segal *et al.* 2006; Pfaller and Diekema 2007). Following bacterial infections caused by *Staphylococcal* and *Enterococcal* species, invasive *C. albicans* infections are the most common cause of bloodstream infections in the United States (Pfaller and Diekema 2010; Antinori *et al.* 2016). In immunocompromised patients, mortality rates resulting from invasive *C. albicans* infections can reach as much as 40% (Low and Rotstein 2011). The repertoire of therapeutic antifungal agents is rather limited. Only four chemically distinct classes of therapeutic agents are currently available to treat invasive fungal infections: flucytosine, polyenes, azoles and echinocandins. Unfortunately, none of them is without limitations (Kuchler *et al.* 2016). Echinocandins and third generation triazoles have enhanced the therapeutic efficiency of antifungal agents, but the mortality rates associated with invasive infections have not improved accordingly (Pasqualotto and Denning 2008; Robbins *et al.* 2016). In addition, non-optimal routes of administration and limited spectrum of activity against different fungal pathogens often limit the use of some antifungal agents (Brown *et al.* 2012). Azoles are most frequently used to treat fungal infections because they are administered orally and some of the azole compounds

are relatively inexpensive. These issues are particularly salient in developing countries where *C. albicans* infections are widespread. Unfortunately, the emergence of azole-resistant strains is facilitated by the fact that azoles are cytostatic, rather than cytocidal compounds.

In eukaryotic cells DNA is packaged into chromatin, which consists of repeating units known as nucleosome core particles (NCPs) that are connected to each other by linker DNA. Each NCP is composed of 147 base pairs of DNA wrapped around an octamer of histone proteins that consists of two molecules each of H2A, H2B, H3 and H4 (Davey *et al.* 2002). A number of studies indicate that covalent modifications of histones exert a major influence on the virulence of fungal pathogens. Targeting enzymes that covalently modify histones represents a novel therapeutic strategy (Pfaller *et al.* 2009; Lopes Da Rosa and Kaufman 2013; Pfaller *et al.* 2015; Kuchler *et al.* 2016). Compelling evidence indicates that histone acetyltransferases (HATs) and histone deacetylases (HDACs) influence fungal virulence by perturbing profiles of histone acetylation (Lopes Da Rosa *et al.* 2010; Wurtele *et al.* 2010; Hnisz *et al.* 2011; Dahlin *et al.* 2014; Nobile *et al.* 2014). In *C. albicans,* modulation of histone H3 lysine 56 acetylation (H3K56ac) affects virulence and viability (Lopes Da Rosa *et al.* 2010; Wurtele *et al.* 2010). H3K56 is acetylated and deacetylated by Rtt109 (HAT) and Hst3 (HDAC), two enzymes with fungal-specific properties. While there were worthwhile efforts to screen for small molecules that inhibit the HAT Rtt109 (Dahlin *et al.* 2013; Lopes Da Rosa *et al.* 2013), we propose that inhibition of the HDAC Hst3 is also an appealing strategy to uncover novel antifungal agents. Hst3 is a deacetylase of the sirtuin family that, in addition to K56-acetylated H3, requires nicotinamide adenine dinucleotide (NAD^+) as co-substrate (Celic *et al.* 2006; Hachinohe *et al.* 2011). During the deacetylation reaction, the acetyl group is transferred from H3K56 to the ADP-ribose moiety of NAD^+ and the remaining portion of NAD^+ is released as free nicotinamide (NAM). In turn, NAM is an inhibitor of the deacetylase activity of

Hst3 and other sirtuins (Landry *et al.* 2000; Jackson *et al.* 2003; Sauve and Schramm 2003). When *C. albicans* cells are exposed to 2-3mM NAM, Hst3 inhibition results in hyperacetylation of H3K56, abnormal morphological transitions and either cell death or a prolonged delay in cell division (Wurtele *et al.* 2010). Furthermore, in a mouse model of systemic infections, NAM attenuated *C. albicans* virulence and reduced fungal invasion of the kidneys and the heart (Wurtele *et al.* 2010).

NAM meets some of the key criteria required of an effective antifungal agent (Chapman *et al.* 2008). First, NAM exhibits a broad spectrum of antifungal activity. For instance, NAM inhibits the growth of azole- or echinocandin-resistant clinical isolates of *C. albicans*, other *Candida* species, and even *Aspergillus fumigatus* (Wurtele *et al.* 2010). Second, the anti-fungal properties of NAM are exerted, at least in part, through inhibition of Hst3, a sirtuin with fungal-specific properties that is essential for *C. albicans* viability (Wurtele *et al.* 2010). Third, unlike echinocandins, NAM can be administered orally. Fourth, NAM is FDA-approved as a food supplement and clinical trials for a number of human conditions demonstrated that oral administration of high daily doses of NAM, up to 3-5 grams a day for up to several weeks, results in minimal side effects (Knip *et al.* 2000; Mackay *et al.* 2012; Lenglet *et al.* 2013; Libri *et al.* 2014). The fact that NAM is well tolerated is, at least in part, because it is readily absorbed by human cells and incorporated into NAD^+-related metabolites that cannot inhibit sirtuins or other important enzymes that also consume NAD^+ and generate NAM as product [*e.g.* mono- and poly-ADP ribosyltransferases and ADP-ribosyl cyclase] (Rankin *et al.* 1989; Banasik *et al.* 1990; Donnelly *et al.* 1995).

Although the results of pharmacokinetic studies are difficult to compare owing to differences in experimental approaches and instrumentation, peak NAM concentrations in plasma were reported to range from 0.125 mM to 1.6 mM

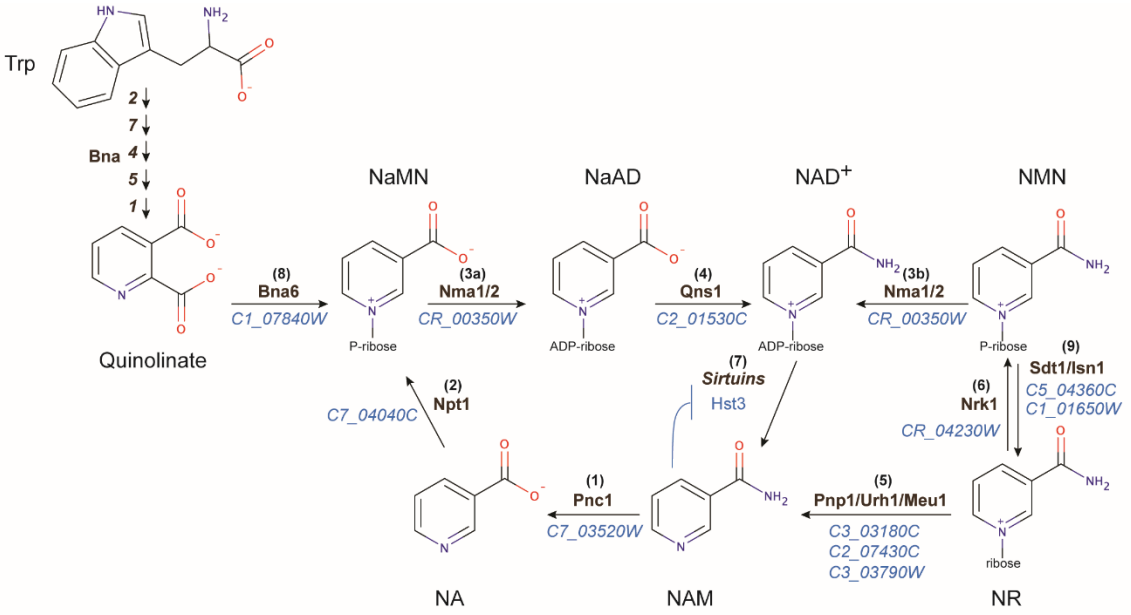

Figure 3.1 Enzymes involved in yeast NAM and NAD$^+$ metabolism

S. cerevisiae enzymes are listed above the arrows and numbered. *C. albicans* genes that encode sequence homologues of *S. cerevisisae* enzymes are indicated in pale grey below the arrows. In *S. cerevisiae*, nicotinamide adenine dinucleotide (NAD$^+$) can be synthesized via three pathways: a *de novo* pathway and two salvage pathways that recycle the different forms of vitamin B_3 known as nicotinamide (NAM), nicotinate/nicotinic acid (NA) and nicotinamide riboside (NR). The first portion of the *de novo* pathway, also known as the kynurenine pathway, converts tryptophan (Trp) through a series of reactions catalyzed by Bna enzymes, culminating in Bn6-catalyzed formation of nicotinic acid mononucleotide (NaMN) **(8)**.

The canonical salvage pathway recycles NAM and NA to produce NAD$^+$. The first step is the deamidation of NAM to produce NA, which is catalyzed by the nicotinamidase Pnc1 **(1)**. This is followed by the conversion of NA into NaMN catalyzed by Npt1 **(2)**. The *de novo* and canonical salvage pathways merge at NaMN, and subsequently share two reactions: adenylation of NaMN catalyzed by either Nma1 or Nma2 in *S. cerevisiae* produces nicotinic acid adenine dinucleotide (NaAD) **(3a)**, and amidation of NaAD to generate NAD$^+$ **(4)**, a reaction catalyzed by the NAD$^+$ synthetase Qns1.

The nicotinamide riboside (NR) salvage pathway begins by conversion of NR into nicotinamide mononucleotide (NMN), a reaction catalyzed by the NR kinase Nrk1 **(6)**. This is followed by adenylation of NMN to produce NAD$^+$, which is catalyzed by either Nma1, Nma2 or Pof1 in *S. cerevisiae* **(3b)**. Alternatively, conversion of NR into NAM by the nucleosidase Urh1 or the phosphorylases Pnp1 and, to a lesser extent Meu1 **(5),** provides a conduit for the NAM moiety of NR to enter the canonical salvage pathway described above for NAM and NA. The 5'-nucleotidases Sdt1 and Isn1 hydrolyze the phosphate group of NMN to generate the nucleoside NR **(9)**. Sirtuins such as Hst3 **(7)** require NAD$^+$ as a substrate to deacetylate proteins, and one of their reaction products is NAM. NAM can also act as a sirtuin inhibitor through the so-called NAM exchange reaction.

(Horsman *et al.* 1993; Dragovic *et al.* 1995; Stratford *et al.* 1996; Lenglet *et al.* 2013; Libri *et al.* 2014). Unfortunately, high concentrations of NAM (2-3 mM) are necessary to inhibit the growth of *C. albicans in vitro* (Wurtele *et al.* 2010).

In *S. cerevisiae*, the first step of NAM salvage to generate NAD^+ is NAM deamidation by the nicotinamidase Pnc1 (Fig 3.1, reaction **1**) (Preiss and Handler 1958). This reaction generates nicotinate (NA) (Ghislain *et al.* 2002) that, in turn, serves as precursor for biogenesis of NAD^+ through the canonical pathway for salvage of NA, known as the Preiss-Handler pathway (Fig 3.1, reactions **2-4**) (Preiss and Handler 1958). This pathway exists in *Candida albicans* (Chaffin et al. 1979), *Candida glabrata* (Ma *et al.* 2007) and, based on evolutionary conservation of the enzymes involved, likely exists in other fungal pathogens (Gossmann *et al.* 2012). Given its relatively short half-life in circulation, a possible strategy to enhance the therapeutic potential of NAM would be to exploit nutritional or pharmacological means to delay or completely block the conversion of NAM into NA by the pathogen. For instance, an appealing pharmacological strategy would be to inhibit the nicotinamidase Pnc1, an enzyme that does not exist in humans (Gazzaniga *et al.* 2009). There are crystal structures of Pnc1 and several nicotinaldehyde and NAM derivatives inhibit fungal nicotinamidases (French *et al.* 2010; Smith *et al.* 2012). Thus, inhibitors of Pnc1 may enhance the therapeutic potential of NAM simply by augmenting its intracellular concentration above the threshold required for robust inhibition of Hst3 and hyperacetylation of H3K56 (Wurtele *et al.* 2010).

Instead of employing Pnc1 inhibitors that may have off-target effects, we investigated the possibility of augmenting NAM's cytotoxicity with a genetic approach. First, we showed that the Pnc1-dependent canonical pathway to salvage NAM and NA in fungi does exist in the pathogen *C. albicans*. We unexpectedly found that cells lacking Pnc1 were, at best, mildly sensitive to NAM. In an effort to

understand why *pnc1* null mutants were not strongly sensitive to NAM, we discovered that cells lacking Pnc1 were capable of incorporating NAM into NMN and NAD^+ in media containing near physiological NAM concentrations (0.1mM). This is unprecedented in *C. albicans*. We show that a first mechanism for non-canonical incorporation of NAM into NAD^+ results from the so-called NAM exchange reaction that inhibits the deacetylase activity of sirtuins. In contrast, the second mechanism involves incorporation of NAM into NMN is unlikely to occur via the NAM exchange reaction. We discuss how the existence of these mechanisms might influence intracellular NAM concentrations and, therefore, its cytotoxicity and therapeutic potential.

3.3 Results

PNC1 deletion mildly sensitizes *C. albicans* to NAM

Jacobson and colleagues demonstrated that *C. albicans* possesses a *de novo* pathway that employs tryptophan to generate NAD^+, and a canonical NAM salvage pathway (Chaffin *et al.* 1979). In addition, the nicotinamide riboside (NR) salvage pathway and many of the *C. albicans* enzymes involved in NAD^+ biosynthesis were not known at the time. Based on amino sequence similarity, we found that the *C. albicans* genome likely encodes all the enzymes involved in the *de novo* NAD^+ biosynthetic pathway, the canonical salvage pathway for NAM and NA, and the NR salvage pathway (Fig 3.1). A sequence homology search identified a single *C. albicans* gene that likely encodes the nicotinamidase Pnc1. *C. albicans* Pnc1 shares a considerable degree of amino acid sequence similarity with *S. cerevisiae* Pnc1 and a triad of catalytic residues that are crucial for nicotinamidase activity (Fig 3.S1F) (Smith *et al.* 2012). To study the phenotypes of cells lacking Pnc1, a homozygous null mutant hereafter referred to as *pnc1*Δ/Δ was generated by replacing both alleles of the *PNC1* gene by *HIS1* and *ARG4* (Noble and Johnson 2005). Our working hypothesis was that, when challenged with supra-physiological

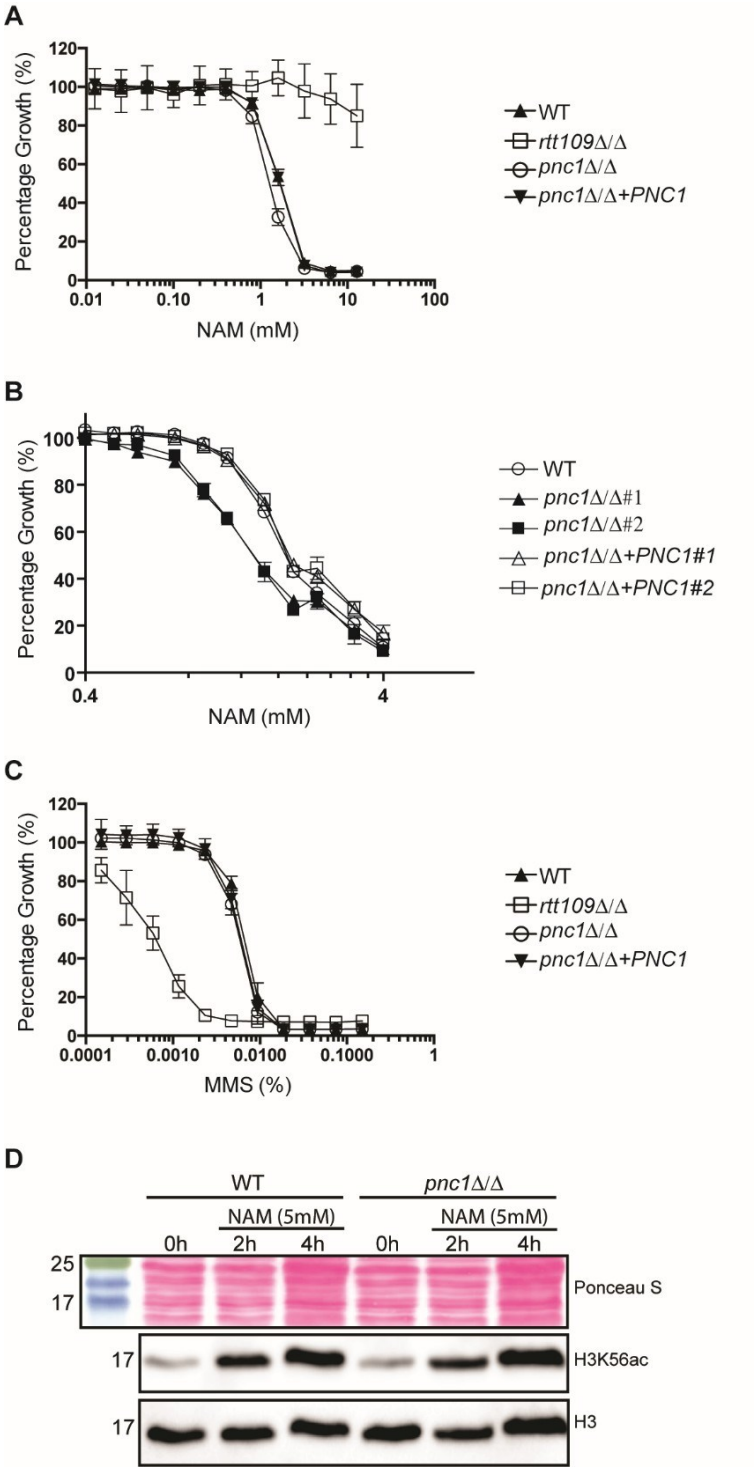

Figure 3.2. Cells lacking Pnc1 are mildly sensitive to NAM, but insensitive to MMS

(A-C) Growth inhibition assays in liquid cultures. Strains were grown at 30°C for 24h in SC-Niacin medium containing increasing concentrations of either NAM (A and B) or MMS (C) prior to measuring the optical density at 595nm (OD595). The percentage growth is the

ratio of OD595 values in wells containing either NAM or MMS over the OD595 values of control wells lacking those chemicals.

(D) Wild-type (WT) cells and *pnc1*Δ/Δ mutants grown in SC-Niacin were exposed to 5mM NAM for 0 hour (aliquots of cells were harvested prior to the addition of NAM), 2 or 4 hours at 30□C. Whole-cell lysates were analyzed by immunoblotting with antibodies against K56-acetylated histone H3 (H3K56ac) or non-modified H3 as loading control. Ponceau S staining of the nitrocellulose membrane served as a second loading control.

concentrations of NAM, cells lacking Pnc1 would accumulate significantly higher NAM concentrations than wild-type cells and the resulting inhibition of the sirtuin Hst3 would sensitize *pnc1*Δ/Δ cells to NAM. To test this hypothesis, liquid cultures of wild-type and *pnc1*Δ/Δ cells were grown in synthetic medium lacking NAM, NA and NR (SC-niacin medium). We found that *pnc1*Δ/Δ cells are, at best, mildly sensitive to NAM (Fig 3.2A, and 3.S4A); the NAM sensitivity of cells lacking Pnc1 was most striking over a narrow range of NAM concentrations (0.4 to 4mM NAM, Fig 3.2B). In contrast to wild-type and *pnc1*Δ/Δ cells, *rtt109*Δ/Δ mutants were resistant to NAM over a broad range of NAM concentrations (Fig 3.2A and 3.S4A). Because *C. albicans* cells lacking Rtt109 cannot acetylate H3-K56 (Lopes Da Rosa *et al.* 2010; Wurtele *et al.* 2010), their significant resistance to NAM suggests that the cytotoxicity of high NAM concentrations in wild-type cells is mainly caused by hyperacetylation of H3-K56.

We observed that the *PNC1* RNA was reproducibly induced when wild-type cells were treated with the alkylating agent methyl methane sulphonate (MMS, data not shown). This result suggested that Pnc1-mediated conversion of NAM into NA might occur more efficiently in response to DNA damage. We felt that this was of interest because we have evidence that inhibition of Hst3 with NAM causes DNA damage. Based on the above, it seemed formally possible that an increase in the abundance of Pnc1 following DNA damage might mitigate NAM cytotoxicity. However, this proved incorrect because mutant cells lacking Pnc1 were not more sensitive to MMS than wild-type cells (Fig 3.2C). We also constructed two independent *PNC1* revertants (*pnc1*Δ/Δ+*PNC1* #1 and #2 in Fig 3.2B) in which

one copy of the wild-type *PNC1* gene was re-introduced to its original locus to generate heterozygous *pnc1*Δ/*PNC1* strains. This restored NAM resistance to a level comparable to that observed in wild-type cells (Fig 3.2B), showing that the mild sensitivity to NAM of *pnc1*Δ/Δ cells was truly due to the absence of *PNC1*, rather than other genetic alterations that might have occurred during strain construction. The mild sensitivity of *pnc1*Δ/Δ cells is in keeping with the fact that, when exposed to 5 mM NAM, cells lacking Pnc1 did not show significantly higher levels of histone H3K56 acetylation than wild-type cells (Fig 3.2D).

Pnc1 is the predominant nicotinamidase in *C. albicans*

The mild sensitivity of *pnc1*Δ/Δ cells to NAM was unexpected because Pnc1-mediated deamidation of NAM into NA, followed by NA export, is an established mechanism to reduce NAM concentrations in *S. cerevisiae* (Belenky et al. 2011). One possibility that may account for the mild NAM sensitivity of *C. albicans pnc1*Δ/Δ cells is that enzymes that normally deamidate substrates other than nicotinamide may compensate for the absence of Pnc1 by converting NAM into NA, possibly at reduced efficiency compared with Pnc1. To address this possibility, we exposed *pnc1*Δ/Δ mutants and wild-type cells to 5 mM NAM and determined the abundance of NAM and NAD^+-related metabolites. We used a method optimized for extraction of NAD^+-related metabolites (see Methods), followed by LC-MS/MS operated under selected reaction monitoring (SRM) conditions (see Materials and Methods and (Trammell and Brenner 2013). Cells were initially grown in SC-niacin, a medium devoid of NAM, NA and NR. Within 7 min after addition of 5 mM NAM, we observed a sharp and rapid increase in NAM concentrations (from 30 to 70 µM in the absence of exogenous NAM up to 1.5 – 2 mM within 7 minutes of cell exposure to 5mM NAM) (Fig 3.3A). Upon continuous exposure to 5 mM NAM for up to 2 hours, intracellular NAM concentrations were similar in wild-type (SN152), *pnc1*Δ/Δ, and *PNC1* revertant cells (Fig 3.3A). Following addition of 5 mM NAM, the intracellular concentration of NA rose

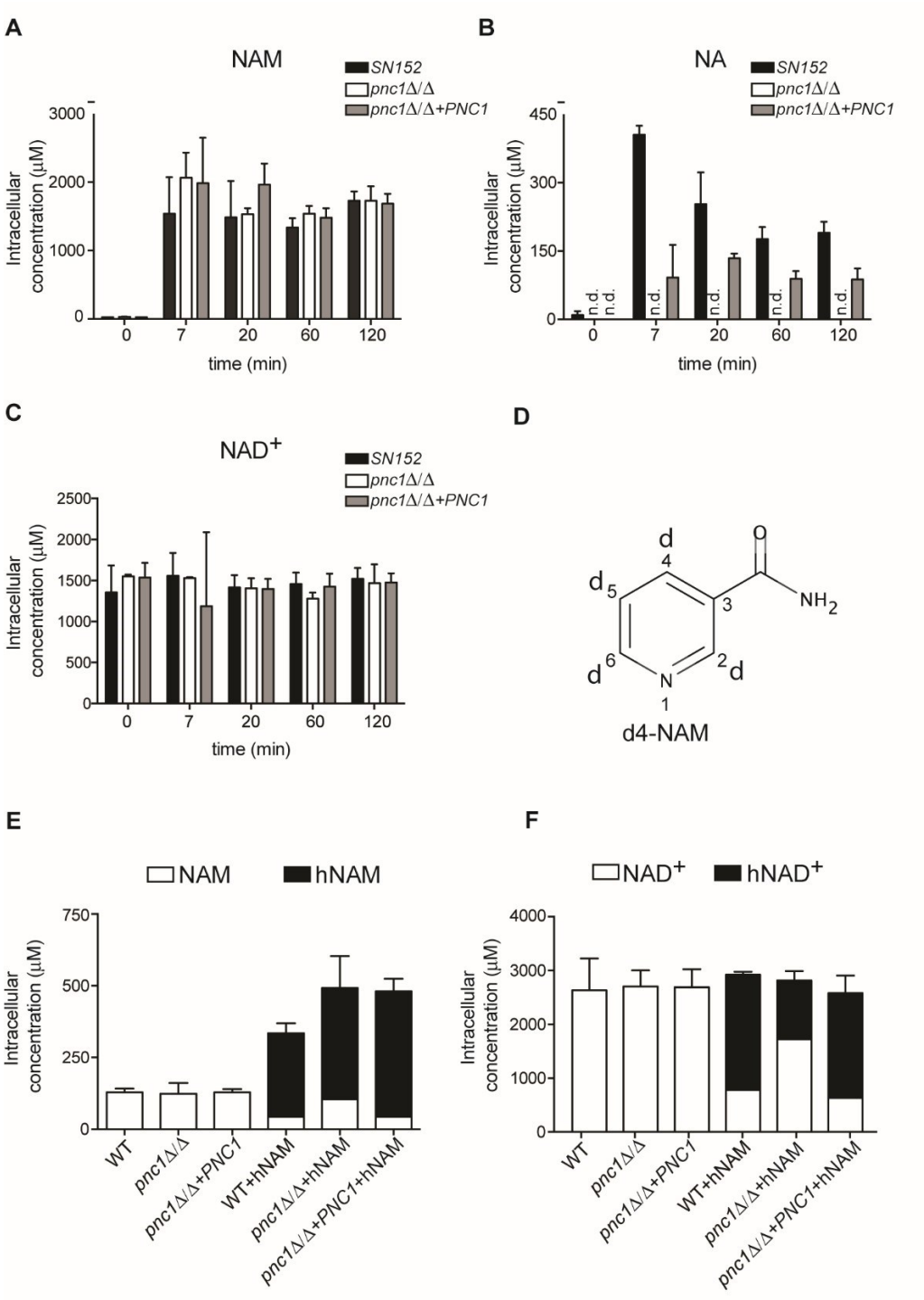

Figure 3.3. *C. albicans* cells lacking the nicotinamidase Pnc1 cannot convert NAM into NA, but nonetheless incorporate NAM into NAD^+

(A-C) Cells exponentially growing in SC-niacin medium at 30˚C were continuously exposed to 5mM NAM for 7.5min up to 120min. Aliquots of those cells were harvested as a function of time and intracellular concentrations of NAM (A), NA (B) and NAD^+ (C) were determined by LC-MS/MS. n.d.: not detected.

(D) Positions of deuterium atoms in tetra-deuterated [2,4,5,6-d_4]-NAM (heavy NAM or hNAM).
(E-F) Cells growing in SC-Niacin were exposed to 5mM hNAM for 2 hours or left untreated. Intracellular concentrations of light and hNAM (E) or light and $hNAD^+$ (F) were determined by LC-MS/MS.

rapidly (within 7 minutes) in wild-type and *PNC1* revertant cells. *PNC1* revertant cells are in fact heterozygous mutants (*pnc1*Δ/Δ+*PNC1*) and, consistent with this, NA concentrations were lower than in wild-type (SN152) cells throughout the time course (Fig 3.3B). In striking contrast to wild-type and *PNC1* revertant cells, NA was below our limit of quantification (12 pmol) in *pnc1*Δ/Δ cells (Fig 3.3B). This result indicates that, even at high NAM concentrations, cells cannot convert NAM into NA in the absence of Pnc1. This suggests that, at least in SC-niacin medium, Pnc1 is the only enzyme that can convert NAM into NA.

Non-canonical incorporation of NAM into NAD^+

Despite the fact that the first step of canonical NAM salvage was rendered impossible by the absence of Pnc1, intracellular NAM concentrations were not significantly higher in *pnc1*Δ/Δ mutants than in wild-type SN152 cells (Fig 3.3A). Furthermore, NAD^+ concentrations were not significantly lower in *pnc1*Δ/Δ mutant cells lacking the canonical NAM salvage pathway than in wild-type (SN152) or *PNC1* revertant cells (Fig 3.3C). A possible interpretation of these two results is that *pnc1*Δ/Δ mutants may incorporate a portion of their high NAM concentrations into NAD^+ through a non-canonical mechanism.

In order to assess whether the supra-physiological abundance of NAM may be incorporated into NAD^+ in a non-canonical (Pnc1-independent) manner, we used tetra-deuterated [2, 4, 5, 6] d_4-NAM (hereafter referred to as heavy NAM or hNAM, Fig 3.3D). We confirmed by MS that our commercial source of d_4-NAM was essentially all tetra-deuterated, and devoid of d_2- or d_3-NAM. In spite of this, essentially all of the positively charged NAD^+-related metabolites that we detected were di- or tri-deuterated, rather than tetra-deuterated. This is in part due to the fact that, with the exception or NAM and NA, all the NAD^+-related metabolites that we

analyzed bear a positive charge on the N1 nitrogen of the pyridine ring (Fig 3.1). It is known that the N1 positive charge, combined with the glycosidic linkages formed by N1, render the deuterium atom linked to C2 labile and exchangeable with hydrogen derived from water (San Pietro 1955; Zoltewicz and Helmick 1970). This deuterium-hydrogen exchange likely accounts for the absence of d_4-metabolites, except in d_4-NAM and d_4-NA that lack the positive charge of the N1 nitrogen (Fig 3.1). In addition to tri-deuterated molecules, we also detected di-deuterated metabolites. The latter can be readily explained by a sequence of NAD^+ reduction into NADH, followed by oxidation of NADH into NAD^+ (Fig 3.S2). During this sequence of oxido-reduction reactions, the deuterium linked to the C4 position of the NAM moiety of NAD^+ is replaced by an hydrogen atom (Fig 3.S2). Because of the above, the abundance of NAD^+ and positively charged NAD^+ precursors reported in subsequent bar graphs represents the sum of the d_2- and d_3-containing forms of each metabolite, except for heavy NAM (hNAM), which were only detected in the tetra-deuterated form (d_4-NAM).

In *S. cerevisiae*, NAM salvage begins with the Pnc1-mediated conversion of NAM into NA. Given this, we did not expect to find incorporation of d_4-NAM into $hNAD^+$ (either d_2 or d_3) in *pnc1*Δ/Δ mutant cells. In wild-type, *pnc1*Δ/Δ, and *PNC1* revertant cells continuously exposed to 5 mM d_4-NAM for 2 hours, most of the intracellular NAM was found to be heavy (Fig 3.3E). As expected, we were able to detect the presence of $hNAD^+$ in wild-type and *PNC1* revertant cells but, surprisingly, $hNAD^+$ was also observed in significant amounts in *pnc1*Δ/Δ cells (Fig 3F). Because the presence of $hNAD^+$ in cells lacking Pnc1 was unanticipated, we performed an additional experiment aimed at determining whether the deuterium atoms were truly located in the nicotinamide moiety of $hNAD^+$. Metabolite extracts from wild type and *pnc1*Δ/Δ cells were resolved by LC and the light and tri- deuterated forms of NAD^+ were fragmented under conditions that broke the N- glycosidic linkage and enabled us to detect the experimental mass of the

nicotinamide moiety of NAD^+, namely 123.0348 Da for the singly charged (theoretical $[M+H]^+ = 123.0480$) NAM derived from light NAD^+ and 126.0537 Da (theoretical $[M+H]^+ = 126.0668$) for d_3-NAM derived from d_3-NAD^+ (Fig 3.S3). We ruled out alternative explanations for this result. First, using MS we did not detect any d_3-NAM in our commercial source of d_4-NAM. Second, we did not detect d_2- or d_3-NAD^+ in the commercial product but, even if these molecules had been present, NAD^+ could not penetrate cells as an intact molecule due to the presence of negatively charged phosphate groups. Our results therefore demonstrate the existence of a Pnc1-independent non-canonical incorporation of NAM into NAD^+.

Non-canonical incorporation of NAM into NAD^+ does not require Npt1

We explored the possibility that *C. albicans* nicotinic acid phosphoribosyltransferase (Fig 3.1, Npt1, reaction **2**) might contribute to the non-canonical incorporation of NAM into NAD^+. The rationale to suspect that this might be the case was the following. Although the *S. cerevisiae* enzyme is specific for NA (Anderson *et al.* 2002; Bieganowski and Brenner 2004), there are several precedents for enzymes that act on both the acidic and the amide forms of NAD^+ precursors. This is the case, for example, of *Acinetobacter baumanii* NadM (Sorci *et al.* 2010) and *S. cerevisiae* Nma1/Nma2 that adenylate either nicotinic acid mononucleotide (NaMN) or nicotinamide mononucleotide (NMN) (Fig 3.1, reactions **3a** and **3b**) (Natalini *et al.* 1986; Zhou *et al.* 2002; Kato and Lin 2014). This is also true of nicotinamide riboside kinase (Nrk1) that can phosphorylate either nicotinamide riboside (Fig 3.1, NR, reaction **6**) or nicotinate riboside (NaR, not shown) (Tempel *et al.* 2007). Given this, we sought to test the hypothesis that, in addition to converting NA into NaMN (Fig 1, reaction **2**), *C. albicans* Npt1 might also utilize NAM as substrate to produce NMN. In addition to the aforementioned arguments, conversion of NAM into NMN seemed plausible because it is

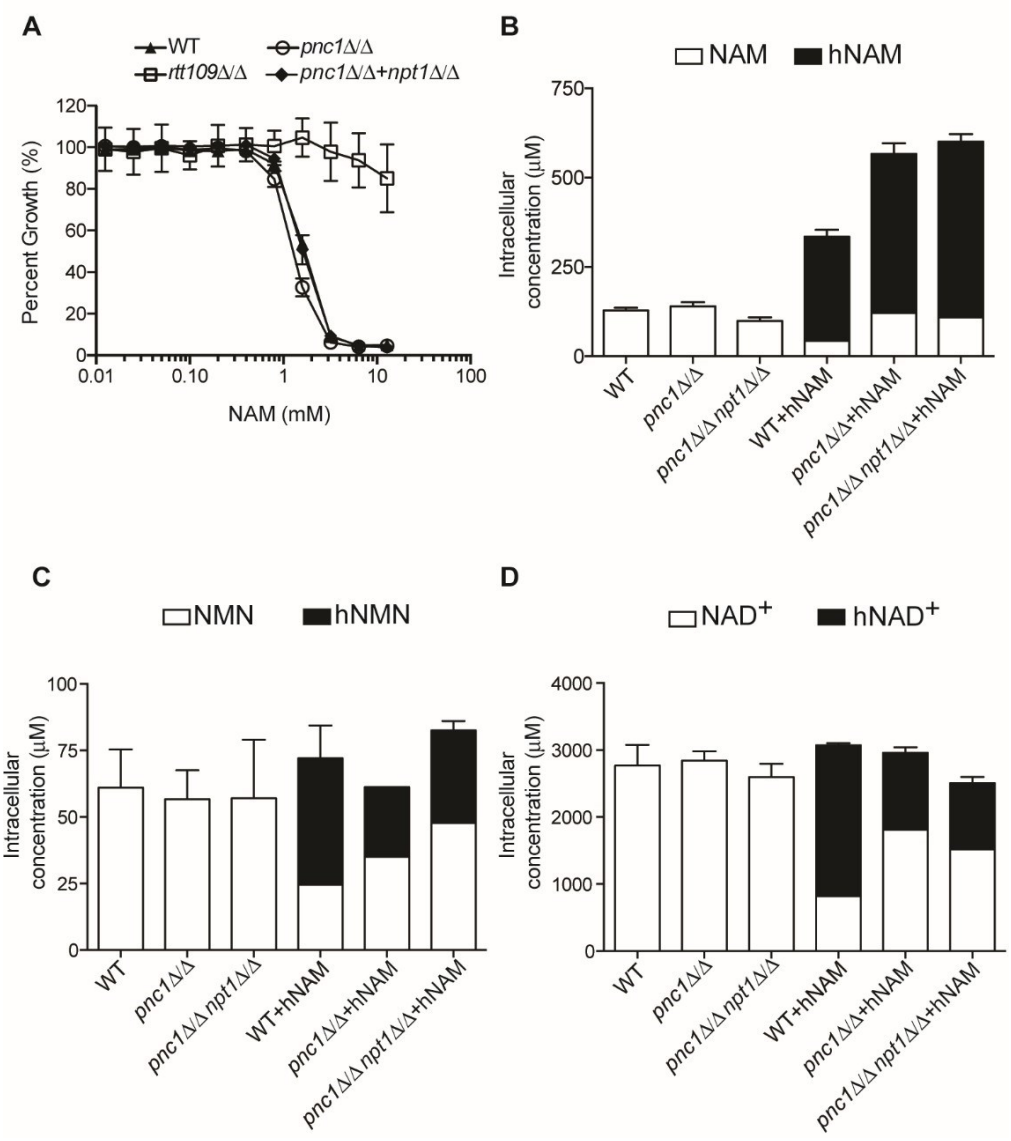

Figure 3.4. Npt1 is not necessary for incorporation of hNAM into hNMN and hNAD$^+$

(A) Growth inhibition assay in liquid cultures. Strains were grown at 30°C for 24h in SC-Niacin medium containing increasing concentrations of NAM prior to measuring the optical density at 600nm (OD600). The percentage growth is the ratio of OD600 values in wells containing NAM over that of control wells that lack NAM.
(B-D) Cells growing in SC-Niacin were exposed to 5mM hNAM for 2 hours or left untreated. Intracellular concentrations of light and hNAM (B), light and hNMN (C) or light and hNAD$^+$ (D) were determined by LC-MS/MS. In panel (D), the data for WT, WT + hNAM, *pnc1*Δ/Δ, and *pnc1*Δ/Δ + hNAM are the same as those presented in Figure 3F.

essentially the same reaction as that catalyzed by NAM phosphoribosyltransferase (NAMPT) in human cells (Wang *et al.* 2006; Burgos and Schramm 2008). To address the role of Npt1 in non-canonical synthesis of NAD^+, we deleted both alleles of the *NPT1* gene in our *pnc1*Δ/Δ null mutant strain. In the resulting *pnc1*Δ/Δ *npt1*Δ/Δ double mutant strain, our hypothesis predicts that NAM cannot be deamidated into NA because of the *pnc1*Δ/Δ mutation or converted into NMN because of the *npt1*Δ/Δ mutation. Hence, NAM should accumulate to higher levels than in wild-type cells because it cannot be converted into either NA or NMN in *pnc1*Δ/Δ *npt1*Δ/Δ double mutants. This did not prove to be the case. First, we found that *pnc1*Δ/Δ *npt1*Δ/Δ double mutants were not more sensitive to NAM than wild-type cells or *pnc1*Δ/Δ single mutants (Fig 3.4A and 3.S4B). Second, when cells were exposed to 5 mM hNAM for two hours, NAM concentrations were not significantly higher in *pnc1*Δ/Δ single mutants than in *pnc1*Δ/Δ *npt1*Δ/Δ mutants (Fig 3.4B). Third, despite the absence of Npt1, significant amounts of hNMN (Fig 3.4C) and $hNAD^+$ (Fig 3.4D) were observed in the *pnc1*Δ/Δ *npt1*Δ/Δ mutant. This result demonstrates that non-canonical incorporation of NAM into NMN or NAD^+ does not require Pnc1 or Npt1.

Non-canonical incorporation of NAM into NMN and NAD^+ does not proceed through formation of NR

In *S. cerevisiae*, nicotinamide riboside (NR) can be salvaged to generate NAD^+ via two distinct routes. First, NR can be phosphorylated by Nrk1 to generate NMN (Fi 1, reaction **6**), followed by adenylation of NMN to produce NAD^+ (Fig 3.1, reaction **3b**) (Bieganowski and Brenner 2004). Second, the NAM moiety of NR can be cleaved from the ribose (Fig 3.1, reaction **5**) and the resulting NAM then enters the canonical NAM salvage pathway (Belenky *et al.* 2007). In *S. cerevisiae*, production of NAM from NR can be catalyzed bythree enzymes: the phosphorylase Pnp1, the nucleosidase Urh1 and, to a much lesser extent, the phosphorylase Meu1 (Fig 3.1,

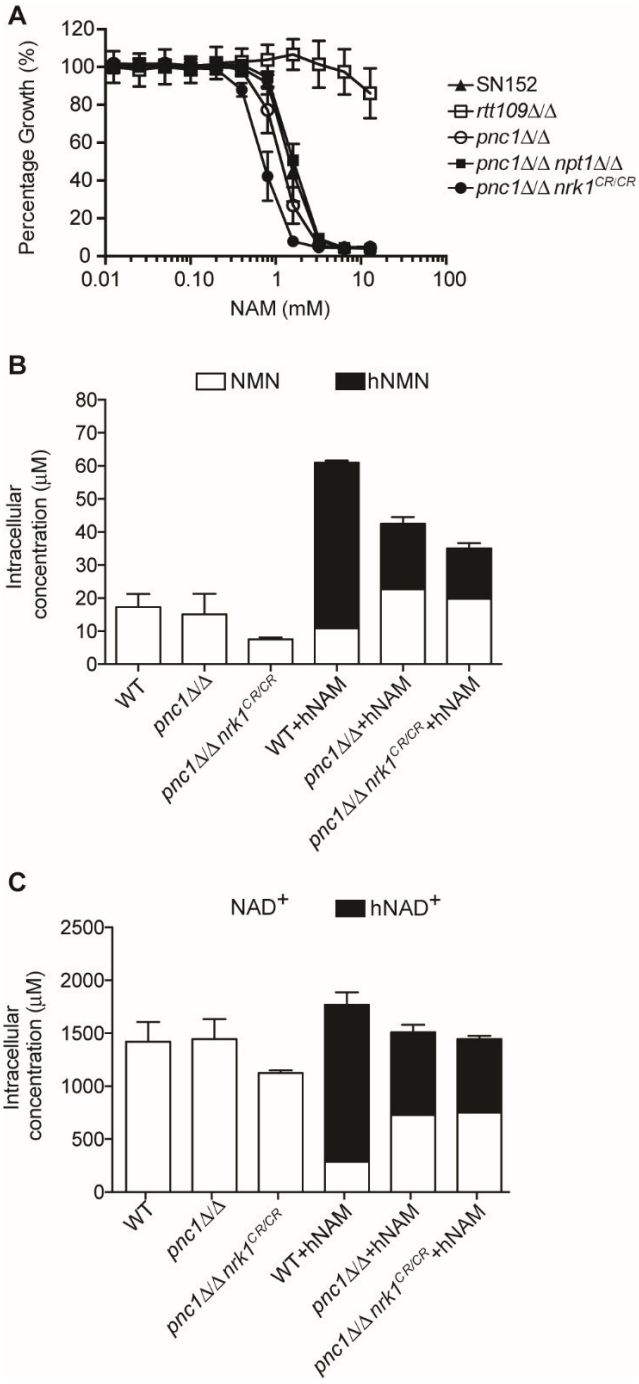

Figure 3.5. Nrk1 is dispensable for incorporation of hNAM into hNMN and hNAD$^+$

(A) Growth inhibition assay in liquid cultures. Strains were grown at 30°C for 24h in SC-Niacin medium containing increasing concentrations of NAM prior to measuring the optical density at 595nm (OD595). The percentage growth is the ratio of OD595 values in wells containing NAM over OD595 values of control wells that lack NAM.

(B-C) Cells growing in SC-Niacin were exposed to 5mM hNAM for 2 hours or left untreated. Intracellular concentrations of light and hNMN (B) or light and $hNAD^+$ (C) were determined by LC-MS/MS.

reaction **5**) (Belenky *et al.* 2007). For steric reasons, the reactions catalyzed by nucleosidases and phosphorylases are considered irreversible but, given the supra-physiological concentrations of NAM employed in our experiments, we could not exclude the possibility that some hNAM may be converted into hNR through reversal of reaction **5** (Fig 3.1). The NR salvage pathway would then lead to phosphorylation of hNR to produce hNMN (Fig 1, reaction **6)**, and the hNMN subsequently adenylated to generate $hNAD^+$ (Fig 3.1, reaction **3b**).

In order to test whether hNAM can be converted into hNR, we initially attempted to disrupt the *PNP1* and *URH1* genes using CRISPR but, despite numerous attempts with different guide RNAs, this did not work. As an alternative strategy, we reasoned that if reaction **5** (Fig 3.1) were reversible at supra-physiological concentrations of hNAM, disruption of the *NRK1* gene should result in an accumulation of hNR because it would be trapped between reactions **5** and **6** in the absence of Nrk1 (Fig 3.1). To address this possibility, we exploited CRISPR (Vyas *et al.* 2015) to introduce premature stop codons within both alleles of the *NRK1* gene in *pnc1*Δ/Δ cells (Fig 3.S6A). Cells lacking both Pnc1 and Nrk1 were, at best, slightly more sensitive to NAM than *pnc1*Δ/Δ mutants (Fig 3.5A and 3.S4C). Due to the absence of Pnc1 and Nrk1, *pnc1*Δ/Δ $nrk1^{CR/CR}$ mutant cells should not be able to incorporate hNAM into either hNMN or $hNAD^+$ via the NR salvage pathway. This is clearly not the case. Upon exposure to 5 mM hNAM, hNMN and $hNAD^+$ were generated at slightly higher levels in *pnc1*Δ/Δ single mutants than in *pnc1*Δ/Δ $nrk1^{CR/CR}$ double mutant cells but hNMN and $hNAD^+$ were clearly produced in both strains (Fig 3.5B and 3.5C). In addition, the hNR concentrations that we detected following a 2-hour exposure to 5 mM hNAM were either below the limit of quantification in some experiments or barely above it in others (data not shown). Hence, the double mutant *pnc1*Δ/Δ $nrk1^{CR/CR}$ clearly did not accumulate high concentrations of hNR. These two results argue against the possibility that high

concentrations of hNAM might drive its conversion into hNR through reversal of reaction **5** (Fig 3.1).

Non-canonical incorporation of NAM into NAD^+ is partially inhibited by isonicotinamide

Unlike deacetylases that simply hydrolyze acetyl groups from their substrates, sirtuins require NAD^+ as an obligate co-substrate to deacetylate proteins (Smith *et al.* 2000; Tanner *et al.* 2000; Jackson *et al.* 2003). During the first step of the reaction, the NAM moiety of NAD^+ is cleaved, while the ADP-ribose portion of NAD^+ becomes covalently linked to the acetyl group of the peptide or protein substrate (Fig 3.6A) (Sauve *et al.* 2001; Hoff *et al.* 2006; Smith and Denu 2006). This reaction intermediate, known as an O-alkylamidate, can then proceed to generate the deacetylated protein and the other reaction products of deacetylation, namely O-acetyl-ADP-ribose and NAM (Fig 3.6A). Alternatively, the O-alkylamidate can react with a NAM molecule (different from the one cleaved off the NAD^+ substrate) to regenerate the initial substrates: NAD^+ and acetylated protein (Fig 3.6B). The reaction of a new NAM molecule with the O-alkylamidate effectively inhibits sirtuin-mediated deacetylation. Because the NAM moiety of the starting NAD^+ molecule is exchanged by a novel NAM molecule, this is often referred to as a NAM exchange reaction or base exchange reaction (Fig 3.6B) (Jackson *et al.* 2003; Sauve and Schramm 2003; Hawse *et al.* 2008).

Isonicotinamide (isoNAM) is an analogue of NAM in which the carboxamide group is linked to C4 of the pyridine ring, rather than to C3 in the case of NAM (Fig 3.6C). Because of its chemical similarity to NAM, isoNAM competes with NAM and prevents it from reacting with the O-alkylamidate intermediate. Because of this, isoNAM inhibits the NAM exchange reaction and, consequently, enhances the deacetylase activity of sirtuins. Consistent with this, high concentrations of isoNAM (25 mM) have been employed in *S. cerevisiae* to repress reporter genes

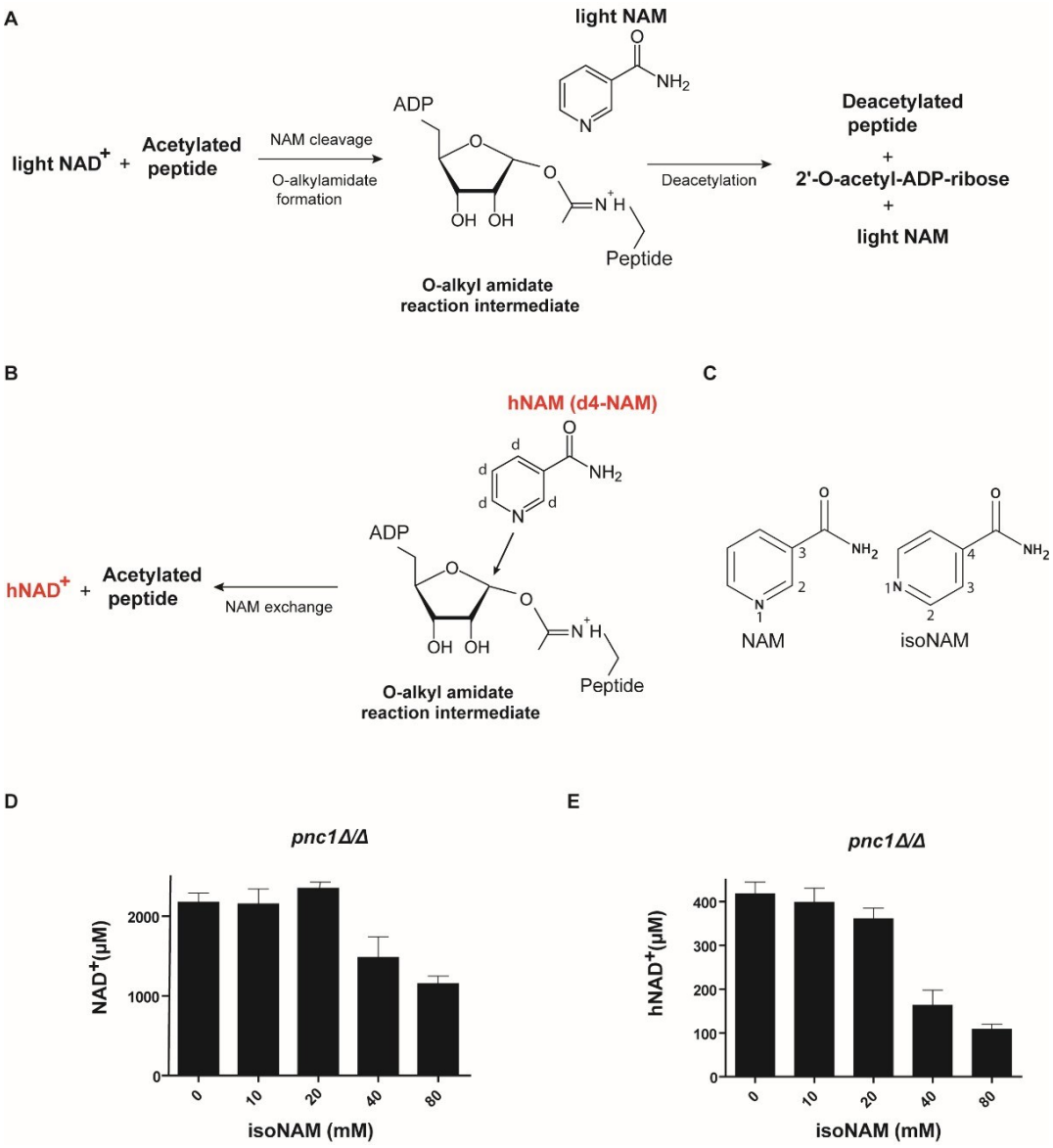

Figure 3.6. Pnc1-independent incorporation of NAM into NAD^+ is partly inhibited by isonicotinamide (isoNAM)

(A) NAD^+-dependent protein deacetylation by sirtuins: the figure emphasizes the early departure of light NAM cleaved from NAD^+. The figure also shows the O-alkylamidate reaction intermediate in which the ADP-ribose portion of NAD^+ is covalently linked to the acetyl group of the target lysine in the protein substrate.
(B) NAM exchange reaction that results in inhibition of sirtuin-mediated protein deacetylation. The diagram highlights the fact that, in our experiments, the NAM exchange reaction is initiated by a heavy molecule of NAM, and culminates in formation of heavy NAD^+.
(C) Chemical structures of NAM and isoNAM, an inhibitor of the NAM exchange reaction.
(D-E) *pnc1*Δ/Δ cells growing in SC-niacin were exposed to 0.2mM hNAM and increasing concentrations of isoNAM for 2 hours and the concentrations of light NAD^+ (D) and heavy NAD^+ (E) were determined by LC-MS/MS.

whose silencing depends upon histone deacetylation by Sir2 (Sauve *et al.* 2005; Mcclure *et al.* 2012). *In vitro*, isoNAM is a weak inhibitor of the NAM exchange reaction mediated by *S. cerevisiae* Sir2 in (Ki = 68mM) (Sauve *et al.* 2005).

Cells lacking Pnc1 were exposed to 0.2 mM hNAM for 2 hours in the presence of increasing concentrations of isoNAM ranging from 0 to 80mM. We observed a progressive decrease in the levels of light NAD^+ as a function of increasing isoNAM concentrations, culminating in an approximately 2-fold decrease in light NAD^+ at 80 mM isoNAM (Fig 3.6D). By comparison, the decrease in $hNAD^+$ concentration was approximately 4-fold at 80 mM isoNAM (Fig 3.6E). Hence, the presence of high concentrations of isoNAM impaired the incorporation of hNAM into $hNAD^+$. This result strongly suggests that one of the non-canonical mechanisms by which hNAM is incorporated into $hNAD^+$ in the absence of Pnc1 involves the NAM exchange reaction, which is inhibited by high concentrations of isoNAM.

Non-canonical incorporation of NAM into NAD^+ cannot sustain viability

When NAM was present at supra-physiological concentration (5 mM), our results showed that non-canonical incorporation of NAM into NAD^+ proceeded, at least in part, through the sirtuin-dependent NAM exchange reaction. In wild-type *C. albicans* grown in SC-niacin, we measured NAM concentrations that varied between 30 and 70 µM by LC-MS/MS. Upon a 2-hour continuous exposure to 100 µM d_4-NAM (a near physiological concentration based on our estimates of basal NAM concentrations), we detected incorporation of hNAM into $hNAD^+$ and hNMN in wild-type cells (Fig 3.7A and 3.7B, WT + d_4-NAM). The $hNAD^+$ and hNMN metabolites were also detected in *pnc1*Δ/Δ cells, but at substantially lower levels than in wild-type cells (Fig 3.7A and 3.7B, *pnc1*Δ/Δ + d_4-NAM versus WT + d_4-NAM). This is expected because the canonical NAM salvage pathway is functional in wild-type cells but inactivated in cells lacking Pnc1.

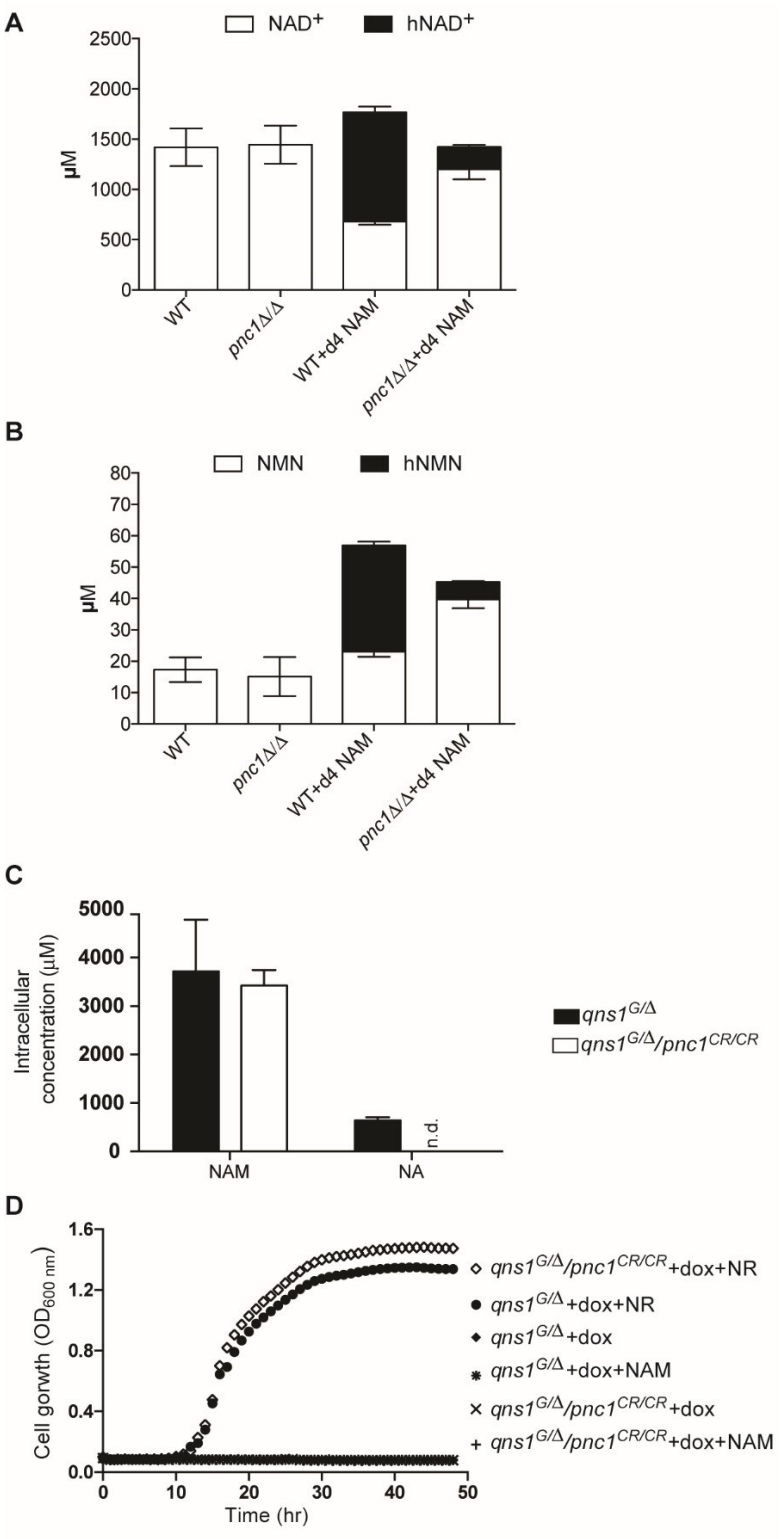

Figure 3.7. Non-canonical NAD$^+$ synthesis occurs at near physiological NAM concentrations, but is insufficient to sustain *C. albicans* viability

(A-B) Cells growing in SC-niacin were exposed to 100 μM hNAM for 2 hours at 30□C and metabolite concentrations were determined by LC-MS/MS. Panel (A) shows the levels of light NAD^+ and $hNAD^+$, whereas panel (B) indicates the concentrations of light NMN and hNMN.

(C) *QNS1* was repressed with doxycycline (DOX) in cells expressing Pnc1 (*qns1*$^{G/\Delta}$ strain) or cells with CRISPR-generated premature stop codons in the *PNC1* gene (*qns1*$^{G/\Delta}$ *pnc1*$^{CR/CR}$ strain). Following overnight repression of *QNS1* with DOX in medium containing 10 μM NR to preserve cell viability, 5 mM NAM was added for 2 hours and the levels of NAM and NA determined by LC-MS/MS. n.d.: NA was below the detection threshold in the *qns1*$^{G/\Delta}$ *pnc1*$^{CR/CR}$ strain.

(D) DOX-induced repression of *QNS1* was conducted overnight in medium containing 10 μM NR to preserve cell viability. Cultures were diluted to OD600 = 0.0005 in SC-Niacin + DOX and either 200 μM NR or 200 μM NAM. Cell growth was monitored every 15min up to 48 hours. Only the strains in media containing NR showed robust growth under these conditions.

The result obtained in *pnc1*Δ/Δ cells demonstrates that non-canonical incorporation of hNAM into $hNAD^+$ does occur at near physiological NAM concentrations.

Next, we sought to determine whether non-canonical incorporation of NAM into NAD^+ was sufficient to maintain cell viability as the only source of NAD^+. To address this possibility, we needed a system in which cells could not synthesize NAD^+ *de novo* from tryptophan or from canonical NAM salvage. For this purpose, we employed a so-called GRACE strain (Gene Replacement and Conditional Expression) that enables conditional depletion of NAD^+ synthetase (Qns1) using doxycycline (dox). In the original strain, which we termed *qns1*$^{G/\Delta}$, one allele of the *QNS1* gene is deleted whereas the remaining allele is under the control of a dox-repressible promoter (*qns1*Δ*/pTET-QNS1)*. In the absence of Qns1 (Fig 3.1, reaction **4**), neither *de novo* synthesis from tryptophan nor canonical NAM salvage can serve as sources of NAD^+. The *qns1*$^{G/\Delta}$ strain exposed to dox therefore loses viability, unless the SC-Niacin medium is supplemented with NR (Bieganowski and Brenner 2004), which can be salvaged to generate NAD^+ even in the absence of Qns1 (Fig 3.1, reactions **6** and **3b**). In order to deplete Qns1 as extensively as possible, we grew cells overnight in SC-Niacin containing dox and 10 μM NR to preserve cell viability. As a control to ensure that Qns1 had been sufficiently

depleted to prevent proliferation in the absence of salvageable NAD^+ precursors, we transferred *qns1*$^{G/\Delta}$ cells to SC-Niacin medium containing dox, but lacking NR. Under those conditions *qns1*$^{G/\Delta}$ cells did not proliferate (Fig 3.7D, strain *qns1*$^{G/\Delta}$ + dox). As judged by monitoring the optical density every 15 minutes, *qns1*$^{G/\Delta}$ cells proliferated normally when SC-Niacin was supplemented with 100 μM NR, but proliferation was curtailed in SC-Niacin containing 100 μM NAM (Fig 3.7D, strain *qns1*$^{G/\Delta}$ + dox and either NR or NAM). Because *qns1*$^{G/\Delta}$ cells cannot generate NAD^+ through the canonical NAM salvage pathway, this result suggests that, in the presence of 100 μM NAM, non-canonical incorporation of NAM into NAD^+ is insufficient to sustain cell viability. In *qns1*$^{G/\Delta}$ cells, the canonical salvage pathway is blocked just prior to NAD^+ synthesis because the Qns1-catalyzed step is blocked (Fig 3.1, reaction **4**). However, all the earlier steps of the NAM salvage pathway (Fig 3.1, reactions **1**, **2**, **3a**) are intact. Given this, Pnc1-mediated conversion of NAM into NA in Qns1-depleted cells would effectively channel a portion of the available NAM into a cul-de-sac (Fig 3.1, reactions **2** and **3**). Given this, it seemed possible that the absence of Pnc1 in Qns1-depleted cells may increase the amount of NAM available for non-canonical synthesis of NAD^+. In order to test this hypothesis, *qns1*$^{G/\Delta}$ cells were genetically modified using CRISPR-mediated insertion of premature stop codons within the two *PNC1* alleles (see Materials and Methods and Supporting Information, Fig 3.S6B). The resulting strain was termed *qns1*$^{G/\Delta}$ *pnc1*$^{CR/CR}$. As a control, we confirmed that even at very high NAM concentrations (>3mM) this strain was incapable of converting NAM into NA because of loss-of-function of *PNC1* (Fig 3.7C), thus validating the CRISPR-mediated inactivation of the *PNC1* gene.

Following overnight depletion of Qns1 in the presence of dox and NR, our *qns1*$^{G/\Delta}$ *pnc1*$^{CR/CR}$ mutant strain thrived in SC-Niacin containing dox and 100 μM NR, but failed to proliferate in the presence of dox and 100 μM NAM (Fig 3.7, strain *qns1*$^{G/\Delta}$ *pnc1*$^{CR/CR}$ + dox and either NR or NAM). This demonstrates that, even in the presence of 100 μM NAM that cannot be diverted into a dead end salvage pathway,

non-canonical incorporation of NAM into NAD^+ cannot serve as the only source of NAD^+ to sustain *C. albicans* viability. In fact, we found that NAM concentrations ranging from 50 μM up to 800 μM were insufficient to rescue the loss of viability of cells lacking either Qns1 alone or cells lacking both Pnc1 and Qns1 (Fig 3.S5A-B). This is in striking contrast to NR, which can rescue the lethality of *C. albicans* cells lacking Qns1 and Pnc1 even when NR is present at concentrations as low as 50 μM NR (Supporting Information, Fig 3.S5B). Our attempts to perform this experiment at NAM concentrations higher than 800 μM were thwarted by the fact that NAM eventually inhibits Hst3 which, in turn, causes DNA damage and cripples cell proliferation irrespective of their ability to synthesize sufficient amounts of NAD^+ or not.

3.4 Discussion

Non-canonical incorporation of NAM into NMN and NAD^+

We previously showed that the cytotoxicity of SCs of NAM in *C. albicans* mainly results from inhibition of the sirtuin Hst3 (Wurtele *et al.* 2010). Given this, we initiated the current study with the hypothesis that cells lacking the nicotinamidase Pnc1, which cannot convert NAM into NA (Fig 3B), would accumulate substantially higher amounts of NAM than wild-type cells. Hence, we expected cells lacking Pnc1 to be considerably more sensitive to NAM than wild-type cells. This did not prove to be the case. Cells lacking Pnc1 were at best mildly sensitive to NAM (Fig 3.2A-B) and, at least in some experiments, NAM concentrations were not significantly higher in *pnc1* mutants than in wild-type cells (Figs 3.3A, E and 3.4B). This led us to speculate that NAM may have metabolic fates other than the canonical Pnc1-dependent conversion into NA. We provided evidence for the existence of non-canonical (Pnc1-independent) processes through which NAM was incorporated into NMN and NAD^+ at supra-physiological (5 mM), and even near physiological (0.1 mM) NAM concentrations (Figs 3.4C-D and 3.7A).

The first non-canonical mechanism is the inhibition of sirtuins through the NAM exchange reaction. During sirtuin-mediated deacetylation, cleavage of the NAM moiety of NAD^+ needs to occur prior to the formation of the O-alkylamidate reaction intermediate (Fig 3.6A). As illustrated in Fig 3.6B, a different NAM molecule (*e.g.* d4-NAM) can only initiate the NAM exchange reaction after formation of the O-alkylamidate reaction intermediate. This has two important implications. First, the NAM exchange reaction is not equivalent to NAM salvage because the exchange reaction does not consume NAM molecules or produce new NAD^+ molecules. Second, the fact that the NAM exchange reaction cannot cause a decrease in NAM concentration implies that this reaction cannot account for the fact that cells lacking Pnc1 are at best mildly sensitive to NAM. However it is important to note that our anti-fungal strategy relies on NAM-mediated inhibition of the deacetylase activity of Hst3. As is the case for other sirtuins, NAM-dependent inhibition of Hst3 likely occurs through the NAM exchange reaction. Because high concentrations of NAM (2-3 mM) are necessary to inhibit Hst3 *in vivo* (Wurtele et al. 2010), the fact that the NAM exchange reaction cannot cause a decrease in NAM concentration is crucial for NAM's cytotoxicity.

The proposed existence of a second non-canonical process stems from the observation that the addition of hNAM elicits the formation of hNMN in cells lacking Pnc1 (Fig 3.4C). Based on several arguments, the formation of hNMN is unlikely to proceed through the sirtuin-dependent NAM exchange reaction. First, a high concentration of isonicotinamide (80 mM), a weak inhibitor of the NAM exchange reaction, reduced but did not abolish the production of $hNAD^+$ (Fig 3.6D-E). This suggests that a significant portion of the $hNAD^+$ was synthesized through a non-canonical mechanism that is distinct from the NAM exchange reaction. An important caveat to this interpretation is that we cannot exclude the possibility that, even in the presence of 80 mM isonicotinamide, the exchange reaction was only partially inhibited which would explain the persistence of $hNAD^+$. In order to account for the production of hNMN, $hNAD^+$ generated by the NAM exchange

reaction could be deadenylated through reversal of the reaction catalyzed by Nma1, which would result in the formation hNMN (Fig 3.1, reaction **3b**). However, this scenario is unlikely because Nma1, and a putative *C. albicans* homologue (systematic gene name: C1_13270W_A) of *S. cerevisiae* Pof1 (Kato and Lin 2014) utilize ATP to adenylate NMN and the reaction products are NAD^+ and inorganic pyrophosphate (iPP). *In vitro*, this adenylation reaction is readily reversible (Kornberg 1948) in the absence of inorganic pyrophosphatase. However, the hydrolysis of iPP by inorganic pyrophosphatases is strongly exergonic, which ensures that adenylation of NMN into NAD^+ is irreversible *in vivo*. Because *C. albicans* encodes a constitutively expressed inorganic pyrophosphatase known as Ipp1 (Fernandez-Arenas *et al.* 2007; Kusch *et al.* 2008), it seems improbable that hNMN is formed by deadenylation of $hNAD^+$.

A path to hNMN that does not imply the participation of sirtuins and NAM exchange is the direct conversion of hNAM into hNMN. In metazoans, this reaction is catalyzed by NAM phosphoribosyltransferase (NAMPT) (Wang *et al.* 2006; Burgos and Schramm 2008) and constitutes the first step of the canonical NAM salvage pathway. However, no functional counterpart of NAMPT has been identified in fungi. This argues that direct conversion of hNAM into hNMN cannot be catalyzed by a phosphoribosyltransferase with a high degree of sequence similarity to NAMPT. Alternatively this reaction may simply not exist in fungi. However, the *C. albicans* genome encodes numerous phosphoribosyltransferases. At least some of these enzymes catalyze reactions that are biochemically similar to the conversion of the base NAM into the mononucleotide NMN. For instance, this is the case of the Fur1 and Apt1 enzymes that respectively incorporate the bases uracil or adenine into the cognate mononucleotides. Because we most often monitored the formation of hNMN and $hNAD^+$ in cells exposed to SCs of hNAM (5 mM), we cannot exclude the possibility that a phosphoribosyltransferase whose natural substrate is not NAM might catalyze inefficient phosphoribosylation of NAM. Given the chemical similarity between NA and NAM, we felt that Npt1

(nicotinic acid phosphoribosyltransferase) was likely to use NAM as a substrate, albeit at low efficiency compared with NA. However, we found that Npt1 was dispensable for production of hNMN in cells lacking Pnc1 (Fig 3.4C). This obviously does not rule out the possibility that other "relaxed specificity" phosphoribosyltransferases may catalyze the direct conversion of NAM into NMN. These arguments suggest, but do not formally prove the existence of a NAM exchange-independent non-canonical pathway for incorporation of hNAM into hNMN and, via Nma1/Pof1-dependent adenylation of hNMN, would lead to $hNAD^+$ (Fig 3.1, reaction **3b**). Unlike the NAM exchange reaction, this would be a *bona fide* NAM salvage pathway that consumes NAM while generating new NAD^+ molecules, and potentially new NADH, $NADP^+$ or NADPH molecules as well. Unfortunately, because we do not currently know how to block this non-canonical pathway by mutation, we cannot evaluate its contribution to the NAM-resistant phenotype of cells lacking Pnc1.

Other potential fates of NAM and therapeutic perspectives

In humans, the first step of NAM excretion into urine is its conversion into N1-methylnicotinamide (N1-meNAM) catalyzed by nicotinamide N1-methyltransferase (NNMT) (Pissios 2017). However, there is no striking homologue of NNMT encoded in the *C. albicans* genome. In addition, even after continuous exposure of cells to 5 mM NAM for 2 hours, we did not detect N1-meNAM in either the extracellular medium or intracellular metabolite preparations. Thus, detoxification of high concentrations of NAM by N1-methylation does not seem to occur in *C. albicans*.

A possibility that we cannot rule out is that of NAM export through an unknown transporter. For technical reasons, we did not assess this possibility rigorously, but in *S. cerevisiae* there is experimental support for Pnc1-independent NAM export

(Croft *et al.* 2018), although NAM transporter(s) have not yet been identified in this species.

Our results showing that *pnc1*Δ/Δ cells are almost as resistant to NAM as wild-type cells (Fig 3.2A-B) suggest that potent Pnc1 inhibitors will not enhance NAM's cytotoxicity. At this stage, the identification of a single fungal-specific enzyme whose pharmacological inhibition might result in a considerable increase in NAM's intracellular concentration seems rather improbable. However, despite the novel findings that we presented here, important aspects of the fates of supra-physiological NAM concentrations in *C. albicans* remain largely unknown. Hence, it remains possible that non-canonical conversion of NAM into other molecules that cannot inhibit Hst3 (*e.g.* NMN) or NAM export may prove an Achilles heel whose pharmacological inhibition would greatly enhance NAM's cytotoxicity in *C. albicans* and other fungal pathogens that are sensitive to NAM (Wurtele *et al.* 2010). Alternatively, the possibility that NAM may act in a synergistic manner with azoles or echinocandins remains worth exploring because combination therapy would likely require lower amounts of NAM and elicit resistance at lower frequency than treatment with each therapeutic agent.

3.5 Acknowledgements

RG and ST were recipients of Mitacs Accelerate awards. ST was also the recipient of the Fonds de recherché santé (FRQS) postdoctoral fellowship. Research in AV's laboratory was supported by funds from the "Fonds de Partenariat pour un Québec Innovant en Santé" (FPQIS), Mitacs (IT07989) and the Canadian Institutes for Health Research (CIHR, FRN 125916), MR (CIHR, MT-15679), We are indebted to Eun-Hye Lee for technical assistance, Valmik Vyas and Gerald Fink for the *C. albicans* CRISPR cassette pV1200 and Brian Wong for the *C. albicans* plasmid pYM70 containing a synthetic hygromycin B resistance gene (*CaHygB).* We are grateful to Merck Sharp & Dohme for making the Grace strain collection available

to the academic research community. We are grateful to Dr. Pierre Thibault for his advice about mass spectrometry. We thank Dr. Brendan Cormack for valuable comments and suggestions regarding the experiments shown in Figure 7. IRIC is supported by infrastructure funds from the Canadian Foundation for Innovation.

3.6 Author contributions

Conceived and designed the experiments: RG, ST and AV; Performed the experiments: RG, ST and MS; Analyzed the data: RG, ST, MS and AV; Contributed reagents, materials and analysis tools: RG, ST, MS, PT, MR, CB and AV; Wrote the manuscript: RG, ST, MR and AV.

3.7 Materials and methods

Culture conditions

Archives of *C. albicans* strains were maintained at -80^{o}C in growth media containing 40% glycerol. YPD (1% yeast extract, 2% Bacto peptone and 2% glucose) was routinely used as rich medium; 2% agar was added for YPD agar plates. *C. albicans* mutant strains constructed using the auxotrophy selection markers (*HIS1* or *ARG4*) were grown in synthetic complete (SC) medium (0.67% Difco yeast nitrogen base, 2% glucose and an amino acid mixture that lacked either arginine or histidine). For both measurements of NAD^{+}-related metabolite concentrations and cell growth assays, cells were grown in SC-niacin media: 0.69% yeast nitrogen base without amino acid and without nicotinic acid (Formedium, Hunstanton, England), 2% glucose and a mixture of amino acids. *Escherichia coli* DH10B or Mach1 cells were used for DNA cloning procedures. *E. coli* cells were grown in Luria-Bertani (LB) medium to which appropriate antibiotics were added. The concentrations of antibiotics used in this study are as follows: chloramphenicol (CM, 34 μg/ml), ampicillin (AMP, 100 μg/ml), nourseothricin (NAT, 200 μg/ml, Werner BioAgents, Jena, Germany).

Strains

All the *C. albicans* strains used in this study are listed in Table S1 and all the oligonucleotide sequences are listed in Table S2. Selection for NAT-resistant strains was performed in the presence of 200 μg/mL NAT. Selection for hygromycin B (HygB)-resistant mutants was conducted in the presence of 800μg/ml HygB (Basso *et al.* 2010). For *Tet* promoter repression, an overnight culture was diluted to an optical density at 600 nm (OD_{600}) of 0.005 in fresh medium containing 20-50 μg/ml doxycycline (DOX, Sigma) with or without 10 μM nicotinamide riboside (NR) and grown for 24 h (Roemer *et al.* 2003; Bieganowski and Brenner 2004; Wurtele *et al.* 2010).

Nicotinamidase (*pnc1*Δ/Δ) mutants

PNC1 (orf19.6684/C7_03520W_A) gene deletion cassettes were amplified by PCR from pSN52 or pSN69 with fusion PCR primer sets (ST8/ST10 and ST9/ST11, Table S2). The *PNC1* gene deletion cassettes carry either the *HIS1* or *ARG4* selection markers flanked by 120-bp sequences homologous to the upstream and downstream regions of *PNC1* (Noble and Johnson 2005; Wurtele et al. 2010). The *HIS1*-containing amplicon was used to transform the *C. albicans* strain SN152 using minor modifications of a standard lithium acetate protocol that previously described (Noble and Johnson 2005; Wurtele *et al.* 2010). At least two independent His^+ strains were tested by PCR and Southern blotting, which confirmed that those strains carried a properly deleted allele. This heterozygous mutant strain was transformed with the *ARG4*-containing amplicon to generate two independent *pnc1*Δ/*pnc1*Δ homozygous gene deletion strains that we termed CaST33 and CaST35.

In a so-called GRACE strain (gene replacement and conditional expression) strain for doxycycline-induced depletion of Qns1, we inserted premature stop codons in

both alleles of the *PNC1* gene using a *C. albicans*-adapted CRISPR mutagenesis system (Vyas *et al.* 2015). For this purpose, a small guide RNA (sgRNA) that targets the region of the *PNC1* gene spanning nucleotide 37 to 56 (+1 corresponds to the adenine of the ATG initiation codon) was generated by annealing two 5'-end phosphorylated primers (ST272 and ST273, see Table S2 for oligonucleotide sequences). The double-stranded DNA product was inserted into pV1200 plasmid digested with *Bsm*BI (Vyas *et al.* 2015). A DNA double-strand break repair template was generated by fusion PCR with primer pairs ST274/ST275 and ST276/ST277, which resulted in a 120-bp DNA fragment with the desired mutation (GGA to TGA) at the centre. This repair template also contained a mutation of the PAM site, a second stop codon as well as a unique restriction site that created a silent mutation. This last feature enabled us to quickly genotype transformants. A *QNS1*-GRACE mutant strain (CaST194, CaST195) was co-transformed with a sequence-verified guide expression plasmid (5 to 10 μg) linearized with *Kpn*I and *Sac*I as well as purified repair templates (3 μg). Two strain isolates containing premature stop codons in both alleles of the *PNC1* gene (CaST207 and CaST208) were confirmed by PCR amplification and sequencing of a DNA fragment spanning the mutation sites (Fig 3.S6). The genotype of the resulting strain is referred to as $qns1^{G/\Delta}$ $pnc1^{CR/CR}$. The G/Δ superscript indicates that one allele of the *QNS1* gene is placed under a doxycycline-repressible promoter, while the second allele of *QNS1* is deleted. The CR/CR superscript indicates that both alleles of the *PNC1* gene contain CRISPR-introduced premature stop codons.

To construct a *PNC1* revertant strain (*pnc1*Δ/Δ+*PNC1*), a PCR-amplified SN152 DNA fragment of *PNC1* downstream region was amplified from SN152 with primer pair RG3/RG4 and cloned into the *Xho*I-*Apa*I sites of plasmid pSFS2A (Reuss *et al.* 2004; Tsao *et al.* 2016), creating $pPNC1_{down}$. Next, a PCR-amplified fragment containing the *PNC1* open reading frame using primer pair RG1/RG2 was cloned into the *Sac*II-*Not*I sites of plasmid $pPNC1_{down}$, resulting in $pPNC1_{rev}$. The *Apa*I-*Apa*I *PNC1-SAT1* fragment derived from $pPNC1_{rev}$ was used to transform the

*pnc1*Δ/Δ#1 strain. At least two independent transformants, CaRG25 and CaRG28 were selected, verified by PCR and Southern blot analysis.

Nicotinic acid phosphoribosyltransferase (*npt1*Δ/Δ) mutants

Putative *NPT1* (orf19.7176/ C7_04040C_A) null mutant was constructed similarly using the PCR-based gene deletion method with fusion PCR primer sets (ST102/ST104 and ST103/ST105) and used to transform CaRG25 or CaRG28 as described for the *pnc1* mutant. At least two independent His^+/Arg^+ protrophs, CaRG80 and CaRG101, were selected and verified by PCR and Southern blotting.

Nicotinamide riboside kinase ($nrk1^{CR/CR}$) mutants

Putative *NRK1* (orf19.511/ CR_04230W_A) was inactivated in the *pnc1* mutant CaST33 using the CRISPR strategy as described for $qns1^{G}$ $pnc1^{CR}$. Small guide RNA (sgRNA) for *NRK1* targeting genomic region (43 to 62bp, relative to ATG at +1) was generated by annealing two phosphorylated primer pair RG32/RG33 cloned into BsmBI-digested pV1200. Repair template was generated by PCR with primer pairs RG48/RG49 resulting a total of 150 bp with desired mutation (GGT to TGA) at the centre. Our repair template contained a mutation to PAM site, a stop codon as well as a unique silent restriction site, which enabled us to quickly genotype transformants. *pnc1* mutant CaST33 was transformed with the *Kpn*I/*Sac*I linearized guide expression plasmid (5 to 10 μg) and purified repair templates (3 μg). Successful mutants, CaRG115 and CaRG117 were verified by amplifying the region with the mutation and sequencing.

Glutamine-dependent NAD^+ synthetase ($qns1^{G/\Delta}$) mutants

QNS1 conditional mutant (Qns1-GRACE, *qns1Δ/pTET-QNS1*) derived from the *C. albicans* CaSS1 strain that expresses a tetracycline-dependent transactivation fusion protein (TetR-ScGal4AD) was obtained from the GRACE library collection (Roemer *et al.* 2003) and verified by PCR. In this study, we constructed a modified

QNS1 conditional mutant strain that is amenable for the CRISPR Solo system pV1200 by replacing the NAT-resistance gene with a *C. albicans* adapted HygB-resistance gene (Basso *et al.* 2010). PCR fusion primer pairs ST266/ST267 and ST268/ST269 were used to amplify the HygB cassette and transform *qns1*$^{G/\Delta}$. HygB-resistant and NAT-sensitive transformants (CaST194 and CaST195) were selected and verified by PCR. Furthermore, the viability of both CaST194 and CaST195 in growth media with addition of DOX were identical to their parental strain Qns1GRACE from the collection.

Liquid culture assays

Liquid minimum inhibition (MIC) assays were performed as described previously in flat-bottomed 96 well plates as follows (Tsao *et al.* 2016). Cells were grown overnight in SC-Niacin medium at 30°C followed by a dilution to OD_{600} of 0.0005 in 100 µl SC-niacin medium containing 2-fold serially diluted testing chemical from the respective highest concentrations. Highest concentrations for nicotinamide (NAM, Sigma) was 12.8 mM and 0.15% for methyl methanesulfonate (MMS, Sigma). At least three independent experiments were performed in duplicates. Data were plotted as percent cell growth in wells containing increasing concentrations of chemicals relative to control wells containing media only. Average percent growth and standard deviations were plotted using Prism 6 (GraphPad Software). For each experiment, the data reflect the average of three biological replicates.

For *pnc1*Δ/Δ *qns1*$^{G/\Delta}$ mutant rescue growth assay, strain CaST207 was grown overnight at 30ºC in SC-niacin medium supplemented with 10 µM NR and addition of DOX to deplete the Qns1 protein. Next day cells were then diluted to OD_{600} 0.0005 in 100 µl SC-Niacin medium in a microtiter plate containing different testing concentrations of NAM or NR (50 µM to 800 µM) either in the presence or absence of DOX. Cell growth was monitored by measuring their optical density at 595 nm every 15 mins continuously for 96 hours using a Sunrise plate reader (Tecan Group). The experiment was performed with three independent strains in duplicates

and the data from one representative strain is shown. Based on the growth curve obtained from the experiment (OD in the function of time), the AUC is derived from the "surface area" underneath the growth curve: above OD >0 in 72 hours (duration of the experiment); y axis cutoff=0.0; x axis cutoff 72h. Therefore this is the arbituratury unit that is directly reflecting the growth of each strain. Instead of showing growth curve lines which would be too confusing to see with so many conditions and strains, this is a visual representation and easy to understand. The value is the arbitrary unit obtained directly from the calculation as explained above (using Prism Graphpad for this calculation), there has been NO normalization nor percentage of total growth adjustment, just raw data (any growth above the OD 0.0 for 72 hours have been calculated by this software; so bigger the number meaning better the growth.

Immunoblotting

Whole-cell lysates were prepared from OD_{600} of 2 cells using an alkaline extraction method (Kushnirov 2000). Proteins from whole-cell lysates were separated on SDS 15% polyacrylamide gels followed by transferred to nitrocellulose membranes by semi-dry transfer system (BioRad) for 75 min at 20V using 1x Towbin buffer (25 mM Tris, 192 mM Glycine, pH 8.3) with additional 20% Methanol and 0.02% SDS. For histone immunoblots, proteins were transferred to nitrocellulose membranes by semi-dry transfer for 1 h at 10 V using 1x Towbin buffer containing 20% Methanol and 0.02% SDS. To probe for H3K56 acetylation, we used an affinity-purified rabbit polyclonal antibody against H3K56ac known as AV105-GE (1:500 dilution) (Masumoto *et al.* 2005). A rabbit polyclonal antibody raised against a non-modified N-terminal peptide of H3 (AV71/72; 1:1000 dilution) was used as loading control (Masumoto *et al.* 2005).

Preparation of internal standard stock solutions for MS detection of NAD^+-related metabolites

For separation A, a combined stock solution was prepared in water containing 100 μM d_3 N-methyl-4-pyridone-3-carboxamide , 200 μM ^{18}O nicotinamide riboside and ^{18}O, d_3 methyl nicotinamide, and 400 μM ^{18}O nicotinamide and d_4-nicotinic acid. A working solution was prepared using 1 part stock solution plus 9 parts water. Sufficient working solution was prepared to add 20 μL to all samples plus 440 μL for standards, controls, and wastage. For separation B, labeled internal standards with either 5 or 10 ^{13}C atoms/molecule were prepared from a yeast culture with U-$^{13}C_6$ glucose (Cambridge Isotope Laboratories, Andover, MA,USA) as described (Trammell and Brenner 2013).

Preparation of standard curve and controls

For each separation, eight working standards containing the amount of each analyte were prepared by adding 20 μL of an appropriate stock solution to labeled microcentrifuge tubes containing 20 μL of the appropriate internal standard working solution. 400 μL of hot EtOH/HEPES (pH 7.1; 3:1) was added to each tube and the volume reduced to dryness on a Labconco Centrivap under vacuum at room temperature.

Metabolite extraction from cell pellets

Exponentially growing cells were treated with 5 mM (or stated otherwise) of either NAM or hNAM and harvested at different time points in duplicates. Cells from 1ml of medium were harvested and counted using a Z2 Coulter counter**.** Cell pellets with a known number of cells were flash frozen using dry ice and stored at -80°C until further use. In groups of four, pellets had the appropriate internal standard added followed by 400 μL hot EtOH/HEPES (Trammell and Brenner 2013). Tubes were vortexed brieflyto mix, held on ice until up to 24 samples were accumulated, vortex mixed at 55 °C for 3 minutes, and centrifuged at 4 °C for 10 min (16.1 rcf). The supernatant was transferred to fresh tubes and solvent removed to dryness on a Centrivap. On the day of analysis samples were reconstituted with 3% acetonitrile in 10 mM ammonium acetate. Cell pellets grown in d_4-Nam were extracted in the same fashion except d_4-NA and ^{18}O, d_3 methyl nicotinamide were the only internal

standards for separation A. To determine if deuterium exchange was caused primarily by hot processing, cells were also extracted with 80:20 methanol/water or 40:40:20 methanol/acetonitrile/water at -20 °C.

LC-MS/MS and SRM

Instrumental analysis was performed using a Waters TQD (Milford, MA, USA) and is a modified version of the published method (Trammell and Brenner 2013). For separation A, the column was a 2 x 100 mm, 3μ, Thermo Hypercarb held at 60° C, the A mobile phase was 10mM ammonium acetate in water with 0.1% formic acid, and the B mobile phase was acetonitrile containing 0.1% formic acid. Analytes were eluted based on a gradient beginning at 5% B for 1.8 min, linearly ramping to 40% B at 11 minutes, ramping to 90% B at 11.3 minutes and holding until 13.3 minutes, ramping down to 5% B at 13.4 minutes and holding until 19.5 minutes. The mass spectrometer was operated in selected reaction monitoring (SRM) mode. SRM is a sensitive and accurate approach that, even within complex samples such as metabolite extracts, can unambiguously identify specific analytes based on the relationship between the intact mass of the analyte and the masses of diagnostic fragments derived from it (Trammell and Brenner 2013). The precursor-to-fragment transitions that we monitored were: NR (255→123); Nam (123→80); NA (124→80); MeNam (137→94); Me-4-py (153→136); Me-2-py (153→110); Nam oxide (139→106);; ^{18}O-Nam (125→80); ^{18}O-NR (257→125); d_4-NA(128→84); ^{18}O, d_3-MeNam (142→97); d_3-Me-4-py (156→139); d_2-NR (257→125); d_3-NR (258→126); d_4-NR (259→127); d_2-Nam (125→82); d_3-Nam (126→83); and d_4-Nam (127→84). For separation B, the column was a 2 x 100 mm, 3μ, Thermo Hypercarb held at 60° C, the A mobile phase was 7.5mM ammonium acetate in water with 0.05% NH_4OH, and the B mobile phase was acetonitrile containing 0.05% NH_4OH. Analytes were eluted based on a gradient beginning at 3% B for 1.8 min, linearly ramping to 50% B at 14 minutes, ramping to 90% B at 14.1 minutes and holding until 16.2 minutes, ramping down to 3% B at 17.1 minutes and holding until 22 minutes. The mass spectrometer was operated in SRM mode, the

transitions monitored were: NAD^+ (664.1→136.1); NADP (744.1→136.1); NaAD (665.1→136.1); NMN (335→123); NAR (256→124); ADPR (560→136.1); d_2-NAD^+ (666→136); d_3-NAD^+ (667→136); d_4-NAD^+ (668→136.1); d_2-NMN (337→126); d_3-NMN (338→126) and d_4-NMN (339→127). While doing the calculations cell number and volume both were taken into consideration. The average cell size in SC-Niacin was determined to be 61 femtolitres (range from 52 to 67 femtolitres) using a Z2 Coulter counter. For each experiment, the reported metabolite concentrations reflect the average and standard deviation calculated from three biological replicates.

3.8 Supplementary information

Supplementary figures

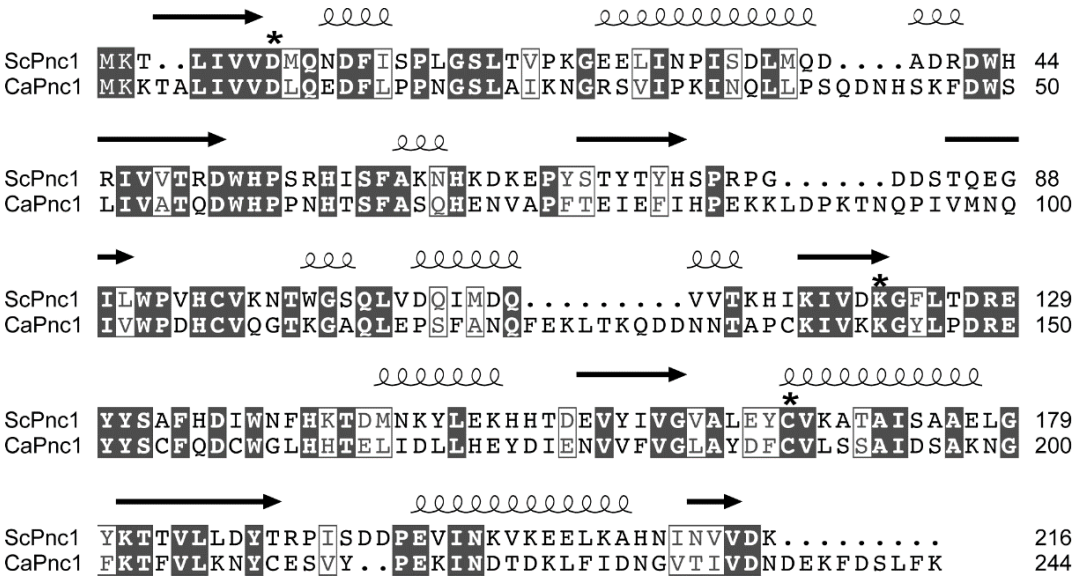

Figure 3.S1 Structure-based sequence alignment of *S. cerevisiae* and *C. albicans* Pnc1.
Secondary structure-based protein alignment of *S. cerevisiae* Pnc1 with the *C. albicans* Pnc1 (C7_03520w). The alignment was obtained using ClustalW modified to exploit structural data of *S. cerevisiae* Pnc1 (PDB 2H0R) using ESpript (Robert

and Gouet 2014). Identical residues are boxed and highlighted in dark gray; homologous residues are boxed and shown in light gray. Conserved residues that form the catalytic triad (*), α-helices (spirals) and β-sheets (arrows) are indicated on top of the sequences.

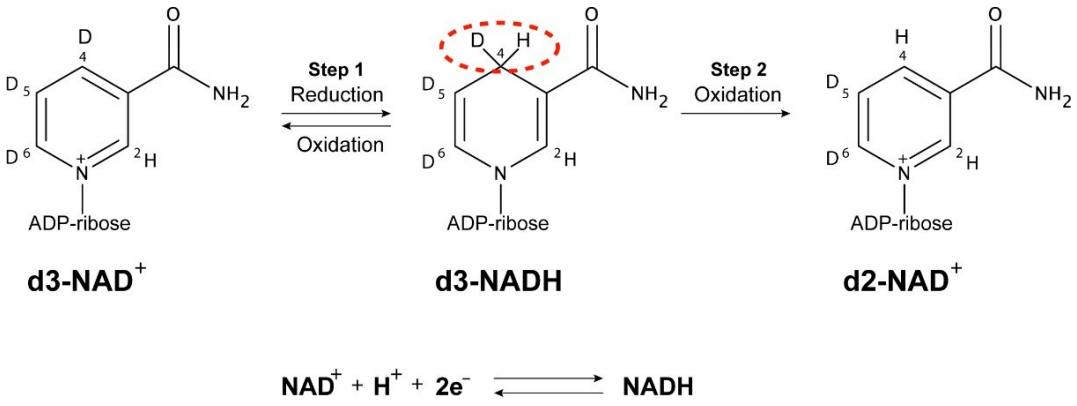

Figure 3.S2 Reversible reduction of NAD^+ results in the loss of a deuterium atom from the C4 position of the NAM moiety of NAD^+.

During step 1, the reduction of d_3-NAD^+ (labeled in positions 4, 5 and 6 of the NAM moiety) to d_3-NADH, the C4 position of the NAM moiety becomes covalently linked to both hydrogen and deuterium atoms (dotted circle). During step 2, the oxidation of NADH that regenerates NAD^+, either the hydrogen or the deuterium can be released, but the loss of deuterium from the C4 position results in the formation of d_2-NAD^+.

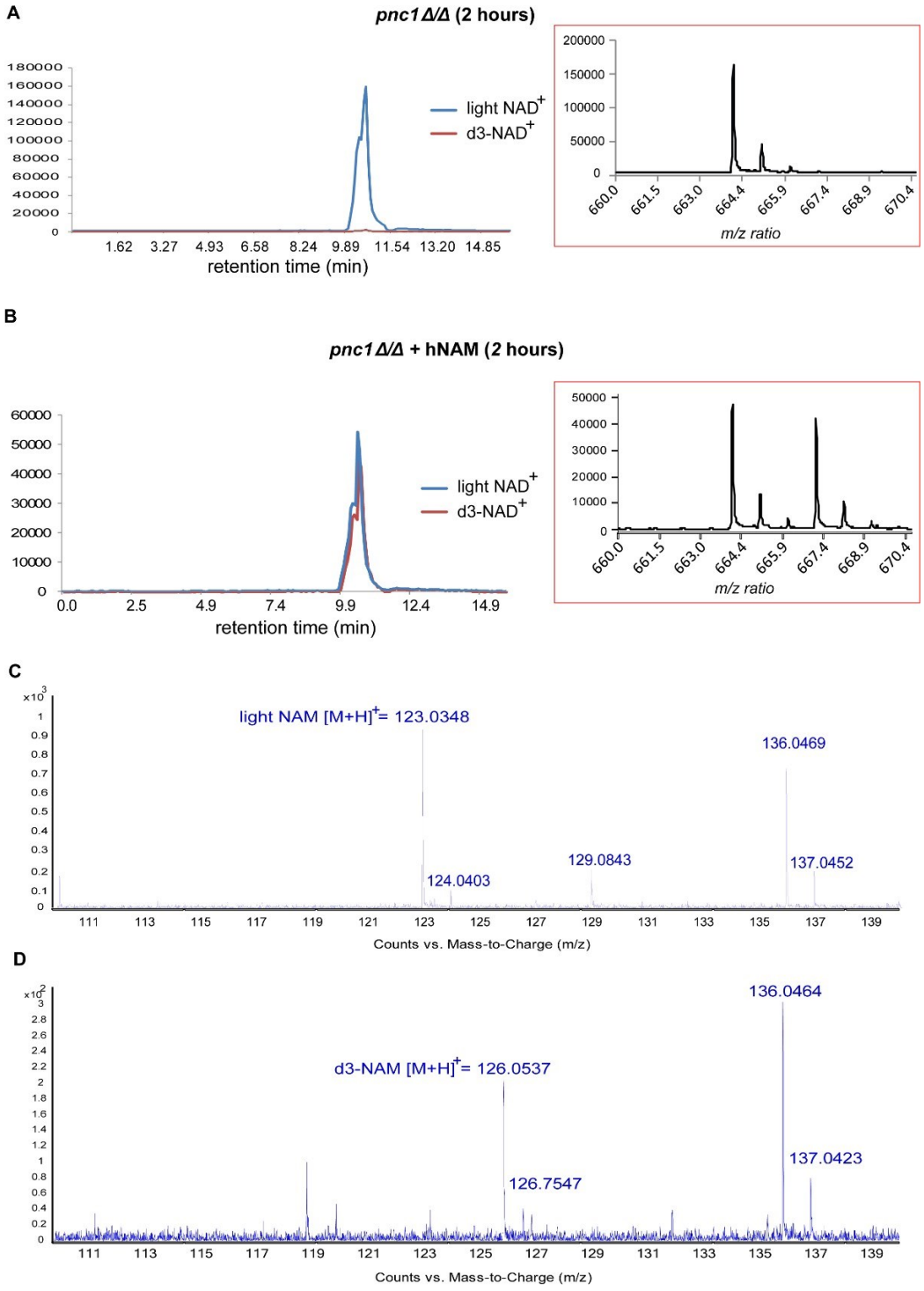

3.S3 Figure. LC-MS/MS detection of nicotinamide moieties derived from light and heavy d3-NAD$^+$.

*pnc1*Δ/Δ cells growing in SC-niacin were exposed to either 5mM NAM (A and C) or 5mM d_4-NAM (B and D) for 2 hours at 30□C and extracted metabolites were analyzed by LC-MS/MS.

(A) Retention time of light NAD^+ during RP-HPLC. Inset: [^{13}C] isotopic series of light NAD^+.
(B) Retention time of light NAD^+ and d_3-NAD^+ (generated by spontaneous loss of a deuterium atom from the C2 position of the NAM moiety) during RP-HPLC. Inset: [^{13}C] isotopic series of both light NAD^+ and d_3-NAD^+.
(C) Fragmentation spectrum of the precursor ion corresponding to light NAD^+ (shown in A). The singly charged ion at *m/z* 123.0348 corresponds to light NAM.
(D) Fragmentation spectrum of the precursor ion corresponding to d_3-NAD^+ (shown in B). The singly charged ion at *m/z* 126.0537 corresponds to d_3-NAM.

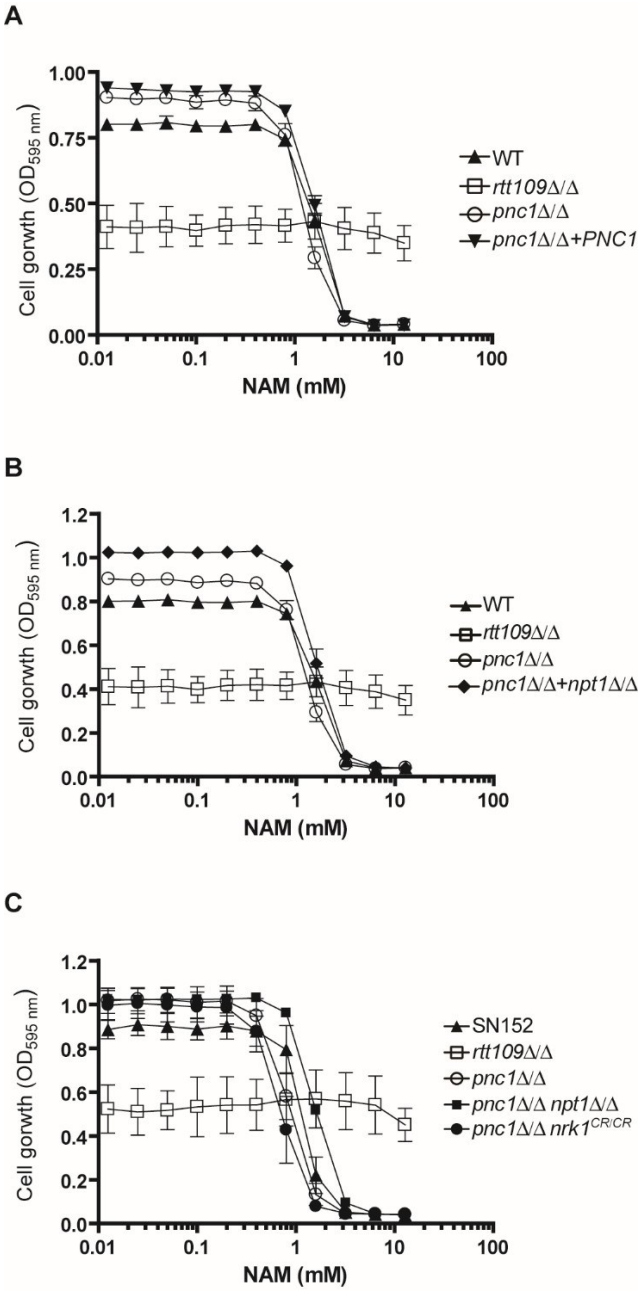

Figure 3.S4 Growth inhibition assays in liquid cultures supplemented with NAM.

(A-C) Strains were grown at 30°C for 24h in SC-Niacin medium containing increasing concentrations of NAM prior to measuring the optical density at 595nm (OD595). Panel (A) corresponds to the data presented in Figure 2A. Panel (B) corresponds to the data presented in Figure 4A. Panel (C) corresponds to the data shown presented in Figure 5A.

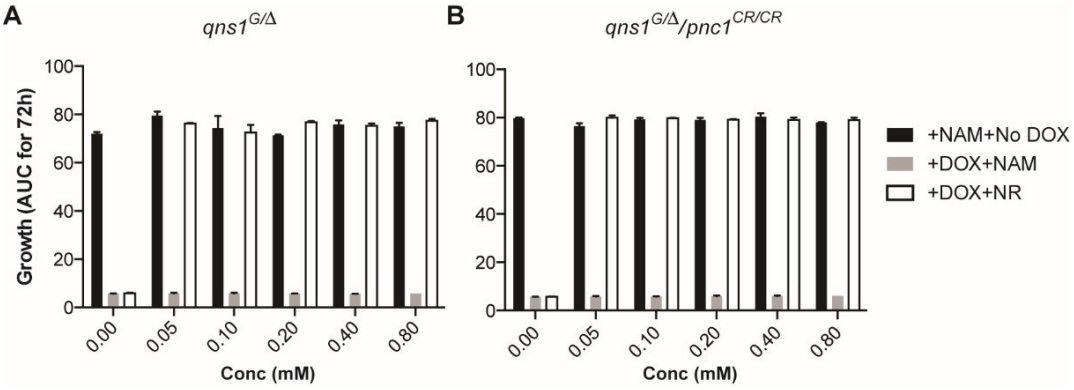

Figure 3.S5 The loss of viability caused by repression of NAD$^+$ synthetase (Qns1) cannot be overcome by NAM addition.

Strains where the only allele of the *QNS1* gene was repressible with doxycycline (*qns1*$^{G/\Delta}$) were incubated overnight in SC-Niacin containing DOX and 10 mM NR to deplete Qns1 while preserving viability. Strains *qns1*$^{G/\Delta}$ (A) and *qns1*$^{G/\Delta}$ *pnc1*$^{CR/CR}$ (B) were grown in SC-Niacin supplemented with increasing concentrations of either NR or NAM, and in the absence or presence of DOX to repress *QNS1*. Growth was monitored by measuring optical density at 600nm every 15 min for up to 72 hours. As described in the Methods sections, the areas under the resulting growth curves were transformed into numerical values (arbitrary units) that are proportional to the areas under the growth curves (AUC).

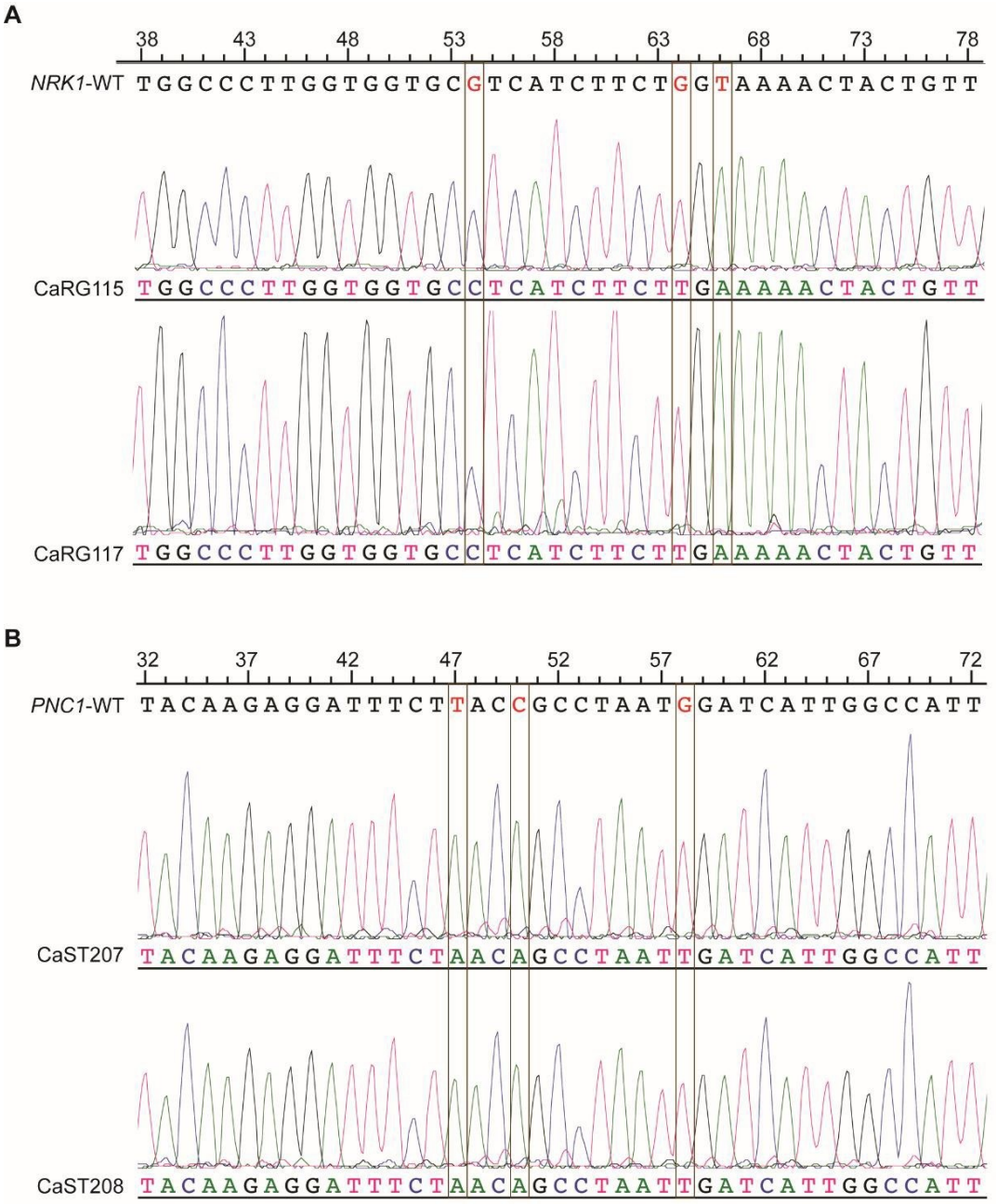

Figure 3.S6 Sequencing of CRISPR-generated loss-of-function alleles.

(A) The wild-type *NRK1* gene (top) is aligned to the DNA sequences of two *nrk1*$^{CR/CR}$ *pnc1*Δ/Δ independent clones (CaRG115 and CaRG117). The G-to-C silent mutation at nucleotide 54 (relative to ATG) was deliberately introduced to create a *Ban*I restriction site and facilitate genotyping during clone screening. The G-to-T and T-to-A mutations at nucleotides 64 and 66 converted a GGT codon to a TGA premature stop codon, and also mutated the sequence of the protospacer-adjacent motif (PAM) to prevent genetic instability caused by multiple cycles of DNA cleavage and repair.

(B) The wild-type *PNC1* gene (top) is aligned to the DNA sequences of two *qns1*$^{G/\Delta}$ *pnc1*$^{CR/CR}$ independent clones (CaST207 and CaST208). The C-to-A silent mutation at position 50 was deliberately introduced to create a *Bcl*I restriction site, and facilitate genotyping during clone screening. The T-to-A mutation at nucleotide 47 converted a TTA codon (nucleotides 46-48, encoding Leu16 of Pnc1) into a premature stop codon. The G-to-T mutation at nucleotide 58 converted of a GGA codon (encoding residue Gly20 of Pnc1) into a second stop codon and, in addition, mutated the PAM sequence to prevent multiple cycles of DNA cleavage and repair. Thus, each of the two mutated alleles of *PNC1* contained two premature stop codons in our isolates of *qns1*$^{G/\Delta}$ *pnc1*$^{CR/CR}$ cells.

Table 3.S1. Strains used in this study.

Name	**Genotype**	**Source**
SN152	*ura3* :: imm^{434} :: *URA3/ura3*::imm^{434} *iro1::IRO1/iro1*::imm^{434} *his1*::hisG/*his1*::hisG *leu2/leu2 arg4/arg4*	(Noble and Johnson 2005)
*rtt109*Δ/Δ	As SN152, *rtt109*Δ *:: C. dubliniensis ARG4/rtt109*Δ *:: C. dubliniensis HIS1*	(Wurtele *et al.* 2010)
CaST33 (*pnc1*Δ/Δ#1)	As SN152, *pnc1*Δ *::C. dubliniensis ARG4/pnc1*Δ *:: C. dubliniensis HIS1*	This study
CaST35 (*pnc1*Δ/Δ#2)	As SN152, *pnc1*Δ *:: C. dubliniensis ARG4/pnc1*Δ*::C. dubliniensis HIS1*	This study
CaRG25 (*pnc1*Δ/Δ+*PNC1*)	As CaST33, *pnc1*Δ*:: C. dubliniensis ARG4/PNC1-FRT*	This study
CaRG28 (*pnc1*Δ/Δ+*PNC1*)	As CaST35, *pnc1*Δ *:: C. dubliniensis ARG4/PNC1-FRT*	This study

CaRG80 (*pnc1*Δ/Δ *npt1*Δ/Δ)	As CaRG28, *npt1*Δ *:: C. dubliniensis ARG4/npt1*Δ*:: C. dubliniensis HIS1*	This study
CaRG101 (*pnc1*Δ/Δ *npt1*Δ/Δ)	As CaRG25, *npt1*Δ*:: C. dubliniensis ARG4/npt1*Δ*:: C. dubliniensis HIS1*	This study
CaRG115 (*pnc1*Δ/Δ/*nrk1*^{CR})	As CaST33, *nrk1*Δ/Δ	This study
CaRG117 (*pnc1*Δ/Δ/*nrk1*^{CR})	As CaST33, *nrk1*Δ/Δ	This study
Qns1-GRACE (*tetO-QNS1*/*qns1*Δ)	As CaSS1, *qns1::HIS3/SAT1-tetp-QNS1*	(Roemer *et al.* 2003)
CaST194 (*tetO-QNS1*/*qns1*Δ)	As Qns1GRACE, *qns1::HIS3/HygB-tetp-QNS1*	This study
CaST195 (*tetO-QNS1*/*qns1*Δ)	As Qns1GRACE, *qns1::HIS3/HygB-tetp-QNS1*	This study
CaST207	As CaST194, *pnc1*Δ/Δ	This study, (Roemer *et al.* 2003)
CaST208	As CaST194, *pnc1*Δ/Δ	This study, (Roemer *et al.* 2003)
CaST209	As CaST194, *pnc1*Δ/Δ	This study, (Roemer *et al.* 2003)
Plasmids		

pYM70	*Candida* adapted Hygromycin B resistance gene	(Basso *et al.* 2010)
pV1200	Solo system CaCas9/sgRNA entry expression vector, which contains the *NatR* gene, and 2-kb targeting arms for the upstream and downstream of the *ENO1* coding region. The Eno1 protein drives CaCas9 expression as above. The *NatR* gene and an *Snr52-sgRNA* cassette are flanked by FRT sites, which mediate recombination when *FLP* expression is induced	(Vyas *et al.* 2015)
pV1200-*PNC1*gRNA	pV1200 encoding a gRNA sequence that targets nucleotides 37 to 56 of *PNC1* (+1 is the adenine of the ATG initiator codon)	This study
pV1200-*NRK1*gRNA	pV1200 encoding a gRNA sequence that targets nucleotides 43 to 62 bp of *NRK1* (+1 is the adenine of the ATG initiator codon)	This study

Table 3.S2. Oligonucleotides used in this study.

Primer	Sequence (5' → 3')
ST8	CACTCCTAACCATACGCCATTATCACTAACAATCTCTTATACT AAAAGCAAACAATAACTTGTGGAATTGTGAGCGGATA
ST9	CTCCGGAACAACACAAAAAAAAAGCACGTAACGATGAATAGAG AAAATATATAAAACCTTCCACTCCTAACCATACGCCAT
ST10	CACCATTATCAATAAATAGTTTATCTGTGTCATTAATTTTCTCT GGATAAACCGATTCACGTTTTCCCAGTCACGACGTT
ST11	CATTGACCATCTCTTATTTAAATAAAGAATCAAATTTCTCATC ATTATCAACTATTGTAACACCATTATCAATAAATAGT
ST272	ATTTGATGGCCAATGATCCATTAGGG
ST273	AAAACCCTAATGGATCATTGGCCATC
ST274	ACTATGAAGAAAACAGCATTAATAGTAGTTGATCTACAAGAG GATTTCTAACAGCCTAATTGATC
ST275	TGGTTGATTTTGGGTATAACTGATCGACCATTTTTAATGGCCA ATGATCAATTAGGCTGTTAGAA
ST276	ACTATGAAGAAAACAGCATT
ST277	TGGTTGATTTTGGGTATAAC
RG1	TCCCCGCGGGCCCCTTAATGGACCAACTACTTTAAATT
RG2	CTAGAGCGGCCGCAGTACGGACAATCTGATAGA
RG3	ACTTCCTCGAGCTTATATTGATCTACTTTTC
RG4	GTACCGGGCCCTGATCAATTGAATGAATTAT
ST102	TTATACTTTTCAGTTACTTCATCGAATACCATTTGCCGAGGCAA GCTATAGTTATTGACCTGTGGAATTGTGAGCGGATA
ST103	CTGCCTGCTCGTGCCGAACTAGGTTTATCAAAAGTTCAACGTT TTTTTTTTATTGGCAATTTATACTTTTCAGTTACTTC
ST104	AATCACTCAACTGTTTGGTAGGGCTTACACACATTAAATTCGA ATACTATACACGACCCTGTTTTCCCAGTCACGACGTT
ST105	AAAAAATGTATACTCATCTAGTCATTCCGAAAAAGAACGAAA GAAGAAGAAAAAAAAAGGAATCACTCAACTGTTTGGTA
RG32	ATTTGCTTGGTGGTGCGTCATCTTCG

RG33	AAAACGAAGATGACGCACCACCAAGC
RG48	TTTTCTAAAATGACTACTACTGGTA
RG49	TGTAAAGTAAAAGTCATCCAAATGT
ST270	TCATGAGGCGCTAACTATAGAG
ST271	CGTCAAAACTAGAGAATAATAAAG

3.9 References

1) Anderson, Bitterman, Wood, Medvedik, Cohen *et al.*, 2002 Manipulation of a nuclear NAD+ salvage pathway delays aging without altering steady-state NAD+ levels. J Biol Chem 277**:** 18881-18890.
2) Antinori, Milazzo, Sollima, Galli and Corbellino, 2016 Candidemia and invasive candidiasis in adults: A narrative review. Eur J Intern Med 34**:** 21-28.
3) Banasik, Komura and Ueda, 1990 Inhibition of poly(ADP-ribose) synthetase by unsaturated fatty acids, vitamins and vitamin-like substances. FEBS Lett 263**:** 222-224.
4) Basso, Bartiss, Mao, Gast, Coelho *et al.*, 2010 Transformation of Candida albicans with a synthetic hygromycin B resistance gene. Yeast 27**:** 1039-1048.
5) Belenky, Racette, Bogan, Mcclure, Smith *et al.*, 2007 Nicotinamide riboside promotes Sir2 silencing and extends lifespan via Nrk and Urh1/Pnp1/Meu1 pathways to NAD+. Cell 129**:** 473-484.
6) Belenky, Stebbins, Bogan, Evans and Brenner, 2011 Nrt1 and Tna1-independent export of NAD+ precursor vitamins promotes NAD+ homeostasis and allows engineering of vitamin production. PLoS One 6**:** e19710.
7) Bieganowski, and Brenner, 2004 Discoveries of nicotinamide riboside as a nutrient and conserved NRK genes establish a Preiss-Handler independent route to NAD+ in fungi and humans. Cell 117**:** 495-502.
8) Brown, Denning, Gow, Levitz, Netea *et al.*, 2012 Hidden killers: human fungal infections. Sci Transl Med 4**:** 165rv113.
9) Burgos, and Schramm, 2008 Weak coupling of ATP hydrolysis to the chemical equilibrium of human nicotinamide phosphoribosyltransferase. Biochemistry 47**:** 11086-11096.

10) Celic, Masumoto, Griffith, Meluh, Cotter *et al.*, 2006 The sirtuins hst3 and Hst4p preserve genome integrity by controlling histone h3 lysine 56 deacetylation. Curr Biol 16**:** 1280-1289.
11) Chaffin, Barton, Jacobson and Jacobson, 1979 Nicotinamide adenine dinucleotide metabolism in Candida albicans. J Bacteriol 139**:** 883-888.
12) Chapman, Sullivan and Cleary, 2008 In search of the holy grail of antifungal therapy. Trans Am Clin Climatol Assoc 119**:** 197-215; discussion 215-196.
13) Croft, James Theoga Raj, Salemi, Phinney and Lin, 2018 A functional link between NAD(+) homeostasis and N-terminal protein acetylation in Saccharomyces cerevisiae. J Biol Chem 293**:** 2927-2938.
14) Dahlin, Kottom, Han, Zhou, Walters *et al.*, 2014 Pneumocystis jirovecii Rtt109, a novel drug target for Pneumocystis pneumonia in immunosuppressed humans. Antimicrob Agents Chemother 58**:** 3650-3659.
15) Dahlin, Sinville, Solberg, Zhou, Han *et al.*, 2013 A cell-free fluorometric high-throughput screen for inhibitors of Rtt109-catalyzed histone acetylation. PLoS One 8**:** e78877.
16) Davey, Sargent, Luger, Maeder and Richmond, 2002 Solvent mediated interactions in the structure of the nucleosome core particle at 1.9 a resolution. J Mol Biol 319**:** 1097-1113.
17) Donnelly, Boyd, Williams, Kelly and Macdermot, 1995 Inhibition of ADP-ribosyltransferase increases synthesis of Gs alpha in neuroblastoma x glioma hybrid cells and reverses iloprost-dependent heterologous loss of fluoride-sensitive adenylate cyclase. Biochem Pharmacol 49**:** 767-776.
18) Dragovic, Kim, Brown and Kim, 1995 Nicotinamide pharmacokinetics in patients. Radiother Oncol 36**:** 225-228.
19) Fernandez-Arenas, Cabezon, Bermejo, Arroyo, Nombela *et al.*, 2007 Integrated proteomics and genomics strategies bring new insight into Candida albicans response upon macrophage interaction. Mol Cell Proteomics 6**:** 460-478.
20) French, Cen, Vrablik, Xu, Allen *et al.*, 2010 Characterization of nicotinamidases: steady state kinetic parameters, classwide inhibition by nicotinaldehydes, and catalytic mechanism. Biochemistry 49**:** 10421-10439.
21) Gazzaniga, Stebbins, Chang, Mcpeek and Brenner, 2009 Microbial NAD metabolism: lessons from comparative genomics. Microbiol Mol Biol Rev 73**:** 529-541, Table of Contents.
22) Ghislain, Talla and Francois, 2002 Identification and functional analysis of the Saccharomyces cerevisiae nicotinamidase gene, PNC1. Yeast 19**:** 215-224.
23) Gossmann, Ziegler, Puntervoll, De Figueiredo, Schuster *et al.*, 2012 NAD(+) biosynthesis and salvage--a phylogenetic perspective. FEBS J 279**:** 3355-3363.
24) Hachinohe, Hanaoka and Masumoto, 2011 Hst3 and Hst4 histone deacetylases regulate replicative lifespan by preventing genome instability in Saccharomyces cerevisiae. Genes Cells 16**:** 467-477.

25) Hawse, Hoff, Fatkins, Daines, Zubkova *et al.*, 2008 Structural insights into intermediate steps in the Sir2 deacetylation reaction. Structure 16**:** 1368-1377.
26) Hnisz, Tscherner and Kuchler, 2011 Targeting chromatin in fungal pathogens as a novel therapeutic strategy: histone modification gets infectious. Epigenomics 3**:** 129-132.
27) Hoff, Avalos, Sens and Wolberger, 2006 Insights into the sirtuin mechanism from ternary complexes containing NAD+ and acetylated peptide. Structure 14**:** 1231-1240.
28) Horsman, Hoyer, Honess, Dennis and Overgaard, 1993 Nicotinamide pharmacokinetics in humans and mice: a comparative assessment and the implications for radiotherapy. Radiother Oncol 27**:** 131-139.
29) Jabra-Rizk, Kong, Tsui, Nguyen, Clancy *et al.*, 2016 Candida albicans Pathogenesis: Fitting within the Host-Microbe Damage Response Framework. Infect Immun 84**:** 2724-2739.
30) Jackson, Schmidt, Oppenheimer and Denu, 2003 Mechanism of nicotinamide inhibition and transglycosidation by Sir2 histone/protein deacetylases. J Biol Chem 278**:** 50985-50998.
31) Kato, and Lin, 2014 YCL047C/POF1 is a novel nicotinamide mononucleotide adenylyltransferase (NMNAT) in Saccharomyces cerevisiae. J Biol Chem 289**:** 15577-15587.
32) Kim, and Sudbery, 2011 Candida albicans, a major human fungal pathogen. J Microbiol 49**:** 171-177.
33) Knip, Douek, Moore, Gillmor, Mclean *et al.*, 2000 Safety of high-dose nicotinamide: a review. Diabetologia 43**:** 1337-1345.
34) Kornberg, 1948 The participation of inorganic pyrophosphate in the reversible enzymatic synthesis of diphosphopyridine nucleotide. J Biol Chem 176**:** 1475.
35) Kuchler, Jenull, Shivarathri and Chauhan, 2016 Fungal KATs/KDACs: A New Highway to Better Antifungal Drugs? PLoS Pathog 12**:** e1005938.
36) Kusch, Engelmann, Bode, Albrecht, Morschhauser *et al.*, 2008 A proteomic view of Candida albicans yeast cell metabolism in exponential and stationary growth phases. Int J Med Microbiol 298**:** 291-318.
37) Kushnirov, 2000 Rapid and reliable protein extraction from yeast. Yeast 16**:** 857-860.
38) Landry, Slama and Sternglanz, 2000 Role of NAD(+) in the deacetylase activity of the SIR2-like proteins. Biochem Biophys Res Commun 278**:** 685-690.
39) Lenglet, Liabeuf, Guffroy, Fournier, Brazier *et al.*, 2013 Use of nicotinamide to treat hyperphosphatemia in dialysis patients. Drugs R D 13**:** 165-173.
40) Libri, Yandim, Athanasopoulos, Loyse, Natisvili *et al.*, 2014 Epigenetic and neurological effects and safety of high-dose nicotinamide in patients with Friedreich's ataxia: an exploratory, open-label, dose-escalation study. Lancet 384**:** 504-513.

41) Lopes Da Rosa, Bajaj, Spoonamore and Kaufman, 2013 A small molecule inhibitor of fungal histone acetyltransferase Rtt109. Bioorg Med Chem Lett 23**:** 2853-2859.
42) Lopes Da Rosa, Boyartchuk, Zhu and Kaufman, 2010 Histone acetyltransferase Rtt109 is required for Candida albicans pathogenesis. Proc Natl Acad Sci U S A 107**:** 1594-1599.
43) Lopes Da Rosa, and Kaufman, 2013 Chromatin-mediated Candida albicans virulence. Biochim Biophys Acta 1819**:** 349-355.
44) Low, and Rotstein, 2011 Emerging fungal infections in immunocompromised patients. F1000 Med Rep 3**:** 14.
45) Ma, Pan, Zupancic and Cormack, 2007 Assimilation of NAD(+) precursors in Candida glabrata. Mol Microbiol 66**:** 14-25.
46) Mackay, Hathcock and Guarneri, 2012 Niacin: chemical forms, bioavailability, and health effects. Nutr Rev 70**:** 357-366.
47) Masumoto, Hawke, Kobayashi and Verreault, 2005 A role for cell-cycle-regulated histone H3 lysine 56 acetylation in the DNA damage response. Nature 436**:** 294-298.
48) Mcclure, Wierman, Maqani and Smith, 2012 Isonicotinamide enhances Sir2 protein-mediated silencing and longevity in yeast by raising intracellular NAD+ concentration. J Biol Chem 287**:** 20957-20966.
49) Natalini, Ruggieri, Raffaelli and Magni, 1986 Nicotinamide mononucleotide adenylyltransferase. Molecular and enzymatic properties of the homogeneous enzyme from baker's yeast. Biochemistry 25**:** 3725-3729.
50) Neville, D'enfert and Bougnoux, 2015 Candida albicans commensalism in the gastrointestinal tract. FEMS Yeast Res 15.
51) Nobile, Fox, Hartooni, Mitchell, Hnisz *et al.*, 2014 A histone deacetylase complex mediates biofilm dispersal and drug resistance in Candida albicans. MBio 5**:** e01201-01214.
52) Noble, and Johnson, 2005 Strains and strategies for large-scale gene deletion studies of the diploid human fungal pathogen Candida albicans. Eukaryot Cell 4**:** 298-309.
53) Pasqualotto, and Denning, 2008 New and emerging treatments for fungal infections. J Antimicrob Chemother 61 Suppl 1**:** i19-30.
54) Pfaller, and Diekema, 2007 Epidemiology of invasive candidiasis: a persistent public health problem. Clin Microbiol Rev 20**:** 133-163.
55) Pfaller, and Diekema, 2010 Epidemiology of invasive mycoses in North America. Crit Rev Microbiol 36**:** 1-53.
56) Pfaller, Messer, Georgopapadakou, Martell, Besterman *et al.*, 2009 Activity of MGCD290, a Hos2 histone deacetylase inhibitor, in combination with azole antifungals against opportunistic fungal pathogens. J Clin Microbiol 47**:** 3797-3804.

57) Pfaller, Rhomberg, Messer and Castanheira, 2015 In vitro activity of a Hos2 deacetylase inhibitor, MGCD290, in combination with echinocandins against echinocandin-resistant Candida species. Diagn Microbiol Infect Dis 81**:** 259-263.
58) Pissios, 2017 Nicotinamide N-Methyltransferase: More Than a Vitamin B3 Clearance Enzyme. Trends Endocrinol Metab 28**:** 340-353.
59) Preiss, and Handler, 1958 Biosynthesis of diphosphopyridine nucleotide. II. Enzymatic aspects. J Biol Chem 233**:** 493-500.
60) Rankin, Jacobson, Benjamin, Moss and Jacobson, 1989 Quantitative studies of inhibitors of ADP-ribosylation in vitro and in vivo. J Biol Chem 264**:** 4312-4317.
61) Reuss, Vik, Kolter and Morschhauser, 2004 The SAT1 flipper, an optimized tool for gene disruption in Candida albicans. Gene 341**:** 119-127.
62) Robbins, Wright and Cowen, 2016 Antifungal Drugs: The Current Armamentarium and Development of New Agents. Microbiol Spectr 4.
63) Robert, and Gouet, 2014 Deciphering key features in protein structures with the new ENDscript server. Nucleic Acids Res 42**:** W320-324.
64) Roemer, Jiang, Davison, Ketela, Veillette *et al.*, 2003 Large-scale essential gene identification in Candida albicans and applications to antifungal drug discovery. Mol Microbiol 50**:** 167-181.
65) San Pietro, 1955 Base-catalyzed deuterium exchange with diphosphopyridine nucleotide. J Biol Chem 217**:** 589-593.
66) Sauve, Celic, Avalos, Deng, Boeke *et al.*, 2001 Chemistry of gene silencing: the mechanism of NAD+-dependent deacetylation reactions. Biochemistry 40**:** 15456-15463.
67) Sauve, Moir, Schramm and Willis, 2005 Chemical activation of Sir2-dependent silencing by relief of nicotinamide inhibition. Mol Cell 17**:** 595-601.
68) Sauve, and Schramm, 2003 Sir2 regulation by nicotinamide results from switching between base exchange and deacetylation chemistry. Biochemistry 42**:** 9249-9256.
69) Segal, Kwon-Chung, Walsh, Klein, Battiwalla *et al.*, 2006 Immunotherapy for fungal infections. Clin Infect Dis 42**:** 507-515.
70) Smith, Anderson, Hoadley, Keck, Cleland *et al.*, 2012 Structural and kinetic isotope effect studies of nicotinamidase (Pnc1) from Saccharomyces cerevisiae. Biochemistry 51**:** 243-256.
71) Smith, Brachmann, Celic, Kenna, Muhammad *et al.*, 2000 A phylogenetically conserved NAD+-dependent protein deacetylase activity in the Sir2 protein family. Proc Natl Acad Sci U S A 97**:** 6658-6663.
72) Smith, and Denu, 2006 Sir2 protein deacetylases: evidence for chemical intermediates and functions of a conserved histidine. Biochemistry 45**:** 272-282.
73) Sorci, Blaby, De Ingeniis, Gerdes, Raffaelli *et al.*, 2010 Genomics-driven reconstruction of acinetobacter NAD metabolism: insights for antibacterial target selection. J Biol Chem 285**:** 39490-39499.

74) Stratford, Dennis, Hoskin, Phillips, Hodgkiss *et al.*, 1996 Nicotinamide pharmacokinetics in humans: effect of gastric acid inhibition, comparison of rectal vs oral administration and the use of saliva for drug monitoring. Br J Cancer 74**:** 16-21.
75) Tanner, Landry, Sternglanz and Denu, 2000 Silent information regulator 2 family of NAD- dependent histone/protein deacetylases generates a unique product, 1-O-acetyl-ADP-ribose. Proc Natl Acad Sci U S A 97**:** 14178-14182.
76) Tempel, Rabeh, Bogan, Belenky, Wojcik *et al.*, 2007 Nicotinamide riboside kinase structures reveal new pathways to NAD+. PLoS Biol 5**:** e263.
77) Trammell, and Brenner, 2013 Targeted, LCMS-based Metabolomics for Quantitative Measurement of NAD(+) Metabolites. Comput Struct Biotechnol J 4**:** e201301012.
78) Tsao, Weber, Cameron, Nehme, Ahmadzadeh *et al.*, 2016 Positive regulation of the Candida albicans multidrug efflux pump Cdr1p function by phosphorylation of its N-terminal extension. J Antimicrob Chemother 71**:** 3125-3134.
79) Vyas, Barrasa and Fink, 2015 A Candida albicans CRISPR system permits genetic engineering of essential genes and gene families. Sci Adv 1**:** e1500248.
80) Wang, Zhang, Bheda, Revollo, Imai *et al.*, 2006 Structure of Nampt/PBEF/visfatin, a mammalian NAD+ biosynthetic enzyme. Nat Struct Mol Biol 13**:** 661-662.
81) Wurtele, Tsao, Lepine, Mullick, Tremblay *et al.*, 2010 Modulation of histone H3 lysine 56 acetylation as an antifungal therapeutic strategy. Nat Med 16**:** 774-780.
82) Zhou, Kurnasov, Tomchick, Binns, Grishin *et al.*, 2002 Structure of human nicotinamide/nicotinic acid mononucleotide adenylyltransferase. Basis for the dual substrate specificity and activation of the oncolytic agent tiazofurin. J Biol Chem 277**:** 13148-13154.
83) Zoltewicz, and Helmick, 1970 Base-catalyzed hydrogen-deuterium exchange of N-substituted pyridinium ions. Inductive effects and internal return. Journal of the American Chemical Society 92**:** 7547-7552.

4 General discussion, perspectives and conclusion

This discussion is divided into two broad sections: fundamental discoveries from this study and applicable targets. In section 4.1, I have discussed the novel findings from this study in detail and in section 4.2 I have discussed enzymes that have the potential to be valuable targets for drug discovery.

4.1 Fundamental discoveries

During the last three decades, the incidence of invasive fungal infections in critically ill individuals has increased drastically. The ever-growing population of immunocompromised patients due to increasing use of broad-spectrum antibiotics that disrupt the microbial flora and opens the doors for fungal colonisation, use of immunosuppressive chemotherapy, incidence of drug resistance, and HIV-AIDS patients have led to an increase in the incidence of invasive fungal infections (Mavor *et al.* 2005; Pfaller and Diekema 2007; Pfaller and Diekema 2010; Badiee and Hashemizadeh 2014). There has been a steady decline in the interest of the pharmaceutical industry in developing new antifungal drugs as different screening campaigns from diverse libraries led to the finding of the same basic scaffolds (Roemer and Krysan 2014). The increase in the number of fungal infections and lack of new antifungal strategies have forced laboratories around the world to find novel targets and explore new therapeutic strategies to combat these infections. Acetylation of lysine 56 on histone H3 is a reversible post-translational modification brought about by enzymes that show fungal-specific properties (Masumoto *et al.* 2005; Schneider *et al.* 2006; Schemies *et al.* 2010). Advantages of targeting this pathway for novel antifungal therapies are described in the introduction of the thesis (section 1.4.3.1 and 1.4.3.2). In this thesis, Chapter 2 is focused on characterizing the H3K56 acetylation pathway in *C. albicans* to enhance its potential as a target for the development of novel antifungal strategies. Hst3 inhibition by NAM leads to hyperacetylation of H3K56 followed by cell death. In

Chapter 3, I have studied *C. albicans* NAM metabolism to find ways to improve its therapeutic efficacy and discover additional targets for antifungal drug discovery.

4.1.1. Novel aspects of Rtt109 HAT complex in *C. albicans*

The role of chromatin-modifying enzymes in fungal virulence and fitness is beginning to be unraveled. There are convincing studies to support the idea that chromatin-modifying enzymes are potential targets for antifungal drug discovery (Lopes Da Rosa *et al.* 2010; Wurtele *et al.* 2010; Lopes Da Rosa and Kaufman 2013; Kuchler *et al.* 2016). Histone-modifying enzymes play important roles in DNA repair, transcriptional activation, and maintenance of genome integrity (Allard *et al.* 2004; Millar and Grunstein 2006; Kouzarides 2007). This thesis is focused on understanding a fungal-specific chromatin modification pathway, acetylation and deacetylation of H3K56. Enzymes that have fungal-specific properties catalyze these modifications of H3K56 and, since targeting fungal-specific processes reduces side effects and host toxicities, the enzymes that acetylate and deacetylate H3K56 represent attractive targets for antifungal therapy. Our studies reveal that i) the catalytic residues of Rtt109 is conserved in *C. albicans*, ii) first evidence that Vps75 contributes to H3K56 acetylation *in vivo*, iii) the function of Vps75 in Rtt109 stabilization is conserved in *C. albicans*, and iv) Rtt109-Vps75 can acetylate H3K56 *in vitro.*

H3K56ac is an abundant post-translational modification found in *C. albicans* where it is catalyzed by the HAT Rtt109 (Wurtele *et al.* 2010). Two residues, D89 and W222 that are important for Rtt109 catalytic activity are conserved among fungal species (Fig 2.1A) (Tang *et al.* 2008). Our results showed that the catalytic activity of Rtt109 is conserved in *C. albicans* (Fig 2.1C). However, the functions of Rtt109's protein co-factors in acetylating H3K56, are somewhat divergent among fungal species. Crystal structures, as well as recent functional studies of ScRtt109, revealed several domains through which its activity is modulated, such as the

interfaces between ScRtt109-Vps75 (Fig 2.1A) (Su *et al.* 2011; Tang *et al.* 2011; Radovani *et al.* 2013). It has been shown that binding of ScVps75 stimulates the catalytic activity of ScRtt109. Furthermore, ScVps75 binding to Rtt109 via the interacting loop I (ScRtt109 residues 128-170, corresponding to CaRtt109 residues 130-175) (Fig 2.1A and 2.S1) could protect ScRtt109 from proteolysis (Berndsen *et al.* 2008; Keck and Pemberton 2011; Tang *et al.* 2011). Rtt109 residues in the region of the interacting loop I are not conserved and do not carry a similar charge in *S. cerevisiae* and *C. albicans* (Fig 2.1A and 2.S1), but the role of Vps75 in Rtt109 stabilization is conserved (Fig 2.3B). In *S. cerevisiae* ScVps75 is not required for H3K56ac *in vivo*, however ScRtt109 mutant (residues of 1-424) lacking a C-terminal Lys/Arg-rich patch required ScVps75 to promote optimum H3K56ac *in vivo* (Radovani *et al.* 2013). The functional divergence of Vps75 in *C. albicans* may be the result of lack of Lys/Arg-rich sequence at the Rtt109 C-terminus that makes the role of Vps75 essential for optimal H3K56 acetylation in *S. cerevisiae* (Radovani *et al.* 2013). In contrast to studies performed in *S. cerevisiae,* our data suggest that *C. albicans* Vps75 has the dual function of stabilizing Rtt109 *in vivo* and promoting H3K56ac both *in vitro* and *in vivo* (Fig 2.2-2.4). These results highlight an intricate control of Rtt109 by Vps75. Interestingly, functional domains of Rtt109 (interacting loops) are not conserved among fungal species, implying that the regulation of Rtt109 by histone chaperones is evolutionarily divergent among fungi (Fig 2.S1). As a future direction, it would be essential to study the mechanism of H3K56ac in other important fungal pathogens to enhance Rtt109's potential as a broad-spectrum antifungal target. The majority of fungal pathogens encode a close homologue of Rtt109 and this is indicative of the presence of an H3K56 acetylation and deacetylation pathway. Fungal Rtt109 vary in size and that might alter the role of its co-factors in acetylating H3K56 (Fig 2S1), hence is will be beneficial to understand this pathway in other pathogenic fungi.

In budding yeast, Rtt109 and Asf1 are responsible for H3K56ac and ScRtt109-Vps75 acetylates N-terminal tail residues (Fig 1.5) (Abshiru *et al.* 2013; Kuo and Andrews 2013). Rtt109 C-terminal tail is required for H3K9 acetylation *in vivo* (Radovani et al. 2013). We did not observe any changes at other sites in the N-

terminal tail of histone H3 in *vps75* null mutant in *C. albicans* (Fig 2.2E). Possibly CaRtt109, which lacks the lysine-rich C-terminal tail requires Asf1 and/or other HATs such as Gcn5 for N-terminal tail acetylation of H3. Recent structural analysis showed that ScRtt109 interacts with Asf1 through its C-terminal tail, making the case of CaRtt109 more interesting (Lercher *et al.* 2017). Our results show that CaRtt109-Vps75 can acetylate H3K56ac *in vitro.* Quantitative mass spectrometry analysis of our HAT assays found a stoichiometry of H3K56ac between 10-15% (Fig 2.4C). It is likely that Rtt109-Vps75 can acetylate H3K56 partially, but optimum acetylation can only be achieved in the presence of Asf1. We observed that CaRtt109-Vps75 can acetylate H3K9 independently of H3K56ac (Fig 2.4C). It would be interesting to know the stoichiometries of acetylation at other N-terminal lysine residues in these HAT reactions. We suspect that CaRtt109-Vps75 can acetylate N-terminal tail lysines more efficiently than H3K56 and we expect that addition of Asf1 in our HAT assays will lead to optimum H3K56ac *in vitro*. I propose a model that in *C. albicans,* maximal H3K56ac is achieved by Rtt109-Vps75 together with Asf1. Altogether, our data show that Rtt109 co-factors, Vps75 and Asf1, show diverged functions of these proteins in the fungal pathogen. It is intriguing that the *C. albicans* Rtt109 HAT complex has evolved a mode of interaction that is somewhat different from that of budding yeast Rtt109. We suspect the different modes of actions of Rtt109 and its co-factors, Vps75 and Asf1 can be attributed to the role of H3K56ac in virulence. This result makes a case for a further understanding of these enzymes in other pathogenic fungi.

4.1.2. Multiple ways to get rid of excess NAM in *C. albicans*

We started working on the NAD^+ biosynthesis pathway in *C. albicans* to understand NAM metabolism in this fungus since our knowledge of this pathway was mostly based on experiments performed in *S. cerevisiae*. NAM is a form of vitamin B_3 that serves as a source of NAD^+. When we started working on NAD^+ biosynthesis in *C. albicans,* genes involved in this pathway were not characterized. We constructed a *C. albicans* NAD^+ metabolism pathway using genes encoding enzymes highly

identical to those of *S. cerevisiae* (Fig 3.1) and studied the *C. albicans* enzymes using a combination of genetics and metabolomics. Our original discoveries from this study include i) first report of characterization of genes involved in NAD^+ metabolism in *C. albicans,* ii) Pnc1 is the only nicotinamidase in *C. albicans* and Npt1 works downstream of it, iii) *C. albicans* have a robust mechanism to maintain constant NAD^+ levels, iv) Qns1 is essential for viability in *C. albicans*, except when the medium is supplemented with nicotinamide riboside as a source of NAD^+ v) existance of a non-canonical pathway that generates NAD^+ from NAM in the absence of Pnc1 *C. albicans,* and vi) evidence that showed non-canonical incorporation of NAM into NAD^+ happens through the NAM exchange reaction that inhibits sirtuins.

Our studies on NAM metabolism in *C. albicans* yielded interesting results. NAM enters *C. albicans* cells quickly and is metabolized to NA in a Pnc1-dependent manner. Contrary to the established notion that NAM cannot be converted into NAD^+ in the absence of Pnc1 (canonical salvage pathway in *S. cerevisiae*), our result proved otherwise in *C. albicans*. Previous studies in *S. cerevisiae* had shown that the only way to get rid of excess NAM was Pnc1-mediated conversion into NA and export of NA (Belenky *et al.* 2011). We showed that NAM is converted into NAD^+ in a Pnc1-independent manner in *C. albicans* (Fig 3.3F). We termed this process a “non-canonical conversion" of NAM into NAD^+ that occurred in a Pnc1- and Npt1-independent manner. To our knowledge, the existence of this pathway has not been reported in any other fungal organism. We tested different possibilities by which this non-canonical conversion of NAM into NAD^+ might be happening. Our results provided evidence that the non-canonical pathway operates, at least in part, through the NAM exchange reaction that inhibits sirtuins. Our results showed that the non-canonical pathway was able to generate NAD^+ from NAM in the absence of Pnc1 at physiological NAM concentrations (0.1 mM) that do not severely inhibit Hst3 (Fig 3.7A). Based on this result, we suspected that the non-canonical pathway might be able to sustain the growth of *C. albicans* on its own. However, in the absence of nicotinamide riboside, when we shut down the *de novo* pathway and the NAM salvage pathway to force cells to generate NAD^+ from NAM

using the non-canonical pathway, it failed to sustain the growth of *C. albicans* on its own (Fig 3.7D). This indicates that the non-canonical pathway is not sufficiently efficient to maintain NAD^+ levels required to sustain the growth of *C. albicans*.

4.1.2.1. NAM exchange and other possibilities for non-canonical pathway

Sirtuins are a group of HDACs that require NAD^+ as a co-substrate. Most HDACs simply hydrolyze acetyl groups from their substrate. However, the fact that sirtuins are entirely dependent upon NAD^+ to deacetylate their substrates suggests that the activity of sirtuins may be regulated by the redox state of the cell (Sauve *et al.* 2001; Sauve and Schramm 2003). Alternatively, because the unusual NAD^+-dependent deacetylation reaction catalyzed by sirtuins produces deacetylated proteins, NAM and 2'-O-acetyl-ADPR, it has been proposed that sirtuin activity may be modulated by fluctuations in the levels of NAM and/or the 2'-O-acetyl-ADPR reaction product may have functions of its own (Fig 1.6 and Fig 3.6A) (Landry *et al.* 2000; Min *et al.* 2001; Sauve *et al.* 2001; Tong and Denu 2010). Previous studies from different groups have shown that the Sir2-mediated deacetylation reaction can be reversed at the level of a reaction intermediate. Sirtuin reversal has been shown to work in the presence of excess NAM (Sauve and Schramm 2003). In the presence of excess NAM, sirtuin-mediated deacetylation reactions can be driven in reverse by an attack of NAM on a reaction intermediate known O-alkylamidate. This reverse reaction, known as the base-exchange reaction, reforms an acetylated peptide (or protein) and NAD^+, rather than forming a deacetylated peptide, 2'-O-acetyl-ADPR, and nicotinamide (Fig 3.6B) (Landry *et al.* 2000; Min *et al.* 2001; Sauve *et al.* 2001). In our case, the intracellular concentration of NAM is sufficiently high to drive the NAM exchange reaction. Our experiments did not allow us to determine the relative efficiencies at which individual sirtuins undergo reversal reaction. To elucidate the relative efficiencies by which the reactions catalyzed by each sirtuin can be reversed, individual sirtuin mutants will need to be generated. There are at least four sirtuins in *C. albicans* (Sir2, Hst1-3) and at least one of them is essential for

viability (Hst3), which would make it difficult to determine the relative contributions of individual sirtuins *in vivo*. Although our results show evidence of sirtuin reversal *in vivo,* they do not rule out the possibility of the existence of other mechanisms to get rid of excess NAM. isoNAM is a weak inhibitor of the NAM exchange reaction. Given the nature of the NAM exchange reaction, it can not help clear excess NAM because it cannot consume NAM molecules. We showed that the NAM exchange reaction occurred when a *pnc1* null mutant was challenged with NAM, but we cannot assess the probability with which the NAM exchange reaction occurs in wild-type cells where the canonical NAM salvage pathway converts NAM into NA. This depends upon the NAM's IC50 or Ki to inhibit different sirtuins and values ranging from 50 μM up to 400 μM for different sirtuins *in vitro.*

We consistently detected formation of hNMN in a *pnc1* null mutant treated with hNAM (Fig 3.4C, 3.5B and 3.7B). We have previously discussed the possibility of conversion of $hNAD^+$ into hNMN by Nma1 reversal and why it is unlikely that presence of hNMN can be attributed to it (Chapter 3.4 discussion). NAM is a base, and with the activity of phosphoribosyl transferase, it can be converted into the nucleotide NMN. The possibility that NAM may be converted into NMN by non-specific phosphoribosyl transferases involved in nucleotide synthesis, which convert RNA or DNA bases into nucleotides, cannot be ruled out based on our results. Humans encode the nicotinamide phosphoribosyl transferase (Nampt) that converts NAM into NMN. A sequence homology search identified Npt1 as the closest sequence homologue of Nampt in *C. albicans*. However, we ruled out a role of Npt1 in the non-canonical pathway (Fig 3.4C-D). As stated, we cannot rule out a role for phosphoribosyl transferases whose natural substrates is not NAM in converting NAM into NMN, when sufficiently high concentrations of NAM are present. Once NMN is formed, the enzymatic activity of Nma1 can convert NMN into NAD^+ (Fig 3.1). The *C. albicans* genome contains several genes that encode enzymes with putative phosphoribosyltransferase activity. However, testing their role in NMM synthesis would be difficult because most of them are involved in nucleotide biosynthesis and are essential for viability. Export seems a likely possibility to get rid of excess NAM. However, given our experimental setup, we

could not test the possibility of NAM export as all our assays were performed in the continuous presence of NAM. It would be impossible to differentiate the NAM that is present in the medium from the NAM that has been exported out by cells. In an experiment, where cells are transiently exposed to NAM and removing it to monitor the accumulation of NAM in the fresh medium, might be possible to assess NAM export.

We identified different fates of NAM in the *pnc1* null mutant. However, it is difficult to predict to what extent these "non-canonical fates" would contribute to decreasing NAM concentration in wild-type cells where Pnc1-mediated conversion of NAM into NA also depletes intracellular NAM. Taken together, our studies revealed that *C. albicans* has multiple ways to get rid of excess NAM, i) convert it to NA by nicotinamidase, Pnc1, ii) convert it into NAD^+ by sirtuin-dependent NAM exchange and iii) convert it into NMN. Due to the existence of multiple mechanisms to get rid of excess NAM, it will be difficult to increase the abundance of intracellular NAM in order to improve its therapeutic efficacy.

4.2 Potential targets identified from this study

There is a valid debate in the field of antifungals about target selection. The relative value of targeting non-essential versus essential processes is part of this debate. Is it better to target virulence factors that are not essential for viability or target essential processes, which makes it a fungicidal target? Both *pros* and *cons* of the fungicidal approach have been discussed in the Introduction (section 1.4.1.). The H3K56 acetylation and deacetylation pathway is unique in this regard. Inhibition of the Rtt109 HAT that acetylates H3K56 reduces virulence, but it is not fungicidal (Lopes Da Rosa *et al.* 2010; Wurtele *et al.* 2010). On the contrary, inhibition of Hst3, a deacetylase that removes H3K56ac, is fungicidal (Wurtele *et al.* 2010). Most of the targets that we propose are discussed in Chapter 2 and Chapter 3, but I would like to elaborate on them further.

4.2.1. Rtt109

Previously, two groups have conducted screens to find small molecule(s) targeting the recombinant *S. cerevisiae* Rtt109 HAT complex. Out of a total of 525,000 compounds that were screened, only two compounds showed inhibitory activity against the Rtt109 HAT complex (Dahlin *et al.* 2013; Lopes Da Rosa *et al.* 2013). These compounds did not show any activity against human p300, which is structurally related to Rtt109 or *S. cerevisiae* Gcn5, demonstrating the selectivity of their action against ScRtt109 (Dahlin *et al.* 2013; Lopes Da Rosa *et al.* 2013). These compounds are far from being antifungal agents and need further medicinal chemistry optimization, but these findings show that it is possible to find small molecules that inhibit Rtt109 HAT activity. The previous screens were performed using *S. cerevisiae* enzymes. Based on our findings (Chapter 2), we now know that the properties of enzymes involved in H3K56 acetylation are not identical in *C. albicans* and *S. cerevisiae*. Vps75 is not required for H3K56ac *in vivo* in *S. cerevisiae*, and the screen performed by Rosa *et al* 2013 did not include the two co-factors (Vps75 and Asf1) together in their assays. However, now that it is established that Vps75 is required for optimal H3K56ac *in vivo* in *C. albicans,* we propose that further screens to identify inhibitors of Rtt109 should be performed using the *C. albicans* enzymes and their co-factors. We have purified the *C. albicans* enzymes and demonstrated their activity *in vitro*. These enzymes will be better suited for antifungal drug discovery. The assay performed using *C. albicans* HAT complex could assist in developing a better screening strategy, taking into account the role of Rtt109 and its co-factors as well as the diversities of chemotypes in the screening libraries.

The absence of H3K56ac leads to accumulation of spontaneous DNA damage. *C. albicans* cells that cannot acetylate H3K56 show reduced virulence, emphasizing the importance of withstanding genotoxic stress for pathogenesis (Lopes Da Rosa *et al.* 2010; Wurtele *et al.* 2010). A functional H3K56ac pathway is necessary for systemic candidiasis. Rtt109 inhibition will reduce virulence and render the pathogen exposed to the host immune system. However, to take advantage of Rtt109 inhibition as a potential treatment option, the host immune system must be

at least partially functional. Given the fact that a majority of people affected by opportunistic fungal infections have a compromised immune system; this might limit the use of Rtt109 inhibition to patients suffering from systemic candidiasis but Rtt109 inhibition may still help in coping with the infection. *rtt109* mutants are sensitive to echinocandins (caspofungin and micafungin) (Wurtele *et al.* 2010) and flucytosine (Lopes Da Rosa *et al.* 2010). Rtt109 inhibitors together with echinocandins and flucytosine can be used in combination therapy. Both echinocandins and flucytosine are clinically approved drugs to treat systemic candidiasis. In theory, Rtt109 inhibitors will sensitize the cells to echinocandins or flucytosine, which will result in effective treatment. In case of flucytosine, which is always used in combination with other antifungal agents, Rtt109 inhibitors can improve its effectiveness. However, this needs to be tested experimentally. Despite of the fact that *rtt109* mutants are not sensitive to other classes of antifungals, it may still be a worthwhile agent to use in combination therapy to circumvent the incidence of drug resistance.

Rtt109 is highly conserved in the fungal kingdom, making it an appealing target for therapeutic intervention against a broad-spectrum of fungal pathogens. Despite the ancestral structural relationship, Rtt109 and human p300/CBP possess different catalytic sites and catalytic mechanisms of action (Schneider *et al.* 2006). Moreover, p300/CBP inhibitors show no activity against fungal Rtt109, making a strong case for Rtt109 being an appealing antifungal drug target (Tang *et al.* 2008).

4.2.2. Asf1

Asf1 is a histone chaperone that plays an important role in packaging the eukaryotic genome into chromatin. Asf1 binds to newly synthesized H3 and H4 dimers and promotes Rtt109-dependent H3K56ac. It transfers newly synthesized histones that are H3K56 acetylated to downstream histone chaperones for replication-coupled and replication-independent nucleosome assembly (Fillingham *et al.* 2008; Dahlin *et al.* 2015). Asf1 is not essential for viability in *S. cerevisiae,* but its absence leads to spontaneous genome rearrangements, sensitivity to genotoxins and persistent

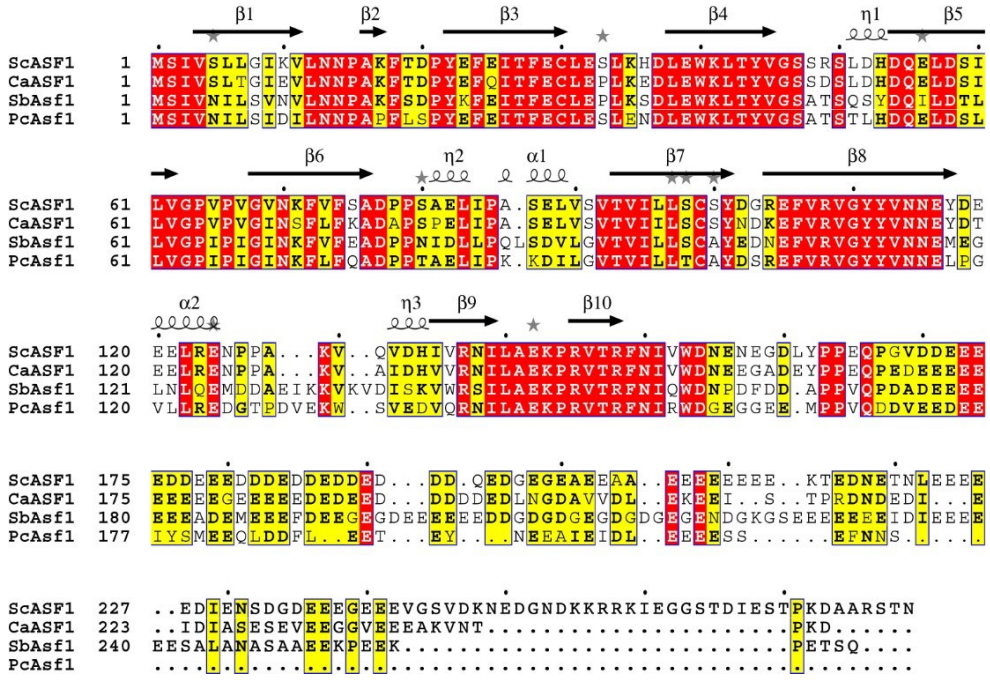

Figure 4.1 Asf1 sequence alignment

Crystal structure of the full-length *S. cerevisiae* Asf1 (PBD: 2HUE) was used as the template for structure-based sequence alignment with other fungal orthologs found in *C. albicans*, *S. pombe* and *P. carinii*. Secondary structures (α-helices or β-sheets) are indicated as spirals or arrows on the top of sequence alignment.

DNA lesions (Daganzo *et al.* 2003). However, our studies showed that Asf1 is essential for cell viability in *C. albicans* (Fig 2.5B). Cells lacking H3K56ac, such as *rtt109* null mutants, are viable. Hence, the essentiality of Asf1 might be due to its role in chromatin assembly or some other function that has not been previously described. Asf1 has been shown to interact with chromatin assembly factors of the Hir1/HIRA family to form silent chromatin, which represses histone gene transcription (Sharp *et al.* 2001; Sutton *et al.* 2001). In *C. albicans*, Asf1 is a stable protein with a long half-life (Chapter 2, Fig 2.5A and D). Asf1 consists of an evolutionarily conserved N-terminal histone-binding domain and a divergent C-terminal tail (Fig 4.1) (English *et al.* 2006). The availability of crystal structures of

the target protein facilitates computational high throughput screens (HTS) for selection of candidate compounds prior to a biochemical HTS (Miknis *et al.* 2015). A virtual screen to identify inhibitors of human Asf1 binding to H3/H4 yielded positive hits (Miknis *et al.* 2015). Such screens will facilitate biochemical assays with fewer compounds that are very selective against the protein of interest. Similar assays can be performed to find inhibitors of *C. albicans* Asf1 binding to H3/H4 that are fungal-specific and do not target human Asf1-H3/H4.

4.2.3. Hst3

Hst3 orthologues that deacetylate H3K56ac exhibit fungal-specific properties. Fungal Hst3 has conserved motifs involved in acetylated peptide binding that are not present in human sirtuins (Frye 2000; Schemies *et al.* 2010; Wurtele *et al.* 2010). Furthermore, the target acetyl-lysine of Hst3, H3K56, is the last residue of an α-helix. This is never the case in the numerous crystal structures of other sirtuins which show extended polypeptide strands on either side of the acetylated lysine. Consistent with this, unlike other sirtuins, Hst3 shows a very narrow substrate specificity *in vivo*. Hst3 is substrate-specific, as inhibition of Hst3 has been shown not to affect other sites than H3K56ac on the N-terminal tails of H3 or H4 (Wurtele *et al.* 2010). These properties make Hst3 an appealing candidate for antifungal drug development. NAM is a potent inhibitor of Hst3 in *C. albicans,* but not all fungi respond to NAM to the same extent, e.g. *C. glabrata* is much more resistant than *C. albicans* to NAM treatment. It is possible that the differential NAM tolerance of *Candida* species can be attributed to their Hst3 orthologues. May be different Hst3 orthologues respond to NAM differently and hence, activity and abundance of *C. glabrata* Hst3 may be different from *C. albicans* Hst3. We propose to perform a deacetylase assay to find small molecule inhibitors of Hst3 from different *Candida* species. This assay would require purification of nucleosome substrates that are acetylated at H3K56. A previously published method that consists in genetically-encoded incorporation of unnatural amino acids at specific codons was used to produce histone H3 molecules that are acetylated at lysine 56 (De Boor *et al.* 2015). With this method, it is possible to engineer site-specific incorporation of *N*-(ε)-

Acetyl-Lysine to produce proteins that are acetylated at particular lysine residues (De Boor *et al.* 2015). H2A, H2B, and H4 can be purified separately and reconstituted together with K56-acetylated H3 to form nucleosomes as described previously (Elsasser *et al.* 2012). These K56-acetylated histone H3 nucleosomes can be used as substrates to assess the NAD^+ dependent deacetylase activity of Hst3 enzymes from various *Candida* species. Results from this assay will possibly help solving the puzzle of differential NAM tolerance of different *Candida* species. The deacetylase assay with Hst3 can also be modified to find small molecule inhibitors. A small molecule that can inhibit Hst3 specifically and not other sirtuins will be a potential antifungal agent. Solving structures of fungal Hst3 using X-ray crystallography will be the next step in finding inhibitors. Availability of crystal structure opens up many different avenues to find small molecule inhibitors of the enzyme. Recently there have been reports of successful virtual screens to find small molecule inhibitors of sirtuins using the optimised method of consensus docking (Houston and Walkinshaw 2013; Kokkonen *et al.* 2015; Huang *et al.* 2017). Once the structure of Hst3 is solved, similar screens can be conducted to find inhibitors of the enzyme.

4.2.3.1. NAM as an antifungal agent

As discussed in the introduction, NAM meets the key criteria to be an antifungal agent. There are several advantages of NAM as a therapeutic agent. NAM selectively inhibits the growth of fungal cells by blocking deacetylation of H3K56ac. NAM primarily exerts its effect through the hyperacetylation of H3K56, but there have been reports of enzymes inhibited by NAM that play a role in the pathogenesis of *C. albicans* and other pathogenic fungi (Ciebiada-Adamiec *et al.* 2010). In *C. albicans* IC50 of NAM is 0.8 mM, the reason behind its low efficacy can be explained by the fact that it is a vitamin precursor of NAD^+ in the cells. Rapidly following its entry into fungal cells, it is converted into NA, which in not toxic to cells. The low efficacy of NAM *in vivo* can also be caused by pharmaco

kinetic parameters that I have discussed in section 1.4.6. In spite of this, its potential has been successfully demonstrated in a mouse model of systemic fungal infections (Wurtele *et al.* 2010). However, previous studies did not allow assessment of long-term NAM treatment as the A/J mice were extremely susceptible to *C. albicans* infections and died within 48 hours following infection. Further studies of systemic or mucosal murine model of *C. albicans* infections are necessary to improve the parameters of NAM administration and assess long-term effects of NAM treatment. To understand NAM pharmacokinetics better, its concentrations in circulation should also be monitored after administration. These studies are necessary to help bring NAM-based antifungal therapies to the clinic. The argument against the proposal of using NAM as an antifungal agent can be addressed by the fact that clinical trials with up to six grams per day for several weeks have shown minimal side effects. In a few cases, peak plasma concentrations were as high as 1.6 mM, which is inhibitory to *C. albicans* growth *in vitro* (Dragovic *et al.* 1995; Stratford *et al.* 1996; Lenglet *et al.* 2013). Recent studies have shown that NAM reduces sensitivity to the DNA damaging agent methyl methane sulphonate (MMS) in budding yeast (Rossl *et al.* 2016). This phenotype was independent of NAM's ability to inhibit sirtuins or enzymes involved in biosynthesis of NAD^+. Based on this, although NAM has been used in several clinical trials to treat different human conditions, *e.g.* Friedreich's ataxia, Alzheimer's disease and others, it is important to take into consideration the possibility that sirtuin-independent effects may modulate the pharmacological properties of NAM (Rossl *et al.* 2016).

The emergence of resistant strains is a major drawback of the azole class of antifungal agents, which are the most widely used antifungals to treat invasive fungal infections. For any drug to be effective, the rate of resistance emergence should be minimal. Our unpublished data show that frequency of emergence of NAM-resistant strains is less than or equal to the echinocandin micafungin, which shows a much lower incidence of drug resistance than azoles. Interestingly, preliminary studies showed that none of the NAM-resistant strains that we isolated had reduced levels of H3K56ac compared with the parental NAM-sensitive strain. Further investigation is required to understand the mechanism behind the NAM-

resistance phenotype of those clones. Elucidating mechanism of resistance in these strains may help improve the therapeutic potential of. NAM inhibits the growth of azole and echinocandin-resistant clinical isolates, and hence it could be used in combination therapy or as second option in cases of azole and echinocandin resistance. It is also important to study why different fungal species exhibit widely different NAM sensitivities. *C. krusei* is more sensitive to NAM than *C. albicans* whereas *C. glabrata* is highly resistant to NAM (Wurtele *et al.* 2010). The rise in systemic infections caused by *C. krusei* infections is partly due to prophylactic treatment with fluconazole. *C. krusei* shows an acute sensitivity to NAM and an intrinsic resistance to the azole class of antifungals (Wurtele *et al.* 2010; Oberoi *et al.* 2012; Delaloye and Calandra 2014), combination therapy with fluconazole and NAM can help overcome the problem of increasing incidence of *C. krusei* infections. On the other hand, the *C. glabrata* tolerance to NAM is intriguing (Wurtele *et al.* 2010). The *C. glabrata* genome encodes homologues of Rtt109 and Hst3, which likely indicates the presence of an active H3K56ac pathway. *C. glabrata* is an NAD^+ auxotroph that cannot synthesize NAD^+ from tryptophan, and therefore relies on salvage pathways to generate NAD^+ (Ma *et al.* 2009). Its NAM tolerance may be explained by its auxotrophy for NAD^+. Because of this, it seems possible that NAM is very rapidly converted into NA to generate NAD^+ in *C. glabrata*. Based on this assumption, *C. glabrata* cells that lack Pnc1 should be sensitive to NAM. We have developed tools to study the NAD^+ metabolome that can be easily adaptable to other pathogenic fungi and I propose that understanding NAD^+ metabolism in different pathogenic fungi will provide additional targets that can be used to develop novel antifungal therapies.

4.2.4. Qns1

Genes involved in NAD^+ metabolism have been proposed as appealing but poorly explored targets to develop antimicrobial agents (reviewed in (Sauve 2008; Gazzaniga *et al.* 2009). Despite the fact that enzymes involved in NAD^+ biosynthesis are evolutionarily conserved, they are appealing targets for antimicrobial drug discovery. For instance, iterative *in silico* and *in vitro* screens

have successfully identified small molecules that selectively inhibit the bacterial nicotinate mononucleotide adenylyltransferase enzyme without affecting its mammalian equivalent (Sorci *et al.* 2009). Despite being challenged with large concentrations of NAM, *C. albicans* cells maintained their NAD^+ levels constant (Fig 3.3 C and E). This result indicates the presence of regulatory mechanisms to maintain NAD^+ homeostasis. Enzymes that reduce NAD^+ biosynthesis such as the glutamine-dependent NAD^+ synthetase Qns1, are potential drug targets. Choosing rational drug targets involved in NAD^+ metabolism will require a better understanding of the enzymes involved. Characterization of Qns1 in other pathogenic fungi could provide an additional target that can be exploited for drug discovery.

4.3 Conclusion

Enzymes involved in H3K56 acetylation and deacetylation are potential antifungal targets. This thesis provides valuable insights into the mechanism of H3K56ac catalyzed by *C. albicans* Rtt109 together with its co-factors Vps75 and Asf1. My work shows a novel function of Vps75 in promoting H3K56ac in *C. albicans.* I report a HAT assay with *C. albicans* proteins that can be adapted to find novel inhibitors of Rtt109. This work also demonstrates that, independently of its role in promoting acetylation of H3K56, Asf1 has a function that is essential for viability of *C. albicans.* This essential function of Asf1 is likely its role in chromatin assembly but other possibilities (*e.g.* a role in the response to spontaneous DNA damage) cannot be excluded.

This thesis provides a first detailed characterization of genes involved in NAD^+ metabolism pathway in fungal pathogen *C. albicans*. I showed that *C. albicans* has multiple ways to get rid of excess NAM and hence it will be difficult to enhance the efficacy of it. I showed the evidence of the existence of a non-canonical mechanism that can convert excess NAM into NAD^+ in the absence of

nicotinamidase, Pnc1. My results support the hypothesis that NAM or small molecule that specifically modulates H3K56 acetylation and deacetylation pathway will be a potential antifungal agent to treat invasive fungal infections. Finally, our studies provided additional targets that can be used to develop novel antifungal therapies, i.e. Asf1 and NAD^+ synthetase Qns1. Our studies emphasize the fact that fungal pathogens have evolved to adapt to different environments by acquiring distinct biological traits. Sometimes it is achieved by protein family expansions or contractions and this leads to diverged functions of many proteins. Hence, it is essential to study processes that have potential implications on virulence and pathogenicity in the relevant model system to help in developing more targeted therapies.

References for Chapter 1 and 4

1) Abshiru, Ippersiel, Tang, Yuan, Marmorstein *et al.*, 2013 Chaperone-mediated acetylation of histones by Rtt109 identified by quantitative proteomics. J Proteomics 81**:** 80-90.
2) Abu Al-Melh, Andersson and Behbehani, 2005 Reduction of pain from needle stick in the oral mucosa by topical anesthetics: a comparative study between lidocaine/prilocaine and benzocaine. J Clin Dent 16**:** 53-56.
3) Allard, Masson and Cote, 2004 Chromatin remodeling and the maintenance of genome integrity. Biochim Biophys Acta 1677**:** 158-164.
4) Badiee, and Hashemizadeh, 2014 Opportunistic invasive fungal infections: diagnosis & clinical management. Indian J Med Res 139**:** 195-204.
5) Barousse, Espinosa, Dunlap and Fidel, 2005 Vaginal epithelial cell anti-Candida albicans activity is associated with protection against symptomatic vaginal candidiasis. Infect Immun 73**:** 7765-7767.
6) Belenky, Stebbins, Bogan, Evans and Brenner, 2011 Nrt1 and Tna1-independent export of NAD+ precursor vitamins promotes NAD+ homeostasis and allows engineering of vitamin production. PLoS One 6**:** e19710.
7) Berenguer, Allende, Lee, Garrett, Lyman *et al.*, 1995 Pathogenesis of pulmonary aspergillosis. Granulocytopenia versus cyclosporine and methylprednisolone-induced immunosuppression. Am J Respir Crit Care Med 152**:** 1079-1086.
8) Berman, and Sudbery, 2002 Candida Albicans: a molecular revolution built on lessons from budding yeast. Nat Rev Genet 3**:** 918-930.
9) Berndsen, Tsubota, Lindner, Lee, Holton *et al.*, 2008 Molecular functions of the histone acetyltransferase chaperone complex Rtt109-Vps75. Nat Struct Mol Biol 15**:** 948-956.
10) Bieganowski, and Brenner, 2004 Discoveries of nicotinamide riboside as a nutrient and conserved NRK genes establish a Preiss-Handler independent route to NAD+ in fungi and humans. Cell 117**:** 495-502.
11) Bogan, and Brenner, 2008 Nicotinic acid, nicotinamide, and nicotinamide riboside: a molecular evaluation of NAD+ precursor vitamins in human nutrition. Annu Rev Nutr 28**:** 115-130.
12) Brown, Denning, Gow, Levitz, Netea *et al.*, 2012 Hidden killers: human fungal infections. Sci Transl Med 4**:** 165rv113.
13) Bruno, Wang, Marjani, Euskirchen, Martin *et al.*, 2010 Comprehensive annotation of the transcriptome of the human fungal pathogen Candida albicans using RNA-seq. Genome Res 20**:** 1451-1458.
14) Butts, and Krysan, 2012 Antifungal drug discovery: something old and something new. PLoS Pathog 8**:** e1002870.
15) Canto, Menzies and Auwerx, 2015 NAD(+) Metabolism and the Control of Energy Homeostasis: A Balancing Act between Mitochondria and the Nucleus. Cell Metab 22**:** 31-53.

16) Chapman, Sullivan and Cleary, 2008 In search of the holy grail of antifungal therapy. Trans Am Clin Climatol Assoc 119**:** 197-215; discussion 215-196.
17) Chaudhuri, Montag and Heidelberger, 1958 Studies on fluorinated pyrimidines. III. The metabolism of 5-fluorouracil-2-C14 and 5-fluoroorotic-2-C14 acid in vivo. Cancer Res 18**:** 318-328.
18) Chi, Allis and Wang, 2010 Covalent histone modifications--miswritten, misinterpreted and mis-erased in human cancers. Nat Rev Cancer 10**:** 457-469.
19) Ciebiada-Adamiec, Malafiej and Ciebiada, 2010 Inhibitory effect of nicotinamide on enzymatic activity of selected fungal strains causing skin infection. Mycoses 53**:** 204-207.
20) Clatworthy, Pierson and Hung, 2007 Targeting virulence: a new paradigm for antimicrobial therapy. Nat Chem Biol 3**:** 541-548.
21) Cote, Quinn, Workman and Peterson, 1994 Stimulation of GAL4 derivative binding to nucleosomal DNA by the yeast SWI/SNF complex. Science 265**:** 53-60.
22) Cowen, Carpenter, Matangkasombut, Fink and Lindquist, 2006 Genetic architecture of Hsp90-dependent drug resistance. Eukaryot Cell 5**:** 2184-2188.
23) Cowen, and Lindquist, 2005 Hsp90 potentiates the rapid evolution of new traits: drug resistance in diverse fungi. Science 309**:** 2185-2189.
24) Cowen, Singh, Kohler, Collins, Zaas *et al.*, 2009 Harnessing Hsp90 function as a powerful, broadly effective therapeutic strategy for fungal infectious disease. Proc Natl Acad Sci U S A 106**:** 2818-2823.
25) D'arcy, and Luger, 2011 Understanding histone acetyltransferase Rtt109 structure and function: how many chaperones does it take? Curr Opin Struct Biol 21**:** 728-734.
26) Daganzo, Erzberger, Lam, Skordalakes, Zhang *et al.*, 2003 Structure and function of the conserved core of histone deposition protein Asf1. Curr Biol 13**:** 2148-2158.
27) Dahlin, Chen, Walters and Zhang, 2015 Histone-modifying enzymes, histone modifications and histone chaperones in nucleosome assembly: Lessons learned from Rtt109 histone acetyltransferases. Crit Rev Biochem Mol Biol 50**:** 31-53.
28) Dahlin, Sinville, Solberg, Zhou, Han *et al.*, 2013 A cell-free fluorometric high-throughput screen for inhibitors of Rtt109-catalyzed histone acetylation. PLoS One 8**:** e78877.
29) Day, Chau, Wolbers, Mai, Dung *et al.*, 2013 Combination antifungal therapy for cryptococcal meningitis. N Engl J Med 368**:** 1291-1302.
30) De Boor, Knyphausen, Kuhlmann, Wroblowski, Brenig *et al.*, 2015 Small GTP-binding protein Ran is regulated by posttranslational lysine acetylation. Proc Natl Acad Sci U S A 112**:** E3679-3688.
31) Delaloye, and Calandra, 2014 Invasive candidiasis as a cause of sepsis in the critically ill patient. Virulence 5**:** 161-169.
32) Denning, 1998 Invasive aspergillosis. Clin Infect Dis 26**:** 781-803; quiz 804-785.
33) Denning, 2003 Echinocandin antifungal drugs. Lancet 362**:** 1142-1151.

34) Denning, and Hope, 2010 Therapy for fungal diseases: opportunities and priorities. Trends Microbiol 18**:** 195-204.
35) Denning, Riniotis, Dobrashian and Sambatakou, 2003 Chronic cavitary and fibrosing pulmonary and pleural aspergillosis: case series, proposed nomenclature change, and review. Clin Infect Dis 37 Suppl 3**:** S265-280.
36) Deorukhkar, Saini and Mathew, 2014 Non-albicans Candida Infection: An Emerging Threat. Interdiscip Perspect Infect Dis 2014**:** 615958.
37) Diasio, Bennett and Myers, 1978 Mode of action of 5-fluorocytosine. Biochem Pharmacol 27**:** 703-707.
38) Dragovic, Kim, Brown and Kim, 1995 Nicotinamide pharmacokinetics in patients. Radiother Oncol 36**:** 225-228.
39) Drogaris, Villeneuve, Pomies, Lee, Bourdeau *et al.*, 2012 Histone deacetylase inhibitors globally enhance h3/h4 tail acetylation without affecting h3 lysine 56 acetylation. Sci Rep 2**:** 220.
40) Elsasser, Huang, Lewis, Chin, Allis *et al.*, 2012 DAXX envelops a histone H3.3-H4 dimer for H3.3-specific recognition. Nature 491**:** 560-565.
41) English, Adkins, Carson, Churchill and Tyler, 2006 Structural basis for the histone chaperone activity of Asf1. Cell 127**:** 495-508.
42) Faucher, and Wellinger, 2010 Methylated H3K4, a transcription-associated histone modification, is involved in the DNA damage response pathway. PLoS Genet 6.
43) Fillingham, Recht, Silva, Suter, Emili *et al.*, 2008 Chaperone control of the activity and specificity of the histone H3 acetyltransferase Rtt109. Mol Cell Biol 28**:** 4342-4353.
44) Fisher, Henk, Briggs, Brownstein, Madoff *et al.*, 2012 Emerging fungal threats to animal, plant and ecosystem health. Nature 484**:** 186-194.
45) Fleming, Walsh and Anaissie, 2002 Emerging and less common fungal pathogens. Infect Dis Clin North Am 16**:** 915-933, vi-vii.
46) Fonzi, and Irwin, 1993 Isogenic strain construction and gene mapping in Candida albicans. Genetics 134**:** 717-728.
47) French, Cen, Vrablik, Xu, Allen *et al.*, 2010 Characterization of nicotinamidases: steady state kinetic parameters, classwide inhibition by nicotinaldehydes, and catalytic mechanism. Biochemistry 49**:** 10421-10439.
48) Frye, 2000 Phylogenetic classification of prokaryotic and eukaryotic Sir2-like proteins. Biochem Biophys Res Commun 273**:** 793-798.
49) Garey, Rege, Pai, Mingo, Suda *et al.*, 2006 Time to initiation of fluconazole therapy impacts mortality in patients with candidemia: a multi-institutional study. Clin Infect Dis 43**:** 25-31.
50) Gazzaniga, Stebbins, Chang, Mcpeek and Brenner, 2009 Microbial NAD metabolism: lessons from comparative genomics. Microbiol Mol Biol Rev 73**:** 529-541, Table of Contents.
51) Ghannoum, and Rice, 1999 Antifungal agents: mode of action, mechanisms of resistance, and correlation of these mechanisms with bacterial resistance. Clin Microbiol Rev 12**:** 501-517.

52) Gola, Martin, Walther, Dunkler and Wendland, 2003 New modules for PCR-based gene targeting in Candida albicans: rapid and efficient gene targeting using 100 bp of flanking homology region. Yeast 20**:** 1339-1347.
53) Gow, Brown and Odds, 2002 Fungal morphogenesis and host invasion. Curr Opin Microbiol 5**:** 366-371.
54) Gudlaugsson, Gillespie, Lee, Vande Berg, Hu *et al.*, 2003 Attributable mortality of nosocomial candidemia, revisited. Clin Infect Dis 37**:** 1172-1177.
55) Guillemette, Drogaris, Lin, Armstrong, Hiragami-Hamada *et al.*, 2011 H3 lysine 4 is acetylated at active gene promoters and is regulated by H3 lysine 4 methylation. PLoS Genet 7**:** e1001354.
56) Hamilton, and Goodley, 1996 Virulence factors of Cryptococcus neoformans. Curr Top Med Mycol 7**:** 19-42.
57) Hnisz, Schwarzmuller and Kuchler, 2009 Transcriptional loops meet chromatin: a dual-layer network controls white-opaque switching in Candida albicans. Mol Microbiol 74**:** 1-15.
58) Hnisz, Tscherner and Kuchler, 2011 Targeting chromatin in fungal pathogens as a novel therapeutic strategy: histone modification gets infectious. Epigenomics 3**:** 129-132.
59) Houston, and Walkinshaw, 2013 Consensus docking: improving the reliability of docking in a virtual screening context. J Chem Inf Model 53**:** 384-390.
60) Http://Www.Cdc.Gov/Drugresistance/Threat-Report-2013., Centers for Disease Control and Prevention, Office of Infectious Disease Antibiotic resistance threats in the United States, 2013, pp.
61) Huang, Song, Wang, Zhang, Wang *et al.*, 2017 Discovery of New SIRT2 Inhibitors by Utilizing a Consensus Docking/Scoring Strategy and Structure-Activity Relationship Analysis. J Chem Inf Model 57**:** 669-679.
62) Hubbard, Markie and Poulter, 1986 Isolation and morphological characterization of a mycelial mutant of Candida albicans. J Bacteriol 165**:** 61-65.
63) Jones, Federspiel, Chibana, Dungan, Kalman *et al.*, 2004 The diploid genome sequence of Candida albicans. Proc Natl Acad Sci U S A 101**:** 7329-7334.
64) Karkowska-Kuleta, Rapala-Kozik and Kozik, 2009 Fungi pathogenic to humans: molecular bases of virulence of Candida albicans, Cryptococcus neoformans and Aspergillus fumigatus. Acta Biochim Pol 56**:** 211-224.
65) Keck, and Pemberton, 2011 Interaction with the histone chaperone Vps75 promotes nuclear localization and HAT activity of Rtt109 in vivo. Traffic 12**:** 826-839.
66) Kim, and Sudbery, 2011 Candida albicans, a major human fungal pathogen. J Microbiol 49**:** 171-177.
67) Knip, Douek, Moore, Gillmor, Mclean *et al.*, 2000 Safety of high-dose nicotinamide: a review. Diabetologia 43**:** 1337-1345.
68) Kokkonen, Kokkola, Suuronen, Poso, Jarho *et al.*, 2015 Virtual screening approach of sirtuin inhibitors results in two new scaffolds. Eur J Pharm Sci 76**:** 27-32.

69) Kouzarides, 2007 Chromatin modifications and their function. Cell 128**:** 693-705.
70) Kuchler, Jenull, Shivarathri and Chauhan, 2016 Fungal KATs/KDACs: A New Highway to Better Antifungal Drugs? PLoS Pathog 12**:** e1005938.
71) Kuo, and Andrews, 2013 Quantitating the specificity and selectivity of Gcn5-mediated acetylation of histone H3. PLoS One 8**:** e54896.
72) Kwon, Imbalzano, Khavari, Kingston and Green, 1994 Nucleosome disruption and enhancement of activator binding by a human SW1/SNF complex. Nature 370**:** 477-481.
73) Lamoth, Juvvadi, Gehrke, Asfaw and Steinbach, 2014 Transcriptional activation of heat shock protein 90 mediated via a proximal promoter region as trigger of caspofungin resistance in Aspergillus fumigatus. J Infect Dis 209**:** 473-481.
74) Lamoth, Juvvadi, Gehrke and Steinbach, 2013 In vitro activity of calcineurin and heat shock protein 90 Inhibitors against Aspergillus fumigatus azole- and echinocandin-resistant strains. Antimicrob Agents Chemother 57**:** 1035-1039.
75) Landry, Slama and Sternglanz, 2000 Role of NAD(+) in the deacetylase activity of the SIR2-like proteins. Biochem Biophys Res Commun 278**:** 685-690.
76) Lenglet, Liabeuf, Guffroy, Fournier, Brazier *et al.*, 2013 Use of nicotinamide to treat hyperphosphatemia in dialysis patients. Drugs R D 13**:** 165-173.
77) Lercher, Danilenko, Kirkpatrick and Carlomagno, 2017 Structural characterization of the Asf1-Rtt109 interaction and its role in histone acetylation. Nucleic Acids Res.
78) Li, Zhou, Luo, Ouyang, Hu *et al.*, 2007 Glycosylphosphatidylinositol (GPI) anchor is required in Aspergillus fumigatus for morphogenesis and virulence. Mol Microbiol 64**:** 1014-1027.
79) Libri, Yandim, Athanasopoulos, Loyse, Natisvili *et al.*, 2014 Epigenetic and neurological effects and safety of high-dose nicotinamide in patients with Friedreich's ataxia: an exploratory, open-label, dose-escalation study. Lancet 384**:** 504-513.
80) Lin, Schranz and Teutsch, 2001 Aspergillosis case-fatality rate: systematic review of the literature. Clin Infect Dis 32**:** 358-366.
81) Liu, 2011 *Molecular detection of human fungal pathogens*. CRC Press, Boca Raton.
82) Liu, Wang, Su, Zhang and Sheng, 2016 Strategies in the discovery of novel antifungal scaffolds. Future Med Chem 8**:** 1435-1454.
83) Lohse, and Johnson, 2009 White-opaque switching in Candida albicans. Curr Opin Microbiol 12**:** 650-654.
84) Lopes Da Rosa, Bajaj, Spoonamore and Kaufman, 2013 A small molecule inhibitor of fungal histone acetyltransferase Rtt109. Bioorg Med Chem Lett 23**:** 2853-2859.
85) Lopes Da Rosa, Boyartchuk, Zhu and Kaufman, 2010 Histone acetyltransferase Rtt109 is required for Candida albicans pathogenesis. Proc Natl Acad Sci U S A 107**:** 1594-1599.

86) Lopes Da Rosa, and Kaufman, 2013 Chromatin-mediated Candida albicans virulence. Biochim Biophys Acta 1819**:** 349-355.
87) Lott, Fundyga, Kuykendall and Arnold, 2005 The human commensal yeast, Candida albicans, has an ancient origin. Fungal Genet Biol 42**:** 444-451.
88) Luger, Rechsteiner, Flaus, Waye and Richmond, 1997 Characterization of nucleosome core particles containing histone proteins made in bacteria. J Mol Biol 272**:** 301-311.
89) Ma, Pan, Domergue, Rigby, Whiteway *et al.*, 2009 High-affinity transporters for NAD+ precursors in Candida glabrata are regulated by Hst1 and induced in response to niacin limitation. Mol Cell Biol 29**:** 4067-4079.
90) Mackay, Hathcock and Guarneri, 2012 Niacin: chemical forms, bioavailability, and health effects. Nutr Rev 70**:** 357-366.
91) Mallick, Bergeron, Jones, Newman, Brothers *et al.*, 2016 Phenotypic Plasticity Regulates Candida albicans Interactions and Virulence in the Vertebrate Host. Front Microbiol 7**:** 780.
92) Mao, Cao, Nie, Liu and Chen, 2006 The Swi/Snf chromatin remodeling complex is essential for hyphal development in Candida albicans. FEBS Lett 580**:** 2615-2622.
93) Marie, and White, 2009 Genetic Basis of Antifungal Drug Resistance. Curr Fungal Infect Rep 3**:** 163-169.
94) Martin, Mannino, Eaton and Moss, 2003 The epidemiology of sepsis in the United States from 1979 through 2000. N Engl J Med 348**:** 1546-1554.
95) Masumoto, Hawke, Kobayashi and Verreault, 2005 A role for cell-cycle-regulated histone H3 lysine 56 acetylation in the DNA damage response. Nature 436**:** 294-298.
96) Maubon, Garnaud, Calandra, Sanglard and Cornet, 2014 Resistance of Candida spp. to antifungal drugs in the ICU: where are we now? Intensive Care Med 40**:** 1241-1255.
97) Mavor, Thewes and Hube, 2005 Systemic fungal infections caused by Candida species: epidemiology, infection process and virulence attributes. Curr Drug Targets 6**:** 863-874.
98) Meersseman, Vandecasteele, Wilmer, Verbeken, Peetermans *et al.*, 2004 Invasive aspergillosis in critically ill patients without malignancy. Am J Respir Crit Care Med 170**:** 621-625.
99) Miknis, Stevens, Smith, Ostrov and Churchill, 2015 Development of novel Asf1-H3/H4 inhibitors. Bioorg Med Chem Lett 25**:** 963-968.
100) Millar, and Grunstein, 2006 Genome-wide patterns of histone modifications in yeast. Nat Rev Mol Cell Biol 7**:** 657-666.
101) Miller, and Johnson, 2002 White-opaque switching in Candida albicans is controlled by mating-type locus homeodomain proteins and allows efficient mating. Cell 110**:** 293-302.
102) Min, Landry, Sternglanz and Xu, 2001 Crystal structure of a SIR2 homolog-NAD complex. Cell 105**:** 269-279.
103) Mohr, Johnson, Cooper, Lewis and Ostrosky-Zeichner, 2008 Current options in antifungal pharmacotherapy. Pharmacotherapy 28**:** 614-645.
104) Moore, and Krebs, 2004 Histone modifications and DNA double-strand break repair. Biochem Cell Biol 82**:** 446-452.

105) Mor, Rella, Farnoud, Singh, Munshi *et al.*, 2015 Identification of a New Class of Antifungals Targeting the Synthesis of Fungal Sphingolipids. MBio 6**:** e00647.
106) Mora, Tittensor, Adl, Simpson and Worm, 2011 How many species are there on Earth and in the ocean? PLoS Biol 9**:** e1001127.
107) Morschhauser, 2010 Regulation of white-opaque switching in Candida albicans. Med Microbiol Immunol 199**:** 165-172.
108) Nakayama, Mio, Nagahashi, Kokado, Arisawa *et al.*, 2000 Tetracycline-regulatable system to tightly control gene expression in the pathogenic fungus Candida albicans. Infect Immun 68**:** 6712-6719.
109) Nobile, Fox, Hartooni, Mitchell, Hnisz *et al.*, 2014 A histone deacetylase complex mediates biofilm dispersal and drug resistance in Candida albicans. MBio 5**:** e01201-01214.
110) Noble, French, Kohn, Chen and Johnson, 2010 Systematic screens of a Candida albicans homozygous deletion library decouple morphogenetic switching and pathogenicity. Nat Genet 42**:** 590-598.
111) Noble, and Johnson, 2005 Strains and strategies for large-scale gene deletion studies of the diploid human fungal pathogen Candida albicans. Eukaryot Cell 4**:** 298-309.
112) Noble, and Johnson, 2007 Genetics of Candida albicans, a diploid human fungal pathogen. Annu Rev Genet 41**:** 193-211.
113) Oberoi, Wattal, Goel, Raveendran, Datta *et al.*, 2012 Non-albicans Candida species in blood stream infections in a tertiary care hospital at New Delhi, India. Indian J Med Res 136**:** 997-1003.
114) Park, and Morschhauser, 2005 Tetracycline-inducible gene expression and gene deletion in Candida albicans. Eukaryot Cell 4**:** 1328-1342.
115) Park, Wannemuehler, Marston, Govender, Pappas *et al.*, 2009 Estimation of the current global burden of cryptococcal meningitis among persons living with HIV/AIDS. AIDS 23**:** 525-530.
116) Peleg, Hogan and Mylonakis, 2010 Medically important bacterial-fungal interactions. Nat Rev Microbiol 8**:** 340-349.
117) Pfaller, and Diekema, 2004 Rare and emerging opportunistic fungal pathogens: concern for resistance beyond Candida albicans and Aspergillus fumigatus. J Clin Microbiol 42**:** 4419-4431.
118) Pfaller, and Diekema, 2007 Epidemiology of invasive candidiasis: a persistent public health problem. Clin Microbiol Rev 20**:** 133-163.
119) Pfaller, and Diekema, 2010 Epidemiology of invasive mycoses in North America. Crit Rev Microbiol 36**:** 1-53.
120) Pierce, and Lopez-Ribot, 2013 Candidiasis drug discovery and development: new approaches targeting virulence for discovering and identifying new drugs. Expert Opin Drug Discov 8**:** 1117-1126.
121) Radovani, Cadorin, Shams, El-Rass, Karsou *et al.*, 2013 The carboxyl terminus of Rtt109 functions in chaperone control of histone acetylation. Eukaryot Cell 12**:** 654-664.
122) Raman, Nguyen, Zhang, Cheng, Jia *et al.*, 2006 Candida albicans SET1 encodes a histone 3 lysine 4 methyltransferase that contributes to the pathogenesis of invasive candidiasis. Mol Microbiol 60**:** 697-709.

123) Reuss, Vik, Kolter and Morschhauser, 2004 The SAT1 flipper, an optimized tool for gene disruption in Candida albicans. Gene 341**:** 119-127.
124) Richard, Ibata-Ombetta, Dromer, Bordon-Pallier, Jouault *et al.*, 2002 Complete glycosylphosphatidylinositol anchors are required in Candida albicans for full morphogenesis, virulence and resistance to macrophages. Mol Microbiol 44**:** 841-853.
125) Robbins, Wright and Cowen, 2016 Antifungal Drugs: The Current Armamentarium and Development of New Agents. Microbiol Spectr 4.
126) Roemer, Jiang, Davison, Ketela, Veillette *et al.*, 2003 Large-scale essential gene identification in Candida albicans and applications to antifungal drug discovery. Mol Microbiol 50**:** 167-181.
127) Roemer, and Krysan, 2014 Antifungal drug development: challenges, unmet clinical needs, and new approaches. Cold Spring Harb Perspect Med 4.
128) Rossl, Bentley-Desousa, Tseng, Nwosu and Downey, 2016 Nicotinamide Suppresses the DNA Damage Sensitivity of Saccharomyces cerevisiae Independently of Sirtuin Deacetylases. Genetics 204**:** 569-579.
129) Ruthenburg, Li, Patel and Allis, 2007 Multivalent engagement of chromatin modifications by linked binding modules. Nat Rev Mol Cell Biol 8**:** 983-994.
130) Santos, Keith and Tuite, 1993 Non-standard translational events in Candida albicans mediated by an unusual seryl-tRNA with a 5'-CAG-3' (leucine) anticodon. EMBO J 12**:** 607-616.
131) Sauve, 2008 NAD+ and vitamin B3: from metabolism to therapies. J Pharmacol Exp Ther 324**:** 883-893.
132) Sauve, Celic, Avalos, Deng, Boeke *et al.*, 2001 Chemistry of gene silencing: the mechanism of NAD+-dependent deacetylation reactions. Biochemistry 40**:** 15456-15463.
133) Sauve, Moir, Schramm and Willis, 2005 Chemical activation of Sir2-dependent silencing by relief of nicotinamide inhibition. Mol Cell 17**:** 595-601.
134) Sauve, and Schramm, 2003 Sir2 regulation by nicotinamide results from switching between base exchange and deacetylation chemistry. Biochemistry 42**:** 9249-9256.
135) Schemies, Uciechowska, Sippl and Jung, 2010 NAD(+) -dependent histone deacetylases (sirtuins) as novel therapeutic targets. Med Res Rev 30**:** 861-889.
136) Schneider, Bajwa, Johnson, Bhaumik and Shilatifard, 2006 Rtt109 is required for proper H3K56 acetylation: a chromatin mark associated with the elongating RNA polymerase II. J Biol Chem 281**:** 37270-37274.
137) Schweer, Bangard, Hekmat and Cornely, 2014 Chronic pulmonary aspergillosis. Mycoses 57**:** 257-270.
138) Sellam, Hogues, Askew, Tebbji, Van Het Hoog *et al.*, 2010 Experimental annotation of the human pathogen Candida albicans coding and noncoding transcribed regions using high-resolution tiling arrays. Genome Biol 11**:** R71.

139) Selmecki, Forche and Berman, 2006 Aneuploidy and isochromosome formation in drug-resistant Candida albicans. Science 313**:** 367-370.
140) Selmecki, Forche and Berman, 2010 Genomic plasticity of the human fungal pathogen Candida albicans. Eukaryot Cell 9**:** 991-1008.
141) Shapiro, Uppuluri, Zaas, Collins, Senn *et al.*, 2009 Hsp90 orchestrates temperature-dependent Candida albicans morphogenesis via Ras1-PKA signaling. Curr Biol 19**:** 621-629.
142) Sharp, Fouts, Krawitz and Kaufman, 2001 Yeast histone deposition protein Asf1p requires Hir proteins and PCNA for heterochromatic silencing. Curr Biol 11**:** 463-473.
143) Sheehan, Hitchcock and Sibley, 1999 Current and emerging azole antifungal agents. Clin Microbiol Rev 12**:** 40-79.
144) Singh-Babak, Babak, Diezmann, Hill, Xie *et al.*, 2012 Global analysis of the evolution and mechanism of echinocandin resistance in Candida glabrata. PLoS Pathog 8**:** e1002718.
145) Slutsky, Staebell, Anderson, Risen, Pfaller *et al.*, 1987 "White-opaque transition": a second high-frequency switching system in Candida albicans. J Bacteriol 169**:** 189-197.
146) Sobel, Faro, Force, Foxman, Ledger *et al.*, 1998 Vulvovaginal candidiasis: epidemiologic, diagnostic, and therapeutic considerations. Am J Obstet Gynecol 178**:** 203-211.
147) Sorci, Pan, Eyobo, Rodionova, Huang *et al.*, 2009 Targeting NAD biosynthesis in bacterial pathogens: Structure-based development of inhibitors of nicotinate mononucleotide adenylyltransferase NadD. Chem Biol 16**:** 849-861.
148) Stevenson, and Liu, 2011 Regulation of white and opaque cell-type formation in Candida albicans by Rtt109 and Hst3. Mol Microbiol 81**:** 1078-1091.
149) Stratford, Dennis, Hoskin, Phillips, Hodgkiss *et al.*, 1996 Nicotinamide pharmacokinetics in humans: effect of gastric acid inhibition, comparison of rectal vs oral administration and the use of saliva for drug monitoring. Br J Cancer 74**:** 16-21.
150) Su, Hu, Zhou, Thompson, Xu *et al.*, 2011 Structure and histone binding properties of the Vps75-Rtt109 chaperone-lysine acetyltransferase complex. J Biol Chem 286**:** 15625-15629.
151) Sutton, Bucaria, Osley and Sternglanz, 2001 Yeast ASF1 protein is required for cell cycle regulation of histone gene transcription. Genetics 158**:** 587-596.
152) Tang, Holbert, Delgoshaie, Wurtele, Guillemette *et al.*, 2011 Structure of the Rtt109-AcCoA/Vps75 complex and implications for chaperone-mediated histone acetylation. Structure 19**:** 221-231.
153) Tang, Holbert, Wurtele, Meeth, Rocha *et al.*, 2008 Fungal Rtt109 histone acetyltransferase is an unexpected structural homolog of metazoan p300/CBP. Nat Struct Mol Biol 15**:** 738-745.
154) Tanny, and Moazed, 2001 Coupling of histone deacetylation to NAD breakdown by the yeast silencing protein Sir2: Evidence for acetyl transfer

from substrate to an NAD breakdown product. Proc Natl Acad Sci U S A 98**:** 415-420.
155) Tempel, Rabeh, Bogan, Belenky, Wojcik *et al.*, 2007 Nicotinamide riboside kinase structures reveal new pathways to NAD+. PLoS Biol 5**:** e263.
156) Tenforde, Scriven, Harrison and Jarvis, 2017 Immune correlates of HIV-associated cryptococcal meningitis. PLoS Pathog 13**:** e1006207.
157) Thevissen, Kristensen, Thomma, Cammue and Francois, 2007 Therapeutic potential of antifungal plant and insect defensins. Drug Discov Today 12**:** 966-971.
158) Thompson, Carlisle and Kadosh, 2011 Coevolution of morphology and virulence in Candida species. Eukaryot Cell 10**:** 1173-1182.
159) Tong, and Denu, 2010 Function and metabolism of sirtuin metabolite O-acetyl-ADP-ribose. Biochim Biophys Acta 1804**:** 1617-1625.
160) Treyvaud Amiguet, Petit, Ta, Nunez, Sanchez-Vindas *et al.*, 2006 Phytochemistry and antifungal properties of the newly discovered tree Pleodendron costaricense. J Nat Prod 69**:** 1005-1009.
161) Vengurlekar, Sharma and Trivedi, 2012 Efficacy of some natural compounds as antifungal agents. Pharmacogn Rev 6**:** 91-99.
162) Vermes, Guchelaar and Dankert, 2000 Flucytosine: a review of its pharmacology, clinical indications, pharmacokinetics, toxicity and drug interactions. J Antimicrob Chemother 46**:** 171-179.
163) Vincent, Rello, Marshall, Silva, Anzueto *et al.*, 2009 International study of the prevalence and outcomes of infection in intensive care units. JAMA 302**:** 2323-2329.
164) Vyas, Barrasa and Fink, 2015 A Candida albicans CRISPR system permits genetic engineering of essential genes and gene families. Sci Adv 1**:** e1500248.
165) Vylkova, Carman, Danhof, Collette, Zhou *et al.*, 2011 The fungal pathogen Candida albicans autoinduces hyphal morphogenesis by raising extracellular pH. MBio 2**:** e00055-00011.
166) Waldorf, and Polak, 1983 Mechanisms of action of 5-fluorocytosine. Antimicrob Agents Chemother 23**:** 79-85.
167) Ward, Knights and Gale, 2017 Infant fungal communities: current knowledge and research opportunities. BMC Med 15**:** 30.
168) Wilson, Davis and Mitchell, 1999 Rapid hypothesis testing with Candida albicans through gene disruption with short homology regions. J Bacteriol 181**:** 1868-1874.
169) Wilson, Reyes, Stolpman, Speckman, Allen *et al.*, 2002 The direct cost and incidence of systemic fungal infections. Value Health 5**:** 26-34.
170) Wirsching, Michel and Morschhauser, 2000 Targeted gene disruption in Candida albicans wild-type strains: the role of the MDR1 gene in fluconazole resistance of clinical Candida albicans isolates. Mol Microbiol 36**:** 856-865.
171) Wurtele, Tsao, Lepine, Mullick, Tremblay *et al.*, 2010 Modulation of histone H3 lysine 56 acetylation as an antifungal therapeutic strategy. Nat Med 16**:** 774-780.

172) Yan, Du, Zhao, Hartmann, Lu *et al.*, 2013 Transcriptome and biochemical analysis reveals that suppression of GPI-anchor synthesis leads to autophagy and possible necroptosis in Aspergillus fumigatus. PLoS One 8**:** e59013.